



Reviews and syntheses: Parameter identification in marine planktonic ecosystem modelling

Schartau Markus¹, Wallhead Philip², Hemmings John^{3,4}, Löptien Ulrike¹, Kriest Iris¹, Krishna Shubham¹, Ward Ben A.⁵, Slawig Thomas⁶, and Oschlies Andreas¹

¹GEOMAR Helmholtz Centre for Ocean Research Kiel, Germany

²NIVA, Norwegian Institute for Water Research, Bergen, Norway

³Wessex Environmental Associates, Salisbury, United Kingdom

⁴now at Met Office, Exeter, United Kingdom

⁵University of Bristol, School of Geographical Sciences, Bristol, United Kingdom

⁶Christian-Albrechts-Universität zu Kiel, Department of Computer Science, Kiel, Germany

Correspondence to: Markus Schartau (mschartau@geomar.de) and Phil Wallhead (philip.wallhead@niva.no)

Abstract. To describe the underlying processes involved in oceanic plankton dynamics is crucial for the determination of energy and mass flux through an ecosystem and for the estimation of biogeochemical element cycling. Many planktonic ecosystem models were developed to resolve major processes so that flux estimates can be derived from numerical simulations. These results depend on the type and number of parameterisations incorporated as model equations. Furthermore, the values assigned to respective parameters specify a model's solution. Representative model results are those that can explain data, therefore data assimilation methods are utilised to yield optimal estimates of parameter values while fitting model results to match data. Central difficulties are 1) planktonic ecosystem models are imperfect and 2) data are often too sparse to constrain all model parameters. In this review we explore how problems in parameter identification are approached in marine planktonic ecosystem modelling. We provide background information about model uncertainties and estimation methods, and how these are considered for assessing misfits between observations and model results. We explain differences in evaluating uncertainties in parameter estimation, thereby also addressing issues of parameter identifiability. Aspects of model complexity will be covered and we describe how results from cross-validation studies provide much insight in this respect. Moreover, we elucidate inferences made in studies that allowed for variations in space and time of parameter values. The usage of dynamical and statistical emulator approaches will be briefly explained, discussing their advantage for parameter optimisations of large-scale biogeochemical models. Our survey extends to studies that approached parameter identification in global biogeochemical modelling. Parameter estimation results will exemplify some of the advantages and remaining problems in optimising global biogeochemical models. Our review discloses many facets of parameter identification, as we found many commonalities between the objectives of different approaches, but scientific insight differed between studies. To learn more from results of planktonic ecosystem models we recommend finding a good balance in the level of sophistication between mechanistic modelling and statistical data assimilation treatment for parameter estimation.



1 Introduction

The growth, decay, and interaction of planktonic organisms drive the transformation and cycling of chemical elements in the ocean. Understanding the interconnected and complex nature of these processes is critical to understanding the ecological and biogeochemical function of the system as a whole. The development of biogeochemical models requires accurate mathematical descriptions of key physiological and ecological processes, and their sensitivity to changes in the chemical and physical environment. Such mathematical descriptions form the basis of integrated dynamical models, typically composed of a set of differential equations that allow credible computations of the flux and transformation of energy (light) and mass (nutrients) within the ecosystem (U.S. Joint Global Ocean Flux Study Planning Report Number 14, *Modeling and Data Assimilation*, 1992).

Generalised mechanistic descriptions of how energy is absorbed and how mass becomes distributed in an ecosystem, already exist, such as dynamic energy budget models (Kooijman, 1986) or the metabolic theory of ecology (Brown et al., 2004). But these theories still have limitations, and include incompatible assumptions (van der Meer, 2006). So far no fundamental ecophysiological principle has been further exacted beyond the conservation of mass. To achieve balanced mass budgets is one straw that biogeochemical modelers grasp at. A consistent theme running through most ecosystem models is therefore the determination of the mass flux of certain biologically important elements, such as nitrogen, phosphorus, iron and carbon (N, P, Fe and C). Nonetheless, the precise details of how mass is transformed and allocated within an ecosystem is far from being established. For this reason, we find a large variety of plankton ecosystem models that differ in their number of state variables as well as in their parameterisation of individual physiological and ecological processes.

1.1 Mass flux induced by plankton dynamics

Dynamical marine, as well as limnic, ecosystem models usually start from a description of the build-up of biomass by photoautotrophic organisms (phytoplankton) as these take up dissolved nutrients from the water column and exploit light energy by photosynthesis. Phytoplankton biomass, as a product of primary production, is subsequently removed by natural mortality (cell lysis due to starvation, senescence, and viral attack), predation by zooplankton, and vertical export away from surface ocean layers via sinking of single or aggregated cells and of fecal pellets. Parameterisations of these three loss processes can be interlinked e.g. grazing of phytoplankton aggregates by large copepods. Depending on the trophic levels considered, the predation among different zooplankton types (e.g. between herbivores, carnivores or omnivores) can be explicitly parameterised. Mortality and aggregation of phytoplankton cells and the excretion of organic matter (fecal pellets) by zooplankton act as primary sources of dead particulate organic matter (detritus) that can be exported to depth via sinking. Exudation by phytoplankton and bacteria can be a major source of labile dissolved organic matter that represents diverse substrates for remineralisation. The transformation of particulate and dissolved organic matter back to inorganic nutrients are parameterised as hydrolysis and remineralisation processes. Often hydrolysis and remineralisation are assumed to be proportional to bacterial biomass, which is considered in many models. Bacterial biomass remains unresolved in some models where microbial remineralisation is parameterised only as a function of concentration and quality of organic substrates. At some level most models



include a parameterisation to account for the net effect of higher trophic levels that are not explicitly resolved in the model. This is usually formulated as a closure flux back to nutrient pools and whose rates simply depend on the biomass of the highest trophic level resolved. These closure assumptions ensure mass conservation while neglecting the actual mass loss to higher trophic levels like fish, which would be subject to changes in biomass on multi-annual rather than seasonal time scales. Every
5 marine planktonic ecosystem model can thus be described as a simplification of the dynamics inherent to a system of nutrients, phytoplankton, zooplankton, detritus, dissolved organic matter, and bacteria.

In many cases marine ecosystem models are embedded in an existing physical model setup that simulates environmental conditions, advection and mixing of the biological and chemical state variables. Feedbacks from the ecosystem model states on physical variables can be relevant (e.g., Murtugudde et al., 2002; Oschlies, 2004; Löptien et al., 2009; Löptien and Meier,
10 2011) but are hardly considered in current marine biogeochemical studies. With such feedbacks resolved, solutions of the plankton ecosystem model may also induce changes in physical environmental conditions. So far, results of the physical model component remain unaffected by ecosystem states in most studies and changes in mass flux are only attributed to alterations in the planktonic ecosystem component, e.g. as a result of varying parameter values.

1.2 Parameters of plankton ecosystem models

15 Amongst the most influential model approaches to study the nitrogen flux through such marine plankton ecosystem at a local site was proposed by Fasham et al. (1990). Their model involves 27 parameters and the simulated N cycle was shown to already depend on the value assigned to a single parameter, namely the sinking velocity of detritus. This stresses the invidious situation of finding a reliable ecosystem model solution by choosing parameter values that are either uncertain or even unknown. Laboratory measurements, as well as ship-based experiments with field samples, can provide information about the range of
20 typical values for some parameters, for example the maximum growth rate of photo-autotrophs or the maximum ingestion rate of herbivorous plankton. Other model parameters are extremely difficult to measure, like exudation rates of dissolved organic carbon by phytoplankton or by bacteria. Another difficulty is that parameter values from laboratory experiments are often specific with respect to plankton species, temperature, and light conditions. Their values may not be directly applicable for ocean simulations where parameter values need to be representative for a mixture of different plankton species in a continuously
25 varying physical environment. For example, for a natural composition of diverse phytoplankton cells that all differ in their genotypic- and phenotypic characteristics, we may expect values of some model parameters to follow a distribution rather than having a single fixed value. In practice, fixed parameter values are prescribed and are assumed to reflect some prevailing behaviour or characteristic (trait) of a mixed plankton community or of a particular plankton functional type. In the end, it is the choice of these parameter values that determines a specific model solution of any ecological- or biogeochemical model
30 setup.

1.3 The vital role of data

Model solutions of interest are typically those that can simulate and explain complex data. Data assimilation (DA) methods can be utilised to obtain a best possible model solution in association with a particular set of parameter values. The comparison



between model results and data is substantial and parameter estimates can be retrieved by indirect means. Parameter values of a planktonic ecosystem model are adjusted until simulation results match available observations, which is a procedure of model calibration. Optimal parameter values are regarded as those that minimise deviations between model results and observations (data-model misfit) but are also in accordance to the range of values known from experiments or from preceding DA studies.

5 To determine optimal parameter estimates we have to account for uncertainties in data and in model dynamics as well, which is specified by an error model. Parameter estimates are thus conditioned by a) the dynamical model equations, b) the data, c) our prior knowledge about the range of possible parameter values, and d) the underlying error model introduced to the data-model misfit function (Evans, 2003).

Situations can occur where model results that are compared with data are insensitive to variations of some parameters. Values of those parameters remain unconstrained by the available data, which is a problem of parameter identifiability. The availability of data thus places limitations on the number of model parameters whose values become identifiable. This in turn sets restrictions on the complexity of plankton interactions that can be unambiguously confined during ecosystem model calibration (Matear, 1995). Choosing appropriate model complexity is ambiguous and is still subject to discussion (e.g., Franks, 2002; Denman, 2003; Fulton et al., 2003; Anderson, 2005; Le Queré, 2006; Friedrichs et al., 2007; Franks, 2009; Kriest et al., 15 2012; Ward et al., 2013), a situation which sustains large differences in the level of complexity of current plankton models.

1.4 Inferences from data assimilation

Novel DA methods are predominantly devised for improving forecasts of model states and data-model misfits are treated as errors due to some unresolved and unspecified system noise. For example, sophisticated sequential filtering methods (e.g., Natvik and Evensen, 2003; Dowd, 2007; Nerger and Gregg, 2008; van Leeuwen, 2010) are applied to account for and com- 20 pensate model deficiencies, improving state estimates e.g. for predictions of an algal bloom. This is often achieved to the cost of infringing mass conservation. To identify and gradually eliminate model deficiencies it is helpful to consider model state and flux estimates that remain dynamically and ecologically consistent in terms of mass allocation. DA approaches that assure mass conservation in ecosystem- and biogeochemical modelling also harmonise well with those DA methods that produce dynamically and kinematically consistent estimates of ocean circulation (e.g., Wunsch and Heimbach, 2007; Wunsch et al., 25 2009).

Here we provide an overview of major DA aspects concerning parameter identification in marine ecosystem- and biogeochemical modelling. We adopt a notation more commonly used for DA studies in operational meteorology and oceanography. At the same time we integrate aspects related to ecological and biogeochemical modelling accordingly. On the one hand we provide background information that should facilitate intelligibility when studying DA literature. On the other hand we like to elucidate typical objectives and common problems when simulating a marine planktonic system. In this manner we hope to support a mutual understanding between ecologically/biogeochemically and mathematically/statistically motivated studies.

First we will start with some theoretical background, introducing mathematical notation as well as depicting prevalent assumptions made for parameter identification analyses and model calibration (Sect. 2). Error models will be described in order to elucidate error assumptions made in previous ecosystem modeling studies (Sect. 3). This will be followed by a description



of different approaches to specify uncertainties in parameter values (Sect. 4). In Sect. (5) we branch-off from DA theory in order to accentuate some biological aspects of those parameters we typically have to deal with in plankton ecosystem models. An example of parameter estimation with simulations of a mesocosm experiment connects aspects of Sect. (5) with theoretical considerations of the preceding sections. Thereafter, model complexity will be jointly addressed together with cross-validation in Sect. (6), followed by a review of space-time variations of marine ecosystem model parameters (Sect. 7). Emulator, or surrogate-based, approaches will be briefly explained and exemplified (Sect. 8) before we discuss parameter estimation of large-scale and global biogeochemical ocean circulation models (Sect. 9). Finally, we will summarise major insights that we gained on parameter identification in Sect. 10 and we will briefly address prospects of some marine ecosystem model approaches that could improve parameter identification.

10 2 Theoretical background

The term parameter identification is used broadly to describe parameter estimation problems, including the specification of uncertainties in parameter estimates and model parameterisations. It involves the following procedures:

- a) Parameter sensitivity analyses: the evaluation of how model results change with variations of parameter values.
- b) Parameter estimation: the calibration of model results by adjusting parameter values until a model solution is in best possible (optimal) agreement with observations.
- c) Parameter identifiability analyses: the specification of parameter uncertainties in order to reveal structural model deficiencies and shortages in data availability/information.

All three aspects are interrelated and should not be viewed as mutually exclusive procedures. For example, before starting with parameter estimation it is helpful to include information from a preceding sensitivity analysis, e.g. selecting only parameters to which model results are sensitive to. Likewise, an identifiability analysis complements the sensitivity analysis by providing information about error margins and possible ambiguities of optimal parameter estimates.

2.1 Basic errors in model results and data

2.1.1 Model states, parameters, control variables, and dynamical model errors

The prognostic dynamical equations of a marine ecosystem model can be expressed as a set of difference equations:

$$25 \quad \mathbf{x}_{i+1} = M[\mathbf{x}_i, \theta_e, \mathbf{f}_i, \boldsymbol{\eta}_i(\theta_\eta)] \quad (1)$$

with index i representing a particular time step (i.e. t_i). The model state vector \mathbf{x}_i has dimension $N_x = N_g \times N_s$ where N_g is the number of spatial grid points and N_s is the number of model state variables (e.g. phytoplankton biomass). The dynamical model operator M is typically at least a nonlinear function of the earlier state \mathbf{x}_i , a set of ecosystem parameters θ_e describing rate constants and coefficients in the dynamical model, and a set of time and space dependent forcings and boundary conditions



f_i . If the ecosystem model is coupled ‘online’ with a physical ocean model, f_i includes both physical model forcings (e.g. wind stress) and ecosystem model forcings (e.g. surface short-wave irradiance). If the physics is coupled “offline”, f_i includes ecosystem model forcings and physical model outputs (e.g. seawater temperature).

For stochastic dynamical models, M also depends on random noise variables or dynamical model errors η_i while for deterministic models we have $\eta_i = 0$. These errors are described by distributional parameters θ_η , e.g. location and scale parameters of a probability density function. Dynamical model errors usually enter the dynamics additively, multiplicatively, or as time/space-dependent corrections to f or θ_η . They may represent the individual or combined effects of errors in forcings, boundary conditions, random variability in model parameters, and structural errors in both the physical transport model (e.g. due to limited spatial resolution) and the biological source-minus-sink terms (e.g. due to aggregation of species into model groups). In the geophysical community, error models that explicitly account for dynamical model errors (noise) are often termed *weak constraint* models, while those that assume a deterministic model are termed *strong constraint* (Sasaki, 1970; Bennett, 2002).

2.1.2 True states and kinematic model errors

To relate the dynamical model output of Eq. (1) to observations, it is helpful to first consider how it may relate to a conceptual and hypothetical true state x^t , which is then imperfectly observed. In this respect we must also consider the averaging scales. In marine ecosystem modelling there is almost always a large discrepancy between the spatio-temporal averaging scales of the model, that define the meaning of the “concentrations” in x , and the averaging scales of the observations from in-situ sampling or remote sensing. For example, the spatial averaging scale of a model may be defined by a model grid cell of size 10 km in the horizontal and 10 m in the vertical, while the averaging scale of the observations might be the 10 cm scale, e.g. of a Niskin bottle sample. Even with a perfect model, data from finescale observations may diverge from model output due to unresolved sub-grid scale variability induced by fluid structures such as eddies and fronts, forming patches of high next to low concentrations e.g. of nutrients or organic matter.

A general relationship between the true state and model state can be expressed as:

$$x^t = T[x, \zeta(\theta_\zeta)] \quad (2)$$

where T is a truth operator, and ζ is a set of random variables described by distributional parameters θ_ζ . We will refer to the ζ as *kinematic* model errors because they are associated with the model state, while the *dynamical* model errors η in Eq. (1) act to perturb the model dynamics.

How we interpret and specify Eq. (2) depends on the spatio-temporal averaging scales chosen to define the true state x^t , which in turn depends on the objectives of the modelling study. One approach is to define these averaging scales as equal to or larger than the shortest space and time scales that are fully resolved by the model. Kinematic model errors ζ may then represent the integrated effects of the various dynamical sources of model error, if these are not already accounted for by dynamical model errors η in Eq. (1). Alternatively, the true state can be defined over scales smaller than those resolved by the model, possibly at the scales of the observations. This may lead to a simpler model for observational error (see below), but now



the ζ must account for the unresolved scales, in addition to any error effects in the model dynamics otherwise not accounted for. With stochastic dynamical models ($\eta \neq 0$), the true state is usually defined on the scales of the model and assumed to coincide with the model output for some (θ_e, η) , such that no kinematic error model is needed.

2.1.3 Data and observational errors

5 The observation vector \mathbf{y} can be related to the true state via:

$$\mathbf{y} = O[\mathbf{x}^t, \epsilon(\theta_e)] \quad (3)$$

where O is the generalized observation operator and ϵ is a set of random *observational* errors described by distributional parameters θ_e and accounting for uncertainties associated with the usage and interpretation of the data. These include at least the random measurement error due to, for example, instrument noise. In addition they may include a contribution from *representativeness* error due to finescale variability, if \mathbf{x}^t is defined as an average over larger scales than those of the observations (see above). Alternatively, if the observations are preprocessed into estimates on the larger scales of \mathbf{x}^t , there may be an *undersampling* error component due to inexhaustive coverage of the raw samples. The observation operator O may also contribute to ϵ , for example if the model output needs to be interpolated from the model grid to the data coordinates, or if O includes conversion factors such as chlorophyll *a*-to-nitrogen (Chl*a*:N) ratios.

15 The simplest possible example of an observational error model assumes additive Gaussian errors. Equation (3) then becomes:

$$\begin{aligned} \mathbf{y} &= H(\mathbf{x}^t) + \epsilon \\ &\longrightarrow \epsilon = \mathbf{y} - H(\mathbf{x}^t) \end{aligned} \quad (4)$$

where H accounts for interpolation and units conversion and $\epsilon \sim G(0, \mathbf{R})$ is Gaussian distributed with mean zero and covariance matrix \mathbf{R} . This may be a reasonable error model for most physical variables and chemical concentrations with ranges well above zero (e.g. dissolved inorganic carbon or total alkalinity in the open ocean). However, many nutrients and plankton biomass variables may vary close to their lower bounds of zero, and display positive skew in their observational errors. For such variables, a lognormal observational error model may be more appropriate:

$$\begin{aligned} \mathbf{y} &= H(\mathbf{x}^t) \circ \exp\left(\epsilon - \frac{\sigma^2}{2}\right) \\ &\longrightarrow \epsilon = \ln(\mathbf{y}) - \ln(H(\mathbf{x}^t)) + \frac{\sigma^2}{2} \end{aligned} \quad (5)$$

25 where \circ denotes element-wise multiplication and the bias correction term $\frac{\sigma^2}{2}$ ensures unbiased errors, but is frequently neglected in practice. The various options and challenges of defining an appropriate error model are discussed in detail in Section (3).

2.2 General estimation methods

We now consider how to estimate uncertain parameters Θ given the data \mathbf{y} , where Θ includes all biological parameters θ_e and possibly distributional parameters $(\theta_\eta, \theta_\zeta, \theta_e)$. There are basically two probabilistic approaches for doing this: Bayesian



estimation and maximum likelihood estimation. In the Bayesian approach, we treat the parameters as random variables, and choose parameter values on the basis of their ‘posterior probability’ i.e. the conditional probability density of the parameter values given the data $p(\Theta | \mathbf{y})$. The posterior probability is computed using Bayes’ theorem:

$$p(\Theta | \mathbf{y}) = \frac{p(\mathbf{y} | \Theta) \cdot p(\Theta)}{p(\mathbf{y})} \propto p(\mathbf{y} | \Theta) \cdot p(\Theta) \quad (6)$$

- 5 where $p(\mathbf{y} | \Theta)$ is the likelihood and $p(\Theta)$ is the unconditional or ‘prior’ distribution of the parameter values. The proportionality follows in Eq. (6) because the probability of the data $p(\mathbf{y})$, otherwise known as the “evidence” for the model, is independent of the parameter values.

In general the likelihood can be expressed as an integral over probabilities conditioned on particular values of the model state and true state:

$$10 \quad p(\mathbf{y} | \Theta) = \int \int p(\mathbf{y} | \mathbf{x}^t, \Theta) \cdot p(\mathbf{x}^t | \mathbf{x}, \Theta) \cdot p(\mathbf{x} | \Theta) \, d\mathbf{x}^t \, d\mathbf{x} \quad (7)$$

where the conditional probabilities $p(\mathbf{y} | \mathbf{x}^t, \Theta)$, $p(\mathbf{x}^t | \mathbf{x}, \Theta)$, and $p(\mathbf{x} | \Theta)$ are specified by the chosen models for observational error (Eq. 3), kinematic model error (Eq. 2), and dynamical model error (Eq. 1) respectively. In practice we are unlikely to require such a complex expression for numerical evaluation; aggregation of error terms and redundancy between kinematic and dynamical model error usually allows simplifications.

- 15 The Bayesian approach encourages us to explicitly quantify our prior knowledge about the parameter values through the prior $p(\Theta)$. In marine ecosystem modelling, we are unlikely to ever consider cases of complete parameter ignorance, where a parameter value could possibly switch sign or get incredibly large. Every parameter is expected to have a value that falls into a credible range, otherwise the associated parameterisation would be difficult to defend. In some cases, when broad uniform or “uninformative” priors are assumed, it may not be necessary to specify exact limits of these distributions as the analyses may
20 become insensitive to these limits once the range becomes sufficiently broad. There are inherent difficulties with the concept of “ignorance” priors: for example, a flat prior distribution over ϕ will correspond to an informative prior for some function $g(\phi)$ (see Cox and Hinkley, 1974 for further discussion). In any case, trying to minimise the impact of prior distributions is rather defeating the object of Bayesian estimation, which explicitly aims to synthesise information from new data with prior information from previous analyses.

- 25 Once the likelihood is formulated and a prior distribution is prescribed, classical Bayes estimates (BEs) may be computed from posterior mean or posterior median values of Θ . Assuming the statistical assumptions are correct, these estimators will minimise the mean square error or mean absolute error respectively of the parameter estimate $\hat{\Theta}$ (e.g., Young and Smith, 2005). To obtain BEs can be computationally expensive, requiring sophisticated techniques to sample efficiently from the posterior distribution (e.g. by Markov Chain Monte Carlo, MCMC, methods). An alternative Bayesian estimator, very widely used in
30 geosciences, is the joint posterior mode or maximum a posteriori (MAP) estimator (e.g., Kasibhatla, 2000; Bocquet, 2014), given by maximising the posterior probability $p(\Theta | \mathbf{y})$ as a function of Θ . Such estimates are more computationally feasible in large problems where the search for the maximum of the posterior (or the minimisation of its negative logarithm) can be greatly accelerated by techniques such as the variational adjoint (Bennett, 2002).



In maximum likelihood (ML) estimation we seek the parameter values $\hat{\Theta}_{\text{ML}}$ that maximise the probability of the data given the parameter set, i.e. $p(\mathbf{y} | \Theta)$. When considered as a function of Θ , this probability is called the *likelihood* of the parameter values $L(\Theta | \mathbf{y})$ because it is strictly a probability of the data, not of the parameter values. Indeed, in ML estimation we do not need to consider the parameter values as random variables at all; rather they are considered as fixed, unknown constants.

5 For this reason the ‘|’s are sometimes replaced by ‘;’s to emphasise that, in a non-Bayesian context, the likelihood is not a conditional probability in the sense of one set of random variables dependent on another (e.g., Cox and Hinkley, 1974). In the ML approach, no prior information on the parameter values is used except possibly to define upper or lower plausible limits or allowed ranges for the parameter search (Young and Smith, 2005).

Historically, Bayesian methods (Bayes, 1763; S. and Price, 1763) predate ML methods of Fisher (1922) by some margin.

10 Fisher introduced ML methods partly to avoid problems in defining prior ignorance (see above) but also to avoid the non-invariance property of Bayesian estimators (Hald, 1999). This property means that given the BE of one parameter $\hat{\phi}_{\text{B}}$, the corresponding BE of a nonlinear function of that parameter $g(\phi)$ is not simply given by plugging in the estimate ($\hat{g}_{\text{B}} \neq g(\hat{\phi}_{\text{B}})$), while for ML estimates the invariance property does hold ($\hat{g}_{\text{ML}} = g(\hat{\phi}_{\text{ML}})$). We will see an example of this below.

In marine ecosystem modelling, much recent interest has focused on combined state and parameter estimation, whereby

15 model parameters Θ are estimated together with a true state \mathbf{x}^t (e.g., Simon and Bertino, 2012; Fiechter et al., 2013; Parslow et al., 2013; Weir et al., 2013; Dowd et al., 2014). In the Bayesian approach, model parameters and system state are both random variables. We can therefore apply Bayes’ Theorem to the composite random variable $\Psi = (\Theta, \mathbf{x}^t)$ and decompose the prior as $p(\Psi) = p(\mathbf{x}^t | \Theta) \cdot p(\Theta)$ to obtain an expression for the joint posterior:

$$p(\mathbf{x}^t, \Theta | \mathbf{y}) \propto p(\mathbf{y} | \mathbf{x}^t, \Theta) \cdot p(\mathbf{x}^t | \Theta) \cdot p(\Theta) \quad (8)$$

20 This equation has so far been applied to stochastic dynamic models with no kinematic model error (cf. Fiechter et al., 2013; Parslow et al., 2013). Equation (6) can be recovered from Eq. (8) by integrating (marginalising) both sides over \mathbf{x}^t .

Recent interest has also focused on "hierarchical" error models (Zhang and Arhonditsis, 2009; Parslow et al., 2013; Wikle et al., 2013). Here, the traditional model parameters are replaced with stochastic processes over time and/or space, and parameter identification focuses on the *hyperparameters* that describe the stochastic processes (e.g. means, variances, autocorrelation

25 parameters). This is essentially similar to the case of parameter estimation for a stochastic dynamical model (Eq. 1) and fits into the general formulation in Sect. (2.1) if we treat the stochastic parameters as additional state variables with dynamical model errors $\boldsymbol{\eta}$. The hyperparameters could in principle be estimated by ML, sometimes referred to as an "empirical Bayesian" approach (Cox and Hinkley, 1974), but it appears that computational tractability may favour the "hierarchical Bayesian" approaches (e.g., Parslow et al., 2013). Similar concerns apply to parameter estimation for stochastic dynamical models, where

30 fully Bayesian approaches appear to be favoured using computational strategies based on sequential Monte Carlo methods (van Leeuwen, 2009; Jones et al., 2010; Dowd, 2011; Doucet and Robert, 2013; Dowd et al., 2014).

Another important initiative is the estimation of kinematic model errors and their distributional parameters along with the ecosystem model parameters (Arhonditsis et al., 2008). Posterior distributions of kinematic model errors provide estimates of



the model discrepancy, introduced by Kennedy and O’Hagan (2001) and originally referred to as model inadequacy, and may thus provide useful diagnostics for assessing model bias and skill.

2.3 Likelihoods and priors as (misfit) cost functions

The choice of a suitable estimation method for marine ecosystem model parameters should be mainly based on the availability of relevant prior information, as well as on the basic error assumptions (Eqs. 1, 2, 3). Once the error model and estimation method have been chosen, we can derive the probability densities and cost functions that can be used for parameter estimation.

As a simple but common example, consider a deterministic model with no model error and data with additive Gaussian observational errors, Eq. (4), with known covariance matrix \mathbf{R} . We wish to use a total of N_y data, summing over all data types, to estimate N_Θ parameters by Bayesian estimation. A survey of the literature might lead us to model the prior distribution of Θ as Gaussian with a mean Θ^b and covariance matrix \mathbf{B} . From Eq. (6) the posterior density is proportional to a product of the likelihood and the prior density:

$$p(\Theta | \mathbf{y}) \propto \frac{1}{\sqrt{(2\pi)^{N_y} \det \mathbf{R}}} \cdot \exp \left[-\frac{1}{2} \mathbf{d}^T \mathbf{R}^{-1} \mathbf{d} \right] \cdot \frac{1}{\sqrt{(2\pi)^{N_\Theta} \det \mathbf{B}}} \cdot \exp \left[-\frac{1}{2} \Delta_\Theta^T \mathbf{B}^{-1} \Delta_\Theta \right] \quad (9)$$

where the data-model residual \mathbf{d} is defined by $\mathbf{d} = \mathbf{y} - H(\mathbf{x})$ (see ϵ in Eq. 4). The deviation from the prior is $\Delta_\Theta = \Theta - \Theta^b$. A MAP or joint posterior mode estimate of Θ can then be obtained by minimising the cost function $J(\Theta) = -2 \log p(\Theta | \mathbf{y}) + \text{constant}$, given by:

$$J(\Theta) = \mathbf{d}^T \mathbf{R}^{-1} \mathbf{d} + \Delta_\Theta^T \mathbf{B}^{-1} \Delta_\Theta \quad (10)$$

where constant terms (since independent of Θ) have been dropped.

Alternatively, nonnegativity constraints on the variables and parameters may lead us to prefer the lognormal observational error model. Likewise, we can assume lognormal priors for the parameters. In this case the posterior density becomes:

$$p(\Theta | \mathbf{y}) \propto \frac{1}{\sqrt{(2\pi)^{N_y} \det \mathbf{R}} \prod_j y_j} \cdot \exp \left[-\frac{1}{2} \mathbf{d}^T \mathbf{R}^{-1} \mathbf{d} \right] \cdot \frac{1}{\sqrt{(2\pi)^{N_\Theta} \det \mathbf{B}} \prod_l \Theta_l} \cdot \exp \left[-\frac{1}{2} \Delta_\Theta^T \mathbf{B}^{-1} \Delta_\Theta \right] \quad (11)$$

where the data-model residual here defined by $\mathbf{d} = \log(\mathbf{y}) - \log(H(\mathbf{x})) + \frac{\sigma^2}{2}$ and

$\Delta_\Theta = \log(\Theta) - \log(\Theta^b) + \frac{(\sigma^b)^2}{2}$. A MAP estimator of Θ is then obtained by minimising:

$$J(\Theta) = \mathbf{d}^T \mathbf{R}^{-1} \mathbf{d} + 2 \sum_{l=1}^{N_\Theta} \log(\Theta_l) + \Delta_\Theta^T \mathbf{B}^{-1} \Delta_\Theta \quad (12)$$

The MAP estimator of $\log(\Theta)$ is obtained by maximising $p(\log(\Theta) | \mathbf{y})$. It means that actually the cost function as given by Eq. (10) can be minimised, without the second term, $2 \sum_{l=1}^{N_\Theta} \log(\Theta_l)$, of Eq. (12).



Due to the noninvariance property of Bayesian estimates, the exponent of the MAP estimator of $\log(\Theta)$ will generally differ from the MAP estimator of Θ . By contrast, ML estimates are obtained by minimising the cost functions without any of the prior terms (second terms in Eq. 10, second and third terms in Eq. 12). In each case the same ML estimator for Θ is obtained whether we use Θ or $\log(\Theta)$, as expected from the invariance property of ML estimates.

5 We close this section with some cautionary remarks about different terminology that the reader may encounter the literature. First, many DA papers and textbooks start by assuming a certain cost function, based on variational or optimal control theory, rather than deriving it from a probabilistic treatment as herein (e.g., Le Dimet and Talagrand, 1986; Bennett, 2002; Fletcher, 2010). These studies tend to refer to MAP estimates obtained by minimising cost functions such as Eq. (10) as “weighted least squares estimates”. However, any analogy with regression analysis is stretched because these estimates are fundamentally
10 dependent on, and potentially biased by, the assumed prior distributions. Second, many DA papers and textbooks use the term “likelihood” to refer to the posterior probability $p(\Theta | \mathbf{y})$ in Eq. (6), and the term “maximum likelihood estimators” although modifiers such as “(Bayesian)” (Jazwinski, 2007) or “(posterior)” (Tarantola, 2005) are sometimes added. This obscures the fact that posterior mode estimators, like all BEs, are dependent on assumed prior distributions. Maximum likelihood avoids this dependence, but in doing so tends to be unsuitable for high-dimensional parameter estimation in the partially-observed
15 systems typically encountered in oceanography and geophysics.

3 Error models

Error models define our assumptions about uncertainties and the statistical relationships between observed data, the true state, model output, model inputs (forcings and initial/boundary conditions), and model parameters. Here we review error models that have been applied to address the various sources of uncertainty in marine ecosystem models and consider their implications
20 for parameter identification. An explicit treatment of each source of uncertainty may not be necessary by all means but we do recommend to reflect on how these uncertainties can be accounted for when modelling plankton dynamics and biogeochemical cycles.

3.1 Uncertainty in observations

The simplest and most common models for observational error assume that the observational errors ϵ are: i) additive normal, ii)
25 constant variance between samples, and iii) independent between samples and variable types. Such models are also commonly used to represent aggregated errors accounting for both observational and kinematic model error (see Sect. 2.1); we will refer to these as *residual* errors.

The additive normal assumption (i) is straightforward but also restricted, as it does not capture three common characteristics of some ecosystem data such as Chl_a concentrations: 1) larger values tend to have larger errors, 2) values cannot be negative,
30 and 3) the error distribution has positive skew. Characteristic (1) may be captured by scaling the standard error with modelled values (e.g., Hurtt and Armstrong, 1996) or with observed values (e.g., Harmon and Challenor, 1997), while characteristic (2) can be resolved using truncated error distributions (e.g., Hooten et al., 2011). All three characteristics together can be captured



by gamma distributions (Dowd, 2007) or power-normal distributions whereby normality is assumed on a power-transformed scale (Freeman and Modarres, 2006). The power-normal family includes log-normal (e.g., Hemmings et al., 2003) as well as square-root normal models (e.g., Fasham and Evans, 1995).

For power-normal, gamma, or proportional error assumptions we have the difficulty that the variance on the original scale approaches zero at low values. This may be unrealistic, at least in regard to instrumental noise. Only in normal models this problem can be easily addressed by adding a constant term to the variance (Schartau et al., 2001; Schartau and Oschlies, 2003) or standard deviation (Vallino, 2000). Another difficulty is that some transform-normal models become more complicated by additional unbiasing factors, needed when assuming unbiased errors on the original scale (e.g. $-\sigma^2/2$ for the log transform). More flexible models may be obtained by e.g. fitting the power transform parameter (Box and Cox, 1964; Wallhead et al., 2014), assuming generalised Gaussian distributions (Tarantola, 1987; Evans, 2003), or using ‘anamorphic’ transformations (Bertino et al., 2003; Simon and Bertino, 2012). It is yet unclear whether those distributions will yield better parameter estimates in typical applications, but it has been demonstrated that the choice of transformation can strongly affect estimates of plankton ecosystem fluxes (Evans, 2003).

The validity of the constant variance assumption (ii) may be improved by a scale transformation, although the transformation that best normalizes the error distribution (see above) is not necessarily the best for homogeneity of variance. Spatiotemporal variations in the error variance naturally occur, for example due to seasonal modulations of the unresolved variability and hence the representativeness error component. Accounting for this variation should improve parameter estimates and uncertainty assessment (cf., Hemmings and Challenor, 2012), but in applications this has rarely been attempted (Hemmings et al., 2003; Dowd, 2007).

In some contexts e.g. mesocosms, the error covariance matrix might be estimated from experimental replicates prior to fitting the model (Sect. 5.3.3). In many cases sampling is sparse and/or when the model error contribution is large, the error variances may not be estimable from data alone (Evans, 2003). Here the variances could instead be parameterised and estimated jointly with the ecosystem model by Bayesian or ML estimation, which has been done in few studies (Hurtt and Armstrong, 1996, 1999; Stock et al., 2005; Malve et al., 2007; Lignell et al., 2013).

The assumption of independent errors between samples and variable types (iii) can be invalidated in cases where contributions from representativeness error or kinematic model error are large, or where the data have been derived by interpolation or application of a regression model. Neglected correlation may result in less efficient (higher variance) parameter estimates, accompanied by distinctive correlations between the parameters’ optimised values. Pre-averaging the data is somewhat helpful to promote independence (and normality, via the Central Limit Theorem), but might also remove some of the informative variability in the data. One common intervention in the cost function is to scale the residual error variance with the sample size of each data type, which effectively prevents biasing of the fit in favour of better-sampled variables (e.g., Schartau and Oschlies, 2003; Friedrichs et al., 2007). It is better to elude such weighting between variances, since it might over-interpret scarce data along with a formal neglect of correlation (Evans, 2003). More formal treatments could fit parameterisations of correlations, either by assuming a flexible statistical model for the mean field or by fitting the parameters of covariance matrices jointly with the ecosystem model (e.g., Stock et al., 2005).



Whatever the assumptions of the observational/residual error model, it is possible to test their validity using the assimilated data, either by analysing the residuals and performing lack-of-fit tests (Bennett, 2002; Stock et al., 2005; Wallhead et al., 2014) or by comparing fit statistics with those obtained under alternative error models (using e.g. likelihood ratio tests, information theoretic or Bayesian criteria, as will be recalled in Sect. 6.2).

- 5 Finally, we caution that certain interpolated or derived data may strictly invalidate the observational error model, not only due to error correlation (see above), but also due to the introduction of *smoothing bias*. Data interpolated onto a model grid will tend to systematically underestimate true values where they are high and overestimate them where low; an effect that will be difficult to account for in the observational error model. In this situation parameter estimates can become bias towards values that suppress spatiotemporal variability in plankton dynamics. Similarly, if the data are derived from a regression model, 10 these estimates may also "trim the peaks and fill the valleys", because in a regression model (e.g. $y = a_0 + a_1p + \epsilon$, where p is some predictor data) there is always some part of the true variability that is included in the error term, and therefore subject to smoothing bias. In principle this could be avoided by including an inverted regression relationship in the operator O and assimilating the "raw" predictor or proxy data instead of the regression-based estimates.

3.2 Prior uncertainty in Θ

- 15 Prior uncertainty plays an important role in estimating model parameters. Typically, there is not enough information in the assimilated data to constrain all parameters of a biogeochemical model. The results may well be sensitive to the "error model of prior uncertainty". Prior uncertainty can be represented by prior probability densities in the Bayesian paradigm or plausible ranges in non-Bayesian paradigms. To account for nonnegativity constraints, prior distributions typically include lognormal (Parslow et al., 2013), square-root normal (Gunson et al., 1999), or beta distributions (Dowd and Meyer, 2003), although 20 normal distributions may yet be applicable for parameters that are well constrained above zero (Parslow et al., 2013). To our knowledge no application has yet incorporated prior correlations between parameters in Θ (i.e. off-diagonal terms in matrix \mathbf{B} introduced in Sect. 2.3). This is surprising, given the fact that posterior uncertainty assessments consistently reveal strong correlations (e.g., Matear, 1995; Prunet et al., 1996; Fennel et al., 2001; Faugeras et al., 2003; Kreuz and Schartau, 2015).

- Quantifying the prior uncertainty in Θ is often difficult due to: 1) the existing diversity of model structure, functional 25 forms used in the various parameterisations, and definitions of model state variables, and 2) the intrinsic variability between assimilated data sets in terms of taxonomic composition of the plankton community vs. (usually monospecific) laboratory cultures. As a result, it may not be advantageous to simply set the prior uncertainty in Θ_l as the posterior uncertainty from one previous study. A conservative but useful approach is to first gather best estimates of Θ_l from a series of previous studies that included parameterisations and state variable definitions sufficiently consistent with the present, and then treat these as 30 unbiased data from which a prior distribution or plausible range can be determined.

When posterior uncertainty becomes unacceptably high, it can be reduced by reducing the prior uncertainty in Θ , and there are several strategies for doing this. First, we should incorporate further data, perhaps of a qualitative nature, into the prior constraints. For example, if it is known *a priori* that certain species or functional groups coexist in certain regions at certain times of the year, then any Θ resulting in competitive exclusion of one of these groups might be ruled out *a priori*. Another



possibility within the Bayesian paradigm is to incorporate the subjective opinion of experts (O'Hagan, 2006). A second strategy is to model statistical structure in the prior parameter values, and thereby fill in missing prior parameter estimates for certain species included in the modelled species or groups. Examples here include the use of allometric scaling relationships with cell size (e.g., Edwards et al., 2012) and phylogenetic relationships derived from stochastic modelling of trait evolution (Bruggeman et al., 2009; Bruggeman, 2011). Third, we may seek to reduce the model complexity in terms of the number of free parameters, thereby removing poorly-constrained parameters and parameter correlations which may act to inflate the posterior uncertainty. This may be achieved using sensitivity analysis (e.g., Friedrichs, 2001; Garcia-Gorriz et al., 2003; Hemmings et al., 2003) or model selection criteria (e.g., Ward et al., 2013). A risk here is that parameter estimates and uncertainty assessment may be compromised if model selection uncertainty is not properly accounted for (Burnham and Anderson, 2002).

10 3.3 Uncertainty in initial conditions (ICs)

Dynamical marine ecosystem models are usually specified by differential equations that are first-order in time, and therefore require for solution one initial condition (IC) for each grid cell or spatial location in the model. These inputs are, in general, uncertain, and liable to impact the model output, at least during a transient relaxation period, or indefinitely if the uncertainty spans more than one basin of attraction of the dynamical system or if the model dynamics are chaotic (e.g., Huisman and Weissing, 1999).

In some cases it is possible to neglect IC error because of accurate measurements, or because a steady state (equilibrium or seasonal cycle) that is only sensitive to Θ can be assumed. One must only be careful about neglecting IC uncertainty although initial concentrations are known to be small (e.g. in January); small absolute errors may be large relative errors that can still affect e.g. timing and magnitude of a spring bloom as well as predator control (Evans and Parslow, 1985).

20 In other cases, IC uncertainty may not be negligible, and may strongly impact the estimation of ecosystem parameters. If jointly estimated, ICs may show strong correlations with the other parameter estimates (collinearities). For non-spatial (0D) models, ICs have often been estimated both as fixed parameters (e.g., Vallino, 2000) and as random variables (Bayesian parameters) with specified prior distributions (e.g., Arhonditsis et al., 2008). In mesocosm models, ICs can play an important role in determining the model trajectory and fit to data, and can comprise a large proportion of the fitted parameters (e.g., Lignell et al., 2013). In spatial models, due to the sparse and gappy nature of oceanic observations, IC uncertainty may require a Bayesian treatment centred on a prior estimate. For example, after a suitable transformation the true ICs might be described as: $\tilde{x}_0 = \tilde{x}_0^b + \delta$ where \tilde{x}_0^b is a vector prior estimate and δ is a vector of normal random errors with covariance structure (cf. Bennett, 2002). Joint estimations of (x_0, Θ) have rarely been performed for spatial models (Li et al., 2006; Smith et al., 2009; Pelc et al., 2012) likely due to the computational difficulties of optimising a potentially high-dimensional x_0 in combination with potentially strongly-nonlinear parameters Θ . Dimensional reduction techniques such as principal component analysis could likely help in this regard.



3.4 Uncertainty in forcings and boundary conditions (BCs)

Marine ecosystem models are usually modulated by time and space-dependent environmental drivers (forcings) and boundary conditions that are not predicted by the model dynamics but are necessary inputs to determine the evolution of the model state variables. Studies have demonstrated the sensitivity of biogeochemical variables to errors in bottom-up forcings such as wind stress and vertical mixing (e.g. Evans, 1988; Friedrichs et al., 2006; Béal et al., 2010; Sinha et al., 2010) and top-down forcings such as fishing (e.g., Heath, 2012). BC errors may have little impact, e.g. at sufficient distance from the boundaries, but might become critical when they directly influence e.g. nutrient supply to the model interior (Schartau et al., 2001) or affect the spread of low salinity water that promotes stratification (Ji et al., 2008).

In some parameter identification studies, time-averaging of forcings and assimilated data has been used as a simple way to reduce the impact of forcing errors associated with e.g. the passage of mesoscale eddies (Schartau and Oschlies, 2003; Hemmings et al., 2004). Very few studies have attempted to account for forcing or BC errors explicitly. In principle, these errors could be modelled as random variables and estimated jointly with Θ or marginalised over the likelihood. However, the combination of strong nonlinearity and high dimensionality in the unknowns make such an approach computationally practical only for low-dimensional models (e.g., Kavetski et al., 2006a, b; Arhonditsis et al., 2008) or through application of dimensional reduction and emulator methods (e.g., Leeds et al., 2014, see Sect. 8).

In larger ocean models, with multiple sources of BC/forcing error, it is more practical to treat the errors synthetically, for example using additive or multiplicative model errors (van Leeuwen, 2009, as described in Sect. (2.1). Dynamical model errors will arguably give a more realistic treatment, although the very simple models usually assumed for η (e.g. independent, homogeneous, and normal increments) might not be a very realistic description of the aggregate effects of BC/forcing error. Kinematic model errors are likely more computationally tractable, but this approach may require more complex error variance and correlation structure to maintain sufficient realism (Arhonditsis et al., 2008; Hemmings and Challenor, 2012).

In either case, simple additive or multiplicative models may fall short, in particular regarding potential errors in *phase*, like the timing of nutrient depletion. Model solutions that predict the right sequence of events (e.g. a plankton bloom) but with slightly wrong timing or spatial location, perhaps due to phase error in the atmospheric forcing or ocean circulation, may suffer a double penalty due to changes where none occur in the data and no change where the data do vary. Data assimilation may then "smooth out" the model variability in an attempt to minimise this double penalty (Wallhead et al., 2006; Ravela et al., 2007). The problem of phase/timing error has received substantial attention in numerical weather forecasting and geophysical data assimilation (e.g., Hoffman et al., 1995; Lawson and Hansen, 2005; Mittermaier, 2007; Ravela et al., 2007; Ziegeler et al., 2012) and has been highlighted as an issue for marine ecosystem models (Schartau and Oschlies, 2003; Friedrichs et al., 2006). A simple remedy is to average the data and model over larger spatio-temporal scales in the data assimilation (e.g., Schartau and Oschlies, 2003), but again this may remove informative variability and result in a $\hat{\Theta}$ that is only suited to those larger scales. Wallhead et al. (2006) explored a more explicit approach assuming random time lags between the true state and model state i.e. kinematic model errors in phase, which can be expressed as $\zeta(\theta_\zeta)$ in Eq. (2). Figure (1) demonstrates this approach using data simulated by an NPZ model with a combination of time lag error and independent, additive residual error in log



N, P, Z. Using a joint posterior mode approach to estimate time lags, ecosystem parameters, and residual / time lag variance parameters (see Appendix A), the time lags can be distinguished from the residual errors (Fig. 1b, c). This is associated with a general improvement in the bias and variance of ecosystem parameter estimates compared to a simpler approach assuming only additive residual error (Wallhead et al., 2006, Table A).

- 5 For some problems, in particular for chaotic systems, the phase noise may be too intense or ill-defined to allow effective use of a parametric phase lag model. A better approach here might be to use a ‘synthetic likelihood’ (Wood, 2010), whereby the raw data are replaced with a carefully chosen, informative set of phase-insensitive summary statistics (e.g. means, standard deviations, and lag correlations; cf., Heath, 2012). This approach could incorporate the comparison of modelled vs. observed Fourier spectra and cross-spectra/coherences (e.g., Powell et al., 2006). Whether the statistics e.g. of spectral slopes by them-
- 10 selves provide good constraint on ecological parameters should be tested since it may not be sufficient (Armi and Flament, 1985; Martin, 2003; Franks, 2005).

3.5 Uncertainty in model formulation and structure

Even with perfectly-known parameters, forcings and initial/boundary conditions, we would still not expect the modelled fluxes such as primary productivity and grazing to perfectly reproduce the true fluxes, or the state variables to perfectly follow the true variability. Aggregation of species into model functional groups, effects of finite spatial and temporal resolution, and inherent approximations in the flux parameterisations and model structure may all contribute to “structural error” in the model dynamics.

Structural errors are usually treated synthetically as either dynamical or kinematic model errors, and are often considered in combination with BC/forcing errors. There are difficulties because structural errors can impose persistent and intermittent biases in the model output that may not be amenable to a simple statistical description. For example, a succession in blooming phytoplankton species might extend or multiply the bloom periods in ways that cannot be accounted for by a single model functional group, however much its parameters are adjusted. Limited spatial resolution can also impose persistent biases that cannot be fully corrected by parameter adjustment, and may lead to poor extrapolation properties (Wallhead et al., 2013). In such cases, rather than elaborating the error models to account for structural error, effort might be better spent improving the explicit biological or spatial resolution of the model, or exploring implicit resolution techniques (e.g., Wirtz and Eckhardt, 1996; Merico et al., 2009; Wallhead et al., 2013).

A alternative approach is to employ the tools of multimodel inference (Burnham and Anderson, 2002; Link and Barker, 2006). The idea here is to base inference of target parameters, states and fluxes on a family of candidate models, each differing in structure and parameterisation, rather than on a single model. For example, we might be fairly certain about the form of the photosynthesis-irradiance (P-I) function in phytoplankton, but much less certain about the appropriate formulation of zooplankton grazing. Multimodel inference would allow the P-I parameter values and their uncertainties to be inferred on the basis of several candidate models, each assuming the same P-I function but different grazing parameterisations. The resulting multimodel estimates and uncertainties would be less likely to be biased by a poor choice of grazing formulation than the inference premised on a single *a priori* formulation.



4 Posterior parameter uncertainties

The determination of parameter uncertainties has many facets, getting to the core of discussions between Bayesian and frequentist approaches and interpretations (e.g., Efron, 1986; Cox, 2005; Lele and Dennis, 2009). In general, if we wish to make inference about uncertainties of parameter estimates ($\hat{\Theta}$) we need some knowledge about the distributional shape of the posterior in the broader neighbourhood region of its maximum $p(\hat{\Theta} | \mathbf{y})$. Likewise, we can gather information about the parameter-cost function manifold in the surrounding of $(\hat{\Theta}, J(\hat{\Theta}))$. For this we may consider some threshold offset value Δ_J , which is an upper limit for the deviation from the minimum value $J(\hat{\Theta})$. Such limit embeds all cost function values that are insignificantly larger than $J(\hat{\Theta})$. Large deviations from optimal estimates might be required for some parameters (components of $\hat{\Theta}$) before the corresponding cost function values reach this threshold, while for other components only small variations are enough. Such tolerance limit thus confines an uncertainty region in parameter space:

$$\left\{ \Theta : J(\Theta) - J(\hat{\Theta}) \leq \Delta_J \right\} \quad (13)$$

Typical threshold values are defined as the α quantile of a parametric or nonparametric probability distribution.

For an unbiased ML estimator the χ^2 -distribution with the degree of freedom ($df=N_y - N_\Theta$) has been suggested for deriving a threshold value $\chi^2(df, \alpha)$ (e.g., Kuczera, 1990; Meeker and Escobar, 1995; Raue et al., 2009, 2011). But for nonlinear models the χ^2 -distribution might be inappropriate and the α quantile of the actual distribution, $J(\Theta) - J(\hat{\Theta})$, needs to be evaluated by other means (e.g., Raue et al., 2011). Furthermore, the degree of freedom (df) that specifies location and shape of the χ^2 -distribution may not be representative. The effective number of independent observations can be lower than N_y , in particular during the development of an algal bloom, for example when typical measurements like Chl a and nutrient concentrations become negatively correlated. We therefore expect the effective degree of freedom to be lower than $(N_y - N_\Theta)$ and $\chi^2(df, \alpha)$ would therefore be an optimistic threshold, i.e. likely to underestimate the true range of uncertainty, unless the correct number of degree of freedom is determined.

4.1 Confidence and credible regions

Depending on the estimator, uncertainties in the combination of parameter values may either disclose a credible region of a random distribution of parameter values (Bayesian interpretation) or they mark a confidence region in which other estimates ($\hat{\Theta}^*$) can be expected, e.g. when using other data from a repeated experiment (frequentist interpretation). For maximisations of the likelihood $p(\mathbf{y} | \Theta)$ it is often stated that credible and confidence regions are practically identical. Such interpretation is imprecise since the methods to confine either regions can be very different with respect to the underlying assumptions, e.g. MCMC versus bootstrap approaches.

In case of classical BEs no credibility limit Δ_J is explicitly prescribed. Instead, an efficient sampling of $(\Theta, J(\Theta))$, or of the posterior $p(\Theta | \mathbf{y})$, is applied and credible regions are inferred from selective (acceptance/rejection) sampling schemes in a MCMC approach, e.g. Metropolis-Hastings algorithm (Metropolis et al., 1953; Hastings, 1970). The prominence of MCMC methods for data assimilation is described by Rayner et al. (submitted). MCMC methods for the derivation of credible regions



are also used for ML estimation problems (e.g., Smith and Yamanaka, 2007a). The main point is that here the data are assumed fixed. The credible regions can be interpreted to reflect a system-inherent random parameter distribution, which is a plausible interpretation when thinking of a mixed plankton community.

A fundamentally different approach to the MCMC method is to repeat parameter optimisations many times but with data subsamples or resample data sets. Large data sets can be split up into a series of subsamples that should be as independent as possible. Or many synthetic data sets are created by applying a random number generator to independently draw bootstrap samples (Efron, 1985; Efron and Tibshirani, 1986). This approach accounts for variable data and it mimics a repetition of an experiment or a repeated sampling at ocean sites. For each bootstrap data set (\mathbf{y}^*) a corresponding optimum estimate $\hat{\Theta}^*$ is obtained. A distribution of $\Delta_{\Theta} = \bar{\Theta}^* - \hat{\Theta}^*$ can be derived from a series of optimisations with different bootstrap data sets. Furthermore, nonparametric density estimates of all $J(\hat{\Theta}^*)$ can be derived and the α quantile can then be determined from the cumulative distribution of such probability density. For some situations a bootstrap approach with as few as ten resample data sets may suffice to accentuate specific uncertainties in some model parameters (e.g., Schartau et al., 2007). But to ascertain confidence regions, much larger bootstrap sample sizes are typically needed (Efron and Tibshirani, 1986).

In practice the margins of the multivariate confidence or credible regions are projected onto each component (l) of Θ so that we obtain uncertainty limits (error margins) for every parameter (uncertainty intervals, $[\hat{\Theta}_l - \mathbf{u}_l^-, \hat{\Theta}_l + \mathbf{u}_l^+]$), with lower and upper uncertainty limits possibly being different ($\mathbf{u}_l^- \neq \mathbf{u}_l^+$). To resolve these margins, both approaches, MCMC and bootstrap methods, require a large number of model evaluations, typically $o(10^2)$ - $o(10^4)$. The benefit is that skewed and contorted posteriors can be better resolved. However, because of the computational costs we often find studies where parameter uncertainties of ecosystem models had been approximated point-wise in the immediate vicinity of $\hat{\Theta}$.

4.2 Point-wise approximations of posterior uncertainty covariance matrix

A single point in parameter space is identified by ML and MAP estimators, i.e. $\hat{\Theta}$ where the posterior $p(\Theta | \mathbf{y})$ has its maximum. A common theory for deriving variance information of a ML estimate is based on the inverse of the Fisher information (Fisher, 1922), see also (e.g., Fisher, 1934; Efron and Hinkley, 1978; Cao and Spall, 2010). The underlying assumption is that the posterior $p(\hat{\Theta} | \mathbf{y})$ is nearly normal shaped nearby its maximum, which is tantamount to a quadratic increase of $J(\Theta)$ as parameter values are varied around the estimate. Series expansions, like Taylor power series, around the estimate $\hat{\Theta}$ can be applied to derive relevant properties of $J(\Theta)$ that are theoretically attributed to an uncertainty covariance matrix (\mathbf{U}_{Θ}). Confidence regions for $\hat{\Theta}$ can then be expressed in terms of approximations of \mathbf{U}_{Θ} . For example, for some prescribed df an upper critical confidence levels can be specified by the α quantile of a F-distribution (Marsili-Libelli et al., 2003):

$$\left\{ \Theta : \left(\Theta - \hat{\Theta} \right)^T \mathbf{U}_{\Theta}^{-1} \left(\Theta - \hat{\Theta} \right) \leq N_{\Theta} \cdot F_{df}^{1-\alpha} \right\} \quad (14)$$

Confidence ellipsoids are described with Eq. (14), thus yielding symmetric uncertainty limits around $\hat{\Theta}$, i.e. $\mathbf{u}_l = \mathbf{u}_l^- = \mathbf{u}_l^+$. With an approximation of \mathbf{U}_{Θ} a confidence interval for every single parameter can be described as $[\hat{\Theta}_l \pm \mathbf{u}_l]$. The individual uncertainty limits can be computed as

$$\mathbf{u}_l = t_{df}^{1-\alpha/2} \sqrt{\mathbf{U}_{\Theta_{ll}}}. \quad (15)$$



where $t_{df}^{1-\alpha/2}$ is the two-tails Student's t-distribution for prescribed α and df (Marsili-Libelli et al., 2003). Two approaches to point-wise approximations of \mathbf{U}_Θ are found in ecological and ecosystem modelling studies. One approach uses first derivatives of the model's observation vector with respect to the parameters (Jacobian) whereas the other requires calculations of second derivatives of $J(\Theta)$ (Hessian).

5 4.2.1 Uncertainty covariances based on the Jacobian matrix

A first approach considers a linearisation (first order power expansion) of the model's observation vector $H(\mathbf{x})$ around the point estimate $\hat{\Theta}$. As long as $H(\mathbf{x}(\hat{\Theta}))$ is not subject to strong nonlinearities, its first derivatives (sensitivity) with respect to Θ can be used to estimate \mathbf{U}_Θ . For an unbiased ML estimator the covariance matrix can be approximated as:

$$\mathbf{U}_\Theta = \frac{J(\Theta)}{df} \cdot \left(\mathbf{H}_\Theta^T \mathbf{R}^{-1} \mathbf{H}_\Theta \right)^{-1} \quad (16)$$

10 with the Jacobian matrix $\mathbf{H}_\Theta(\hat{\Theta})$ and with the observational error covariance matrix \mathbf{R} (e.g., Thacker, 1989; Kuczera, 1990; Omlin and Reichert, 1999; Brun et al., 2001; Omlin et al., 2001). The term $J(\Theta)/df$ is added as an approximation of the residual variance of J , which should be considered unless $H(\mathbf{x})$ is in such good agreement with data so that the minimum of $J(\Theta)$ actually matches the exact degree of freedom, df. The rows of the Jacobian \mathbf{H}_Θ are the first derivatives with respect to the parameters $\nabla H(\mathbf{x})$, with $\nabla = (\partial/\partial\Theta_1, \partial/\partial\Theta_2, \dots, \partial/\partial\Theta_{N_\Theta})$ being the Napla operator of first partial derivatives.

15 4.2.2 Uncertainty covariances based on the Hessian matrix

Another more common approach for a point-wise approximation of \mathbf{U}_Θ is derived from a Taylor expansion around $J(\hat{\Theta})$. Since $\nabla J(\hat{\Theta}) \approx 0$ in the minimum, the first order term of the Taylor expansion is negligible. The series expansion then approximates the distribution:

$$J(\Theta) - J(\hat{\Theta}) \approx \frac{1}{2} \left(\Theta - \hat{\Theta} \right)^T \mathcal{H}_\Theta \left(\Theta - \hat{\Theta} \right) \quad (17)$$

20 The matrix \mathcal{H}_Θ is the Hessian whose elements are second derivatives of $J(\Theta)$ with respect to the parameters:

$$\mathcal{H}_\Theta = \nabla^T \nabla J(\Theta) \Big|_{\Theta=\hat{\Theta}} \quad (18)$$

With the Taylor expansion in Eq. (17) we obtain an approximation of the local curvature of $J(\Theta)$ at point $\hat{\Theta}$, also referred to as the *observed* Fisher information. Like in Eq. (16), but instead of using first derivatives of $H(\mathbf{x})$, a posterior uncertainty covariance of $\hat{\Theta}$ is then approximated by computing the inverse of a Hessian matrix:

$$25 \quad \mathbf{U}_\Theta = \frac{J(\Theta)}{df} \cdot 2 \cdot \mathcal{H}_\Theta^{-1} \quad (19)$$

Both approximations (Eqs. 16 and 19) yield, in principle, similar results for accurate ML estimates i.e. when the actual minimum of $J(\Theta)$ has been identified by the optimisation algorithm. In practice search algorithms can terminate at some distance from the actual minimum for numerical reasons, e.g. when the minimum is located in a flat valley of J and the imposed convergence criterion makes an algorithm terminate the search in the periphery of the valley. Marsili-Libelli et al. (2003) proposed



an approach where the accuracy of parameter estimates can be improved by minimising differences between the results of Eq. (16) and Eq. (19).

4.2.3 The Hessian: its approximation and inversion

Hessian matrices have often been approximated with a finite central differences approach for first and second derivatives of J with respect to ecosystem model parameters at the point-estimate $\hat{\Theta}$ (e.g., Matear, 1995; Kidston et al., 2011; Kreuz and Schartau, 2015). A critical issue of finite difference calculations of the Hessian's elements is the choice of an appropriate increment size (δ), which sets the distance of departure from the optimal parameter point estimate $\hat{\Theta}$. Sometimes a compromise between resolving flat regions around $(\hat{\Theta} + \delta, J(\hat{\Theta} + \delta))$ and numerical precision has to be found (Kreuz and Schartau, 2015). To approach a high accuracy of the Hessian approximation it is possible to consider a set of different increment sizes for the central differences approach, as given in Marsili-Libelli et al. (2003).

The problem of increment size reduces if first derivatives of J with respect to the parameters (gradient, ∇J) are readily obtained with an adjoint model, as used in a variational data assimilation approach. Adjoint versions of plankton ecosystem models have been constructed primarily to compute ∇J for an efficient search with gradient descent algorithms in the parameter-cost function manifold (e.g., Lawson et al., 1996; Fennel et al., 2001; Schartau et al., 2001; Spitz et al., 2001; Friedrichs, 2002; Faugeras et al., 2003; Zhao et al., 2005; Friedrichs et al., 2007; Xiao and Friedrichs, 2014a). To elucidate the nature of adjoint model developments is beyond the scope of this paper, but a brief summary about adjoint model developments is given in the Appendix (C). The advantage is that all elements of the Hessian can be approximated with finite differences of adjoint model results (e.g., Fennel et al., 2001; Friedrichs, 2002; Faugeras et al., 2003; Friedrichs et al., 2007).

Computations of the Hessian, Eq. (18), provide valuable identifiability information even if this matrix is not explicitly used to specify confidence regions of parameter estimates. For example, a decomposition of the Hessian matrix into its eigenvalues and the corresponding eigenvectors reveals which parameters are hardly constrained by the data or it helps to identify structural deficiencies of a model. The eigenvectors' components (l) represent the components of Θ . Components of those eigenvectors that belong to small eigenvalues indicate parameter combinations that are poorly constrained or cannot be estimated. In contrast, those eigenvectors that correspond with the largest eigenvalues show parameter combinations that are well constrained. The studies of Fennel et al. (2001) and Faugeras et al. (2003) are informative in this respect, because they provide insight into the range of characteristic eigenvalues and eigenvectors of 0D and 1D marine ecosystem models.

Ideally, every eigenvector would exhibit only one single component, meaning that values of every parameter can be estimated independently of the other parameters' values. In practice this is only the case for few parameters of a planktonic ecosystem model. Eigenvectors with two or more distinct components discloses those parameters whose estimated values are correlated and for which correlation coefficients can be explicitly derived (e.g., Matear, 1995; Prunet et al., 1996). Correlations between parameter estimates are referred to as collinearities. A useful collinearity index was introduced by Brun et al. (2001). Their index expresses how a change in J (or in $H(\mathbf{x})$), due to a shift in the value of one parameter can be entirely compensated by adjusting the value of another (correlated) parameter.



In general, results from an eigenvalue decomposition of the Hessian can expose parameters whose values cannot be constrained with the available data and should not enter the optimisation procedure. Doing so can improve the estimation of the other parameters' values. Often the ratio of a Hessian's largest to smallest eigenvalues is calculated. This ratio is called condition number and it indicates whether the Hessian is well-conditioned and can be inverted. High condition numbers are indicative for an ill-posed inverse problem and a point-wise parameter posterior uncertainty covariance matrix may then not be determinable from an inversion of the Hessian. The topic is complex and, in spite of a high condition number, it might still be possible to consider the generalized inverse and generalized Cholesky decomposition of \mathcal{H}_Θ (e.g., Gill and King, 2003). Whether such numerically feasible inversions still provide valuable information about parameter covariances is difficult to tell. For example, Kreuz and Schartau (2015) used eigenvalue decomposition of the Hessian to identify parameters that have different effects on annual carbon, nitrogen and phosphorus budget calculations. In their twin experiment they found the eigenvectors of the lowest three to six eigenvalues (out of 36) to vary considerably after repeating the analysis several times with noise added to model results. In their case a condition number was not considered for their analysis, since it did not provide unambiguous information about the quality of the Hessian and its inverse.

4.3 Parameter screening and profile likelihoods

It is common to face ill-posed inverse problems in plankton ecosystem modelling, which sometimes can be discouraging, in particular if we had initially hoped to estimate all parameters. The screening for important parameters straightens what to expect from a parameter optimisation; it can be interpreted as a preparatory and integral part of any parameter identifiability analysis (Brun et al., 2002). Likewise, parameter sensitivity analyses in form of twin experiments (e.g., Lawson et al., 1996; Spitz et al., 1998; Faugeras et al., 2003; Kreuz and Schartau, 2015) are useful in setting up well-posed parameter optimisation problems that also allow for the point-wise derivation of uncertainty covariances from matrix inversions in Eq. (16) or Eq. (19).

An alternative to a point-wise determination of posterior uncertainties (confidence regions) is the construction of 1D- or 2D profile likelihoods (Venzon and Moolgavkar, 1988). For a 2D profile likelihood an array of combinations of two parameters (Θ_m, Θ_n) is constructed. For every combination of parameter values (elements of the 2D array) a minimisation of $J(\Theta)$ is repeated while varying all other parameters $(\Theta_{l \neq m, n})$. This is done for all arrays with possible combinations of two parameters, which requires a large number of additional optimisations. Parameter identifiability analyses based on profile likelihoods have been applied to problems where fast evaluations of $J(\Theta)$ were possible (e.g., Brun et al., 2001; Raue et al., 2009, 2011). Brun et al. (2001) evaluated confidence regions for three parameters (rate constants of production, respiration and water-air gas exchange) from profile likelihoods and they showed that the error margins of the parameter estimates can be much larger than derived with a point-wise approach. Unfortunately, the evaluation of a profile likelihood is impracticable for most marine ecosystem model applications, because of the associated computational costs.



5 Typical parameterisations of plankton models and their parameters

Depending on the available data and on the error model imposed, we may end up with some parameter values that compensate errors in the dynamical model. The methods described above can only point towards a deficiency in model structure, forcing, or in boundary conditions. With respect to model structure, parameter estimates of different models may differ even if calibrated with identical data and although having the same physical (environmental) setup. For a comparison of optimal parameter values of different models it is meaningful to compare uncertainty ranges and collinearities. But this may only partially explain why parameter estimates could be different and it is certainly helpful to unravel and understand some of the differences between major parameterisations that e.g. describe growth and loss of phytoplankton.

5.1 Differences between maximum carbon fixation and maximum growth rate

- 10 A crucial element of most plankton ecosystem models is the description of phytoplankton growth as a function of light and nutrient availability. How growth of algae is parameterised is relevant and the associated parameter values usually determine model solutions of bloom development. The build up of phytoplankton biomass depends on how much of the available nutrients can be utilised and how much energy can be absorbed from sun light. Under conditions of nutrient repletion and light saturation the carbon fixation (gross primary production, GPP) reaches a maximum rate, described as a parameter (P_m^C) with unit d^{-1} .
- 15 For models that do not resolve mass flux of carbon explicitly, P_m^C is substituted by a maximum growth rate (μ_m) to express the phytoplankton's maximum assimilation rate of nitrogen (N), or of phosphorus (P). The maximum GPP and the maximum growth rate are interrelated and in principle one can be derived from the other (Smith, 1980). In reality, maximum C-fixation, maximum N- or P-assimilation, and cell doubling rates are highly variable and it requires at least cellular C, N and Chl a to be explicitly resolved, thereby linking e.g. intracellular nutrient allocation to photoacclimation (e.g., Shuter, 1979; Laws et al.,
- 20 1983; Pahlow, 2005; Armstrong, 2006).

In practice an analogy between P_m^C and μ_m is often assumed in N- or P- based biogeochemical models (assuming fixed stoichiometric elemental C:N:P ratios for algal growth). The parameter P_m^C or μ_m is typically multiplied with a dimensionless temperature function (f_T) (e.g., Arrhenius, 1889; Eppley, 1972), allowing for temperature induced changes of metabolic rates. The actual potential maximum rate ($P_m^C \cdot f_T$ or $\mu_m \cdot f_T$) is then reached at some prefixed reference or optimum temperature accordingly. In early N-based plankton modelling studies (e.g., Evans and Parslow, 1985; Fasham et al., 1990; Doney et al., 1996) the maximum growth rate was mainly adopted from Eppley (1972). In subsequent DA studies this maximum rate was either subject to optimisation (e.g., Fasham and Evans, 1995; Spitz et al., 2001) or it was kept fixed because then parameter values of the limitation functions could be better identified (Matear, 1995; Fennel et al., 2001).

5.2 Light- and nutrient limitation

- 30 In many marine ecosystem models two separate limitation functions are combined: one that expresses the P-I curve and another that describes the dependence between ambient nutrient concentrations and nutrient uptake. The two functions are similar in their characteristics, starting from zero (no light or no nutrients) and approaching saturation at some high light and at



replete nutrient concentration. Three approaches are generally found in marine ecosystem models to limit algal growth by photosynthesis and nutrient uptake. The first is to apply Blackman's law (Blackman, 1905), assuming that growth is reduced by the most limiting factor, either by light or by nutrient availability (e.g., Hurtt and Armstrong, 1996; Oschlies and Garçon, 1999; Klausmeier and Litchman, 2001). The second is to multiply both limitation functions (e.g., Evans and Parslow, 1985; 5 Fasham et al., 1990). The third approach leads to more complex representations of growth limitation, as they account for interrelations between cellular C:N (or N:C) ratio, N-uptake and the photoacclimation state of the algae (e.g., Geider et al., 1998; Pahlow, 2005; Armstrong, 2006; Wirtz and Pahlow, 2010). Whether the first, second or third approach is considered can be expected to affect estimates of the associated parameter values.

5.2.1 Photosynthesis as a function of light (P-I curve)

10 In a P-I curve the level of increase from low to high irradiance is specified by the (initial) slope parameter also referred to as photosynthetic efficiency (α_{phot}) (Smith, 1936; Jassby and Platt, 1976; Cullen et al., 1992; Baumert, 1996). Photosynthetic efficiencies were derived from P-I measurements by Platt and Jassby (1976), Peterson et al. (1987), and Platt et al. (1992) and their mean values were used for many N-based models (e.g., Fasham et al., 1990; Sarmiento et al., 1993; Doney et al., 1996; Oschlies and Garçon, 1999). Published measurements of α_{phot} were typically normalised to Chl*a* concentrations. In case of 15 N- or P-based models careful considerations are then needed with respect to the phytoplankton's cellular Chl*a* content, which can vary by a factor of ten and more. Values of α_{phot} were found to vary by a factor of three (Côté and Platt, 1983) during a three month period, which can be attributed to changes in phytoplankton community structure as well as to photoacclimation. Platt and Jassby (1976) reported an even larger variational range over a one year period, from $\alpha_{\text{phot}} = 0.03$ to $0.63 \text{ mg C (mg Chl}a)^{-1} \text{ h}^{-1} \text{ W}^{-1} \text{ m}^2$ within the upper ten meters.

20 5.2.2 Nutrient uptake by algae

Typical nutrient limitation parameterisations are either expressed with the half-saturation constant (K_s) of a classical Monod equation (Monod, 1942, 2012) or described with nutrient affinity (α_{aff}) (Aksnes and Egge, 1991). Both parameters can be interpreted as being interrelated $\alpha_{\text{aff}} = \mu_m \cdot f_T / K_s$. However, α_{aff} is derived from mechanistic considerations that are fundamentally different from former interpretations of K_s of a Monod equation (Pahlow, 2005; Armstrong, 2008; Pahlow and 25 Oschlies, 2013; Fiksen et al., 2013). The description of nutrient limited growth with the Monod equation, thereby retrieving values for K_s from measurements, had been discussed in the past (e.g., Eppley et al., 1969; Falkowski, 1975; Droop, 1983). This discussion regained importance and the sole application of the Monod equation is currently viewed as a considerable drawback when simulating plankton growth (Flynn, 2003; Smith et al., 2009; Franks, 2009; Smith et al., 2014, 2015).

5.2.3 Algal growth and intracellular acclimation

30 More complex interdependencies between light and nutrient limitation are resolved by models that account for intracellular acclimation dynamics (e.g., Geider et al., 1998; Pahlow, 2005; Armstrong, 2008; Wirtz and Pahlow, 2010). In these models



growth rates become dependent on cell quota, e.g. usually normalised to carbon biomass (N:C), and the amount of synthesized Chl*a* per cell. These approaches involve physiological parameters that are related but not identical to those of classical N- or P-based growth models, which impedes a direct comparison of older estimates of growth parameters with values currently used in models with acclimation processes resolved.

5 Parameter values of acclimation models have typically been tuned to explain laboratory measurements (Geider et al., 1998; Flynn et al., 2001; Pahlow, 2005; Armstrong, 2006; Smith and Yamanaka, 2007a; Pahlow and Oschlies, 2009; Wirtz and Pahlow, 2010). So far, there is a limited number of experimental studies whose data were used to calibrate these acclimation models (Laws and Bannister, 1980; Terry et al., 1983, 1985; Healey, 1985; Flynn et al., 1994; Anning et al., 2000). Model calibrations were usually done by adjusting parameter values so that model solutions provide a qualitative good fit to the laboratory data. In many cases the parameter adjustments relied on the researchers' experience and intuition, sometimes accounting for prior parameter values obtained from preceding model analyses (e.g., Flynn et al., 2001). Analyses of parameter uncertainties of recent acclimation models are usually lacking. Most laboratory modelling studies had put emphasis on the physiological mechanistic model behaviour while error assumptions for quantitative data-model comparison were hardly considered.

Explicit error assumptions for parameter optimisations and for comparisons of acclimation model results with laboratory data were introduced by Armstrong (2006) and by Smith and Yamanaka (2007a). In both studies additive uncorrelated Gaussian observational errors were assumed and optimised model output of different model versions had been compared. Armstrong (2006) applied a "simulated annealing" algorithm (Metropolis et al., 1953) to fit his optimality-based model version to the data of Laws and Bannister (1980). The same data were used to also fit the model of Geider et al. (1998) and he evaluated the likelihood ratio of the two ML estimates, to discuss and underpin the improved performance of his refined acclimation parameterisations. Smith and Yamanaka (2007a) also compared the performance of two acclimation models, of Geider et al. (1998) and Pahlow (2005) respectively. Optimal parameter values for the two model versions were obtained with the MCMC method, minimising the misfit between model results and data of the Flynn et al. (1994) experiment. Apart from mechanistic considerations, Smith and Yamanaka (2007a) concluded that the models of Pahlow (2005) and Geider et al. (1998) were describing the assimilated data equally well, since both cost function minimum values were comparable. However, the simulated N:C and Chl*a*:N ratios of the model proposed by Pahlow (2005) were in much better agreement with observations during the exponential growth phase, which remained undifferentiated by their imposed error model.

Field data from three ocean sites in the North Atlantic were used by Pahlow et al. (2008) for calibrating their plankton model with intracellular acclimation dynamics. They conducted a two-step approach for parameter optimisation. First they optimised parameter values so that depths and dates of minimum and maximum observed values become well represented by their model at all three sites. In a second step they refined their parameter estimates by minimising weighted data-model residuals. Their optimised parameters of photo-acclimation and maximum C-fixation (α_{phot} , F_m^C) turned out to agree with those values derived from model calibrations with laboratory data. Besides the acclimation aspect they also addressed the difficulty in parameterising phytoplankton biomass losses due to grazing along with other losses like the algal release of organic matter.



5.3 Phytoplankton losses

Parameterisations of phytoplankton losses involve cell lysis, the aggregation of cells together with all other suspended matter, and grazing by zooplankton. Cell lysis, excretion and leakage are usually expressed as a single rate parameter and the mass loss is assumed to be proportional to the phytoplankton biomass. The principle theory of coagulation to describe the aggregation of phytoplankton and of detritus is well established but the representativeness of the parameterisations (simplifications) assumed for model simulations remains an open task (e.g., Burd and Jackson, 2009). Aggregation parameters in marine ecosystem models are often assumed to represent the combination of a collision rate and the probability of two particles (e.g. cells) sticking together after collision. One problem is to find constraints that allow for a clear distinction between phytoplankton losses due to the export of aggregated cells and the loss because of grazing. Both processes can be responsible for the drawdown of phytoplankton biomass, and data that cover the onset, peak and decline of a bloom are needed for a possible distinction.

5.3.1 Loss rates of algae due to complex grazing dynamics

How the complex nature of predator-prey interaction is parameterised remains a critical element of plankton ecosystem models. Compared to the approaches that describe algal growth an even larger number of different parameterisations exist for grazing (Gentleman et al., 2003). Experimental data of grazing rates and collections of field data of zooplankton abundance are therefore of great value.

Elaborate analyses of meso- and microzooplankton biomass, grazing and mortality rates were done by Buitenhuis et al. (2006, 2010). For their two studies they compiled an extensive database with laboratory and field measurements. With their data syntheses they could derive parameter values for simulations with a global ocean biogeochemical model. Furthermore, independent field data, not used to derive the meso- and microzooplankton parameter values, were considered for assessing the performance of their model on global scale. Their work reflects the large effort that can be dedicated to this topic for achieving reliable simulation results of zooplankton grazing.

The explicit distinction between zooplankton size classes, like meso- and microzooplankton, was bypassed in Pahlow et al. (2008). Their model allows for omnivory within a the zooplankton community, which is resolved by introducing adaptive food preferences. These preferences are treated as trait (property) state variables that adapt to the relative availability of different prey. This reduces the number of parameters needed to describe a variety of different behaviour in grazing responses. After parameter optimisation they identified distinctive complex patterns between zooplankton grazing and plankton composition for the three simulated ocean sites.

5.3.2 Mesocosm data of onset, peak and decline of natural phytoplankton bloom

To collect diverse data that fully resolve build up and decay of an algal bloom at ocean sites is difficult to achieve. Data derived from remote sensing, e.g. *Chl a* concentration and primary production rates, provide limited information to explain relevant differences between processes described before, like N-utilisation, fixation and release of C, and synthesis and degradation of *Chl a*. Mesocosm experiments that enclose a large volume of a natural plankton and microbial community can be helpful in



this respect, if they provide a good temporal resolution of the exponential growth phase as well as of the post-bloom period. Vallino (2000) highlighted the advantage of using mesocosm data to test plankton ecosystem models, as done before by Baretta-Bekker et al. (1994, 1998). Drawbacks are uncertainties in initial conditions and also the representativeness of mesocosm data to reflect the real dynamics in the ocean is subject to discussion (e.g., Watts and Bigg, 2001). In spite of these limitations, simulations of mesocosms or of enclosures experiments (e.g. with large carboys deployed in the field) have helped to assess model performance. This is particularly true for tracing microbial dynamics (Van den Meersche et al., 2004; Lignell et al., 2013) or for details in the composition and fate of particulate organic carbon and nitrogen (POC and PON) (Schartau et al., 2007; Joassin et al., 2011).

5.3.3 Estimating phytoplankton loss parameters: a mesocosm example

In the following example we will illustrate typical uncertainties in the estimation of phytoplankton loss parameters in the absence of explicit zooplankton observations like micro- and mesozooplankton abundance or grazing rates. Three parameters that affect the loss of phytoplankton biomass have been optimised together with other parameters. For this we assimilated five different types of daily observations (dimension of \mathbf{y} is $N_y = 5$) over a period of $N_t = 23$ days from a mesocosm study into a plankton ecosystem model. The model resolves fluxes of C and N through phytoplankton, zooplankton, detritus and dissolved organic matter, with a total of twelve state variables ($N_x = 12$). The model includes optimal nutrient allocation and photo-acclimation described before, following Pahlow (2005). As an error model we assume additive Gaussian errors applying Eq. (4) in Sect. (2.1.3). Details of the corresponding mapping from model results \mathbf{x} to observations $H(\mathbf{x})$ are given in the Appendix (B).

In our example we consider two cost functions, with and without covariances respectively. We disregard any prior information and we assume mesocosms to be homogeneously mixed. Equation (10) in Sect. (2.3) then reduces to:

$$J(\Theta) = \sum_{i=1}^{N_t} (\mathbf{y}_i - H_i(\mathbf{x}))^T \mathbf{R}_i^{-1} (\mathbf{y}_i - H_i(\mathbf{x})) \quad (20)$$

The standard errors (σ_i) represent the observed variability between the nine mesocosms, based on daily measurements. Residual error covariance matrices can thus derived for every sampling day: $\mathbf{R}_i = \mathbf{S}_i \mathbf{C}_{(y)} \mathbf{S}_i^T$. The matrices \mathbf{S}_i include diagonal elements with σ_i at date t_i , while off-diagonal elements are zero. The elements of matrix $\mathbf{C}_{(y)}$ represent correlations between the different types of observations, which were determined for two time intervals: exponential growth and post-bloom period (see Appendix B). The distinction between periods of bloom buildup and post-bloom becomes relevant if C and N (or P) data are assimilated. Correlations can switch sign and thus the sign of the data-model residual $\mathbf{d}_i = \mathbf{y}_i - H_i(\mathbf{x})$ matters. For example, PON and dissolved inorganic carbon (DIC) are strongly negatively correlated during the exponential growth phase. During the post-bloom period DIC may still decrease at times when PON concentration declines as well, which yields a weak but positive correlation.



For our second cost function we assume all data to be independent (i.e. all off-diagonals of $C_{(y)}$ are zero) and Eq. (20) can be further simplified to a sum over all individual vector components (indexed with j):

$$J(\Theta) = \sum_{i=1}^{N_t} \sum_{j=1}^{N_y} \frac{(y_{ij} - H_{ij}(\mathbf{x}))^2}{\sigma_{ij}^2} \quad (21)$$

Figure (2) shows contours of $J(\hat{\Theta}_m \pm \Delta_m, \hat{\Theta}_n \pm \Delta_n; m, n = 1, 2, 3)$ around the optimum at $(\hat{\Theta}_m, \hat{\Theta}_n, \min(J))$, while all other parameters are fixed to their optimal estimates $(\hat{\Theta}_{l \neq m, n})$. Each plot is thus a combination of two loss parameters: maximum grazing ($\Theta_1 = g_m$) and carbon loss rate ($\Theta_2 = \gamma_C$) on top; γ_C and aggregation parameter ($\Theta_3 = \Phi_{agg}$) in the middle; Φ_{agg} and g_m on the bottom. Results from MCMC (dots and asterisks) reveal similar collinearities between parameter combinations that involve g_m for the two cost functions (right and left sides of top and bottom row in Fig. (2)). It means that g_m can only be estimated in combination with Φ_{agg} and γ_C . If g_m remains fixed, we do not find such strong collinearity expressed between γ_C and Φ_{agg} and their estimates seem to be rather independent (middle row of Fig. 2), given the mesocosm data.

Another peculiarity is that the ranges of the MCMC's posterior indicate larger uncertainties if the cost function without covariance information is applied (right side of Fig. 2), although model and data are identical. This behaviour is also resolved by the 95% confidence regions that are obtained with a point-wise approximation of error ellipses (lines), based on approximated and inverted Hessian matrices according to Eq. (19). Furthermore, collinearities according to the error ellipses are smaller for the cost function with covariances compared to the case of independent data. Here, confidence regions of the error ellipses correspond well with the credible regions of the MCMC results. We stress that this may not be the general case and the good correspondance is likely attributable to the low dimension of the example looked at.

Overall, these results exemplify the uncertainty in constraining major loss parameters in the presence of grazing, if no explicit prior information about grazing rates or data of zooplankton biomass are available. Collinearities between grazing parameters and other phytoplankton biomass losses may be reduced by testing model performance against independent data, e.g. as done for the meso- and microzooplankton grazing in Buitenhuis et al. (2010). In cross-validation studies some combinations of parameters that produce indistinguishable solutions for one experiment or for one ocean site are compared with data of another experiment or at another ocean site.

6 Cross-validation and model complexity

Good performance should be attributable to a model capturing the predominant plankton dynamics under varying conditions in different environments. Parameter values are often optimised for local ocean sites, but ideally, parameter estimates from one site should improve model performance at other locations as well. The generality of optimised models can be tested by cross-validating against independent data, providing a direct and effective test of predictive skill (Gregg et al., 2009).



6.1 Cross-validation

Parameter optimisations can often improve the fit of a model by selecting unrepresentative parameter values that serve only to compensate for misfits between data and model results. It is therefore essential to check whether the resultant 'optimised' model is giving the right answer for the correct reasons.

- 5 Xiao and Friedrichs (2014b), for example, found that while the optimisation of a range of NPZD models to satellite data tended to reduce model-data misfit, this was often achieved through the adoption of extremely unrealistic parameter estimates, sometimes being multiple orders of magnitude higher or lower than their best a priori estimates. The same authors (Xiao and Friedrichs, 2014a) showed that adding synthetic noise to assimilated satellite data led to the introduction of similar errors, and a significant deterioration of one model's predictive skill. The extreme parameter estimates were not representative for the
- 10 system and the model performance turned out to be poor when the model was tested against independent data that were not used during the optimisation procedure.

- This is the principle of cross-validation, in which an optimised model is tested in terms of its ability to reproduce data that were not included in the calibration phase. This is often achieved by excluding a subset of the original calibration dataset, for later use in model evaluation. For example, in a variational data assimilation exercise for the Arabian Sea, Friedrichs et al.
- 15 (2006) repeated their optimisation a number of times, each time excluding data from a particular season. The calibrated models were then used to predict the system behaviour during the withheld season, with the resultant model-data misfit labelled the 'predictive cost function'.

- The cross-validation approach has the advantage of testing one of the key attributes of marine biogeochemical models, namely their predictive skill. The technique is, however, not without its difficulties. The first issue is that it is important to
- 20 ensure the test data are truly independent from the training data. In this regard, Friedrichs et al. (2006) took advantage of the highly seasonal nature of the Arabian Sea, but it would perhaps be less appropriate in regions with a less pronounced seasonal cycle, such as at the centre of a subtropical gyre. A potentially more serious problem occurs when researchers simply divide the available data at random, such that highly correlated data appear in the assimilated and the test data. Under such circumstances, the cross-validation would give no indication as to the ability of the model to predict independent data.

- 25 The potential to select unrealistic, compensatory, parameter values may not always be obvious, especially if good estimates of the 'true' (or at least sensible) values of the model parameters are not well known a priori. Such errors may, nonetheless, strongly impact the ability of a model to reproduce anything but the assimilated data. This issue appears to be a common theme in simple marine biogeochemical models calibrated to time-series data, as a number of studies (Fennel et al., 2001; Friedrichs et al., 2006; Ward et al., 2010) have found that parameter optimisation resulted in decreased predictive skill, relative
- 30 to 'off-the-peg', prior parameterisations. A notable counterpoint to those studies is given by Oschlies and Schartau (2005), who found that simultaneous optimisation of an NPZD model at three time-series sites (Schartau and Oschlies, 2003) led to improved performance when the model was applied within a 3D simulation of the North Atlantic. On the one hand, it seems likely that this improvement was dependent on assimilating data from three highly dissimilar North Atlantic locations, which prevented the inclusion of compensatory errors that were highly specific to any one site (see also Xiao and Friedrichs, 2014a).



On the other hand, in Schartau and Oschlies (2003) and in Oschlies and Schartau (2005) it is also stressed that the apparent improvement is associated with some ambiguous rapid nitrogen remineralisation pathway in their simple NPZD model, which can be incorrect in either simulations (1D and 3D), but with the same positive effect on primary production rates in the central North Atlantic.

5 6.2 Model performance as a function of model complexity

Of the many factors that affect the ability of a biogeochemical model to reproduce and predict observations, the appropriate degree of model complexity in any given situation is both one of the most important, and one of the least well defined. This is because there exists a fundamental trade-off between simplicity and complexity. Simple models have the advantage of being easier to understand, and with fewer parameters they should also be better constrained (both before and after optimisation). Nonetheless, simplification requires a degree of abstraction, and it can sometimes be difficult to draw parallels with the complexities of the observed system.

At the other end of the spectrum, a highly complex model can explicitly resolve more processes, allowing more detailed comparison with observations. As models become more complex, the number of degrees of freedom increases, and the calibrated model will generally be able to match the observations better than a simpler model. If insufficient observations are available, the extra degrees of freedom can lead to the introduction of compensatory errors at the assimilation site, which could then increase uncertainty at other locations. Similarly, an extra flexibility may lead to very different model solutions with only small variations in the assimilated data, also leading to increased uncertainty in model predictions.

A range of statistical techniques are available to assess this trade off, and a useful review is given by Johnson and Omland (2004). One of the most practical (if not the most general) techniques is cross-validation, as described in the previous section. In their experiments looking at the effects of adding noise to assimilated remote sensing data, Xiao and Friedrichs (2014a) found that the most complex model they evaluated was also the most sensitive to the introduction of synthetic errors in the assimilated data (Fig. 3). They attributed this result to the extra degrees of freedom that could be 'fit to noise'. This is consistent with earlier findings that model predictive skill deteriorates as complex models can become "overfit" to the data (i.e. too many parameters are fit to inadequate data) (Friedrichs et al., 2006, 2007; Ward et al., 2010).

Aside from directly assessing a model's predictive skill using cross-validation, a number of alternative approaches are available to identify the minimum number of model parameters that are supported by the available data. One of the simplest techniques (in terms of its applicability), is the Akaike Information Criterion (AIC). The AIC considers two opposing terms corresponding to the maximum log-likelihood of the parameters given the data ($\ln[L(\hat{\Theta} | \mathbf{y})]$, measuring model data misfit) and a bias-correction factor, that increases with the number of free parameters (N_{Θ}).

$$30 \quad \text{AIC} = -2 \ln \left[L \left(\hat{\Theta}_p | \mathbf{y} \right) \right] + 2N_{\Theta} \quad (22)$$

Note that for a model fitted by least-squares, the log-likelihood can be approximated by the residual sum of squares (RSS), following (Johnson and Omland, 2004): $\ln[L(\hat{\Theta}_p | \mathbf{y})] \approx -N_y/2 \cdot \ln(\text{RSS}/N_y)$, with N_y being the total number of observations. The AIC, and alternative techniques (weighted AIC, or Bayesian Information Criterion, BIC), seek to quantify the trade-off



between bias and variance. Of a range of competing models, the one with the lowest AIC has the greatest empirical support. A perhaps more intuitive approach is given by the Likelihood Ratio Test (LRT) for e.g. comparing so-called nested models, in which the simpler model is a special case of the more complex model, in the sense that $M_p = f_1$ is a special case of $M_{p+1} = f_1 + f_2$ where $f_2=0$. Like the AIC, the LRT aims to account for model complexity in the sense that it compares log-likelihoods:

$$\text{LRT} = J(\hat{\Theta}_p) - J(\hat{\Theta}_{p+q}) \quad (23)$$

with $J(\hat{\Theta}) = -2 \ln[L(\hat{\Theta} | \mathbf{y})]$ and index $p+q$ indicating the number of free parameters of the full model. An alternative simpler model (with p parameters) that is not significantly worse than the full model (with $p+q$ parameters) can be selected using this ratio. There is a clear analogy to Eq. (13) in Sect. (4). In other words, although having removed individual parameters (going from Θ_{p+q} to Θ_p) we may still have an increase in the data-model misfit that is tolerable or insignificant within some limit Δ_J . For nested models only, a value for Δ_J can be derived from a $\chi^2(\text{df} = q, \alpha)$ distribution. The respective degree of freedom (df) is then assumed to be equal to the difference in the number of free parameters between the full and the reduced model, which is q . For LRT with non-nested models an empirical, non-parametric distribution needs to be derived by other means instead, for instance using synthetic (or resample) data sets (e.g., Lewis et al., 2011).

The theory mentioned above is well described by Johnson and Omland (2004), and have already been applied in few ecosystem modelling studies (e.g., Crout et al., 2009; McDonald and Urban, 2010; Ward et al., 2013). The techniques for model selection have generally shown that more complex models are more vulnerable to over-tuning than simpler models. This appears to be because the number of uniquely identifiable parameters in marine biogeochemical models is often very low. Studies based on classic NPZD type models have typically found that the inclusion of as few as three to 15 parameters were supported by the assimilated data (Matear, 1995; Friedrichs et al., 2007; Ward et al., 2013; Löptien and Dietze, 2015). It should however be noted that these studies made use of only very limited datasets, and a higher level of complexity would likely be supported with the incorporation of more comprehensive datasets, especially those describing fluxes.

Ward et al. (2013) sequentially removed parameters from a relatively simple 2NPZD model to show that much of the model structure was redundant, with respect to the assimilated data, Fig. (4). They applied an F-score where the relative change in LRT is related to the relative change in parsimony (i.e. difference in the number of free parameters between the reduced and the full model divided by the degree of freedom of the full model, $\text{df}_{p+q} = N_y - N_{\Theta_{p+q}}$):

$$F = \left[\frac{\text{LRT}}{J(\hat{\Theta}_{p+q})} \right] \cdot \left[\frac{N_{\Theta_{p+q}} - N_{\Theta_p}}{\text{df}_{p+q}} \right]^{-1} \quad (24)$$

As model complexity was reduced, model predictive skill was initially very slow to deteriorate, and J remained similarly low. The increased parsimony of the simpler models led to improved performance in terms of the LRT, and the AIC and Bayesian information criterion (BIC). Once all of the redundant components of the model were removed, removal of essential components led to a rapid increase in J , with an associated increase in the other metrics. The LRT selects the simplest model with an F-score below a variable threshold value. The AIC and BIC select the model with the lowest overall score. Among models with a similar score, the simplest should be favoured.



7 Space-time variations in model parameters

With the previously described cross-validation approach we question how representative local estimates are if applied at larger scales, e.g. in basin-wide or global models. As outlined before, the extent to which this is feasible is far from clear. Theoretical arguments, as well as results from cross-validations, revealed problems with the portability of locally calibrated models (e.g.,
5 Hurtt and Armstrong, 1999; Friedrichs et al., 2007). These limitations encourage estimators that allow spatial and/or temporal variations of parameter values.

For spatial or temporal variation to be useful we have to make sure that the corresponding parameter adjustments reflect changes in the actual underlying (real-world) dynamics. To assess whether this condition is met is a particularly challenging problem that has yet to be adequately addressed. Direct comparisons are needed between optimisations that allow variation
10 in posterior parameter vectors and those that do not. In studies where direct comparisons are made, a common finding is a reduction in the model misfit to the assimilated data by allowing these kinds of variations, but this tells us little. A reduction of the cost function is expected, as a direct consequence of an effective increase in the number of adjustable parameters. As pointed out by Gregg et al. (2009), “skill assessment using assimilated data lacks the independence necessary for a comprehensive, objective evaluation”. Furthermore, any ad hoc fixing of local parameter values would be difficult to justify in prognostic
15 simulations of changing environmental conditions. Switching between different parameter sets in time or for specific regions is not a solution *per se* but it stresses where model refinements have to be investigated (Huret et al., 2007). From analyses of spatially- and temporally varying parameter estimates we can learn where and when particular model equations are limited in reproducing changes in plankton dynamics with fixed parameter values, which should provide important feedback information on revising these parameterisations.

20 7.1 Regional differences between parameter estimates

Satellite ocean colour data are widely used to investigate spatial differences in parameter estimates. In many cases, a local calibration method is applied where parameters are optimised separately to fit Chl a data for a number of pre-defined sites or regions spanning a domain of interest. For example, parameters of a 3D-NPZ model were optimised by Garcia-Gorriz et al. (2003) for January and June for two regions, the North- and South Adriatic basin in the Mediterranean Sea. They inferred
25 comparable parameter vectors for the two regions during bloom conditions in January but considerable differences between the regionally optimised parameter sets emerged for June. Garcia-Gorriz et al. (2003) attributed this difference to unresolved variations in plankton composition and changes in biomass concentration between the two basins. Huret et al. (2007) performed a similar assimilation experiment for the Loire and Gironde river plumes in the Bay of Biscay. On the one hand, they found some similarities between parameter estimates for the two distinct river plumes for particular conditions during spring, suggesting
30 the possibility of a common set of parameter values for both plume areas. On the other hand, the authors stressed their optimal parameter estimates to be based on data for a specific period, which seemed inappropriate for simulations of the entire season of phytoplankton production. An interesting finding was that Huret et al. (2007) obtained too high Chl a concentrations in the Bay of Biscay for the entire simulation year when utilising the mean of parameter estimates of the two plume regions.



Pronounced regional and seasonal differences are not restricted to adjacent seas and coastal areas. Large scale studies for the North Atlantic have shown comparably strong regional differences between parameter estimates (Hemmings et al., 2003; Losa et al., 2004; Doron et al., 2013). A set of sites representing distinct latitude bands was considered for a one year calibration of a NPZ model in Hemmings et al. (2003). The annual cycle at locations on a five degree grid was simulated with variable parameter estimates of a NPZD model in Losa et al. (2004) and individual parameter estimates for thirteen provinces in the North Atlantic, pre-defined according to Longhurst (1995), were derived for a six-compartment 3D biogeochemical model in Doron et al. (2013). Although these studies included different models, the optimised parameters were common to all three studies, but little consistency is seen in the spatial patterns between their estimates. Patterns of spatial variation in parameters are not easily validated as most parameters do not have well-observed equivalents in nature. Nevertheless, Losa et al. (2004) were able to document the plausibility of their posterior photosynthesis parameter values for the maximum growth rate μ_m and initial slope α_{phot} by comparison with observational estimates of Platt et al. (1991). These posterior parameter fields were cross-validated in a 3D version of their model by comparing the output with an independent SeaWiFS chlorophyll data from 1997-2003 (Losa et al., 2006). The spatially-varying parameter set of Losa et al. (2004), obtained by assimilating Coastal Zone Color Scanner (CZCS) data for the period 1979-1985, enabled the model to simulate the seasonal patterns in SeaWiFS data much better than with a fixed prior parameter vector. An important caveat is that the calibration and validation data sets are essentially two realisations of the same emerging spatio-temporal patterns. To demonstrate improved predictive skill attributable to its dynamics the model would be expected to resolve differences between the two independent data sets, given physical forcing data specific to each period.

7.1.1 Combining sites or regions

The presence of parameter variation between sites or regions for which a model was calibrated independently does not refute the existence of a common parameter vector with which the model could achieve similar results. Garcia-Gorriz et al. (2003) and Hemmings et al. (2003) performed alternative experiments in which regions were combined under a uniform parameter vector constraint, but did not include predictive skill tests for direct comparisons of the performance of spatially-varying and uniform parameter solutions. In other studies, sites have been combined without considering the alternative of allowing parameters to vary spatially. By optimising a 13-parameter model for locations of the Ocean Weather Ship India (OWSI) and of the Bermuda Atlantic Time-series Study (BATS) simultaneously Hurtt and Armstrong (1999) found that it could capture the primary observed characteristics of the annual cycle at both sites, despite being unable to reproduce the cycle at BATS when calibrated at OWSI. As mentioned in the previous section, the approach of data assimilation over multiple sites has since been used by Schartau and Oschlies (2003) with some success in improving predictive skill of a 3D North Atlantic simulation (Oschlies and Schartau, 2005) based on a simultaneous three-sites calibration. A relatively complex global model with 45 adjustable parameters was similarly demonstrated to improve the predictive skill after assimilating time series data at five different calibration sites (Kane et al., 2011).

There is a clear advantage of combining sites or regions, in that it makes more data available to constrain parameters. It also creates a representative sample for the domain of interest, reducing the risk of over-fitting. In contrast, when assimilating



data at a single site in models of differing complexity, Friedrichs et al. (2007) found it necessary to limit the number of adjustable parameters (to four or even less) to avoid portability problems. Use of a larger data set representing a wider diversity of ecosystem behaviour should support a greater number of parameters to be constrained, which would allow a model's true flexibility to be more fully exploited. However, there is a potential disadvantage of combining sites or regions, particularly over large spatial scales, in that the resultant parameter vectors may be less suitable for either region than parameter vectors obtained by local calibration.

Hemmings et al. (2004) introduced the idea of allowing provinces that are in a sense optimal for calibration to emerge during the data assimilation process. A sample of sites from the domain of interest is divided into two similarly distributed sets, one for calibration and the other for cross-validation. The objective is to find "the number and geographic scope of parameter vectors which allow the lowest possible cost of the calibrated model, with respect to the stations in the validation set, to be obtained". The method involves first performing a *whole-domain calibration* where parameters are optimised for all calibration sites, then recursively splitting the domain into two geographic provinces to investigate whether a better calibration can be achieved by optimising parameters for each one separately, a procedure referred to as *split-domain calibration*. To define the boundary between the two provinces, an algorithm is employed that identifies natural groups of sites that can be simulated with one parameter vector. The relative merits of the calibration procedure are assessed by cross-validating the posterior parameter vector or vectors against sites from the validation set.

Application of the method to the North Atlantic data set used by Hemmings et al. (2003), with the same NPZ model and twelve adjustable parameters, resulted in the discovery of a two-parameter vector solution having a cross-validation misfit cost 25% lower than that for the single vector solution obtained for all calibration sites. The two sub-domains are shown in Figure (5). The validation cost was also 24% lower than that obtained when the model was calibrated locally using individual sites. This is consistent with subsequent findings of Xiao and Friedrichs (2014b), where combining sites tends to reduce validation costs. Note that the validation scheme used by Hemmings et al. (2004) may not be able to discriminate well between skill associated with the model dynamics and that associated with the ability of the model to interpolate spatio-temporal patterns. This could be resolved by comparison with interpolated output from some purely empirical model fitted to the calibration data.

7.1.2 Spatially varying parameter estimates derived with Bayesian hierarchical modelling

Zhang and Arhonditsis (2009) proposed a Bayesian hierarchical formulation for calibrating aquatic biogeochemical models at multiple sites. In this framework, posterior parameter distributions can vary between sites but the sites share common prior distributions. Fiechter et al. (2013) used this approach to estimate parameter distributions for a 1D-NPZD-iron model at two sites in the Gulf of Alaska. Non-informative prior distributions were employed for each parameter so the influence of the priors on the solution for each site was fairly weak. In a parallel Bayes' hierarchical modelling study for the same model, Leeds et al. (2013) assimilated satellite Chl_a data at nine sites using a spatial Gaussian process model for the parameters with an anisotropic correlation matrix to allow for differences between along-shelf and cross-shelf dependence. The methods employed by Leeds et al. (2013) and Fiechter et al. (2013) seem promising because of their potential for rigorous treatment of



uncertainty. However, in the absence of cross-validation experiments, their potential for improving the predictive skill of the models is not well evaluated at present.

7.1.3 Time-varying parameters

The idea of representing seasonal variation in part by temporal variations in the parameters has been examined in various studies (Losa et al., 2003; Brasseur et al., 2005; Dowd, 2006; Mattern et al., 2012, 2013a, 2014; El Jarbi et al., 2013; Melbourne-Thomas et al., 2013). In some cases, parameters are allowed to vary in space and in time (Tjiputra et al., 2007; Fan and Lv, 2009; Doron et al., 2013; Li et al., 2013). Cross-validation tests comparing the merits of varying and non-varying parameter solutions are mostly lacking, which prevents inferences being drawn about the superiority of these parameter variations for improving predictive skill. Temporal variation is handled naturally by adapting widely used sequential state estimation techniques to obtain parameter values along with state estimates. One such technique, the Sequential Importance Resampling (SIR) method (Gordon et al., 1993; van Leeuwen, 2009, 2010), has been widely used (e.g., Losa et al., 2003; Dowd, 2006; Mattern et al., 2013a). The SIR particle filter approximates the solution of a sequential Bayesian problem in which the joint probability distribution of state and parameters is given by a series of forecast and analysis steps. Given a state vector \mathbf{x} augmented with the model parameters and a set of observations \mathbf{Y} , the forecast at time t_i is described by

$$p(\mathbf{x}_i | \mathbf{Y}_{i-1}) = \int p(\mathbf{x}_i | \mathbf{x}_{i-1})p(\mathbf{x}_{i-1} | \mathbf{Y}_{i-1})d\mathbf{x}_{i-1} \quad (25)$$

where \mathbf{x}_τ is the augmented state vector at time τ and $\mathbf{y}_\tau = (\mathbf{y}'_1, \dots, \mathbf{y}'_\tau)'$ is the cumulative observation data set up to and including observations at time τ . The forecast is combined with new observations \mathbf{Y}_i in the analysis step

$$p(\mathbf{x}_i | \mathbf{Y}_i) \propto p(\mathbf{y}_i | \mathbf{x}_i)p(\mathbf{x}_i | \mathbf{Y}_{i-1}). \quad (26)$$

While the state evolves between analysis times according to the model equations, the parameters remain constant. Both are then updated in the analysis. The time-varying parameter estimates may, in principle, also be used independently of the state estimates in subsequent free-running simulations that preserve model dynamics and conserve mass.

Losa et al. (2003) applied a SIR particle filter to a model with 15 time-varying parameters in an assimilation of multi-year time series at the BATS site. The model was treated as a weak constraint with an additive system noise term that was uncorrelated between state variables. Mattern et al. (2013a) instead added noise to their two parameters in a 7-compartment 3D biogeochemical model of the Middle Atlantic Bight, with the advantage that the state evolution over each forecast step was true to the model and correlated errors between state variables were represented. In both cases, the error model is highly subjective, yet it can have a major impact on the results. For instance, Losa et al. (2003) found the level of noise to be a critical factor affecting their solution. This motivated subsequent experiments in which additional time-varying parameters representing the noise level for each state variable were optimised (Brasseur et al., 2005). The posterior parameter trajectories thus obtained were not consistent with the earlier results. Despite the subjective characteristics of the system noise, the solution of Losa et al. (2003) improved the model prediction of unassimilated bacteria data. The necessity of time-variation in the parameters for achieving this is unclear, since no alternative results for static parameter solutions were analysed.



In a more recent BATS assimilation study with a simpler NPZD model, El Jarbi et al. (2013) did compare the performance of time-varying and static parameter solutions. Rather than employing a sequential method, they opted to solve the optimal control problem. i.e. to find parameter trajectories that minimise a cost function for the complete time period. An annual periodicity constraint on posterior parameter trajectories was introduced to allow the calibrated model to be also applied for time periods
5 beyond the range of observations. Optimal periodic parameters were obtained using a two-year data set and validated against independent data for the following three-year period. In cross-validation tests, this solution was shown to improve predictive skill over the static parameter solution of Rückelt et al. (2010). Their results suggest that the time-varying parameter model may capture some aspects of the inter-annual variability, which would indicate dynamical skill.

Mattern et al. (2014) compared the predictive skill of versions of their two-parameter model with time-varying and static
10 parameter solutions. Here, the time-varying solution was obtained using an alternative, emulator-assisted sequential data assimilation scheme. Their cross-validation experiments show a modest improvement in the ability to predict the annual cycle with time-varying parameters. A prediction of the inter-annual variability was not tested and the achievability of similar predictive skill by purely empirical representations of the annual cycle derived from the observational data is not ruled out. In addition, the supporting evidence for using time-varying parameters is conditional on the restriction to adjust only two model
15 parameters, which places limits on the model's flexibility. It's flexibility could equally well be increased by increasing the size of the parameter vector, rather than allowing it to vary in time.

7.1.4 Learning from space and time variation in parameter estimates

A variety of approaches have been explored for data assimilation with parameters varying in space or time or both. A common finding is that the posterior misfit cost with respect to the assimilated data is reduced by allowing variation, but this provides no
20 evidence in itself to support the case for parameter variation. Goodness-of-fit statistics that penalise model complexity in terms of number of parameters (e.g. the LRT based F-score employed by Ward et al., 2013) could prove more informative, but are not used. In the few studies which do use cross-validation to compare uniform and varying parameter solutions (Hemmings et al., 2004; Mattern et al., 2014; El Jarbi et al., 2013), the cross-validation schemes are not shown to discriminate reliably between predictive skill associated with model dynamics and that due to interpolation of patterns in space or persistence of an annual
25 cycle.

Allowing parameters to vary reduces the extent to which their values can be constrained by a given set of observations, making an already under-determined problem worse. It could therefore be argued that parameter variation is justified only when there is good evidence to infer that a given model cannot adequately represent the observed variability under the uniform parameter vector constraint. The evidence should be statistically robust, taking into account all relevant sources of uncertainty.
30 The consideration of these additional uncertainties, motivated by its potential for improving parameter estimates (Hemmings and Challenor, 2012), may tend to weaken data constraints further and make the introduction of parameter variation less practical, as well as affecting the strength of the evidence in support of it.

Heterogeneity in the parameter vector is most likely to be useful for structurally simple models. Those models may lack the required flexibility to capture some distinct spatial features observed within large domains or they may fail to resolve specific



events during a complete annual cycle. Its introduction may be a sensible alternative to increasing structural complexity as it does not increase the computational demands of 3D simulations. From an ecological point of view, the need to introduce space and time variations in parameter values reflects limitations in resolving physical environmental changes, or deficiencies in physiological or ecological processes, or all of these factors together. For example, variations in plankton elemental stoichiometry, e.g. variable Chl a :C and C:N ratios, induce variations in photosynthetic rates that may not be well described by a model's parameterisation of Chl a synthesis and assimilation of nutrients (as discussed in Sect. 5.2). It is helpful to consider biological or environmental reasons why space or time variations of parameter values are expected to improve model performance.

If good reasons are found to support the use of parameter variation for model improvement, then the issue of how to benefit from this spatio-temporal information must be addressed. Spatially varying parameters can be applied directly in 3D models (e.g., Losa et al., 2006). This should work well for hindcasts and short-term forecasts where the application is not compromised by large scale ecological changes. For forecasting, climatological trajectories such as those estimated by El Jarbi et al. (2013) are likely to be of advantage, although their direct application to long-term prediction in the context of global change would be difficult to justify. Application of spatially varying parameters to long-term predictions of global change is possible but will be more complicated than their use in short-term forecasting and it may be necessary to find ways of allowing spatial patterns in biogeochemical parameters to evolve with predicted changes in the physical regimes.

8 Emulator approaches

Systematic approaches for parameter optimisation, which were successfully applied in 0D or 1D setups, may become too costly as resolution in space is increased and if the time period for integration is prolonged. This is the case when spatially three-dimensional models with high resolution or steady annual cycles (i.e. periodic solutions) are considered. For the computation of a steady annual cycle (or fixed-point) typically thousands years of model time are necessary, which may result in a number of time steps in the order of $o(10^7)$. Since data assimilation usually involves an iterative optimisation process, typically hundreds or more model evaluations are necessary to obtain a satisfactory parameter set. Thus the necessary time steps during procedures of parameter identification can even reach $o(10^{10})$. Recent attempts aim at replacing computationally costly models with approximations that are less expensive; i.e. emulators have the goal to provide an approximation of the model output trajectory $\mathbf{x} := (\mathbf{x}_i)_{i=0}^{N_t}$, recalling Eq. (1) of Sect. (2.1):

$$\mathbf{x}_{i+1} = M[\mathbf{x}_i, \Theta, \mathbf{f}_i, \boldsymbol{\eta}_i], \quad i = 0, \dots, N_t - 1, \quad (27)$$

by substituting the original model M by a simpler one, the emulator (\widetilde{M}). Here we disregard a stochastic model approach and consider $\boldsymbol{\eta}_i = 0$ for simplicity.

The application of emulators has emerged in many different fields of science and thus the theoretical background is relatively well developed (e.g. Bliznyuk et al., 2008; Castelletti et al., 2012; Conti et al., 2009; Kennedy and O'Hagan, 2000, 2001; Lucia et al., 2004; Liu and West, 2009; Phillips, 2003; van der Merwe et al., 2007). Two distinct approaches of emulation exist: one to emulate model dynamics, the other for the emulation of statistical properties, e.g. of $M(\mathbf{x}, \Theta, \mathbf{f})$. Both approaches are outlined in the following. Note that the terminology in literature may vary somewhat depending on the respective research field.



8.1 Dynamic Emulators

A dynamic emulator (or reduced order or surrogate model) is a substitute for the original model M . It makes use of the original model equations but is a simpler representation in terms of resolution or details resolved in the dynamics. The term “simple model” refers here to the computational effort needed to evaluate a solution that is a useful approximation of the solution obtained with the full model. A typical number of model evaluations needed for an automatised optimisation process can easily reach the order of 10^{10} . In this case an emulator becomes particularly valuable, because its application should be much faster than the original model, while as much as possible main properties of the original model are retained. Only then an emulator-based DA approach will give satisfactory results.

Dynamical or physical emulators are based on a simplified model version (\widetilde{M}), which might be additionally aligned with interim evaluations of the original model. The term “dynamic” refers to the fact that the emulator is still based on dynamical physical or biogeochemical equations that can be similar to original model but might have some reduced complexity, either by neglecting some processes or by simplifying e.g. the forcing \widetilde{f} . Another option is the reduction of accuracy in model output by coarsening the spatial or temporal discretization. For instance, the Transport Matrix (TM) method (Khaliwala, 2007) can be interpreted as an emulator approach with a kind of coarse model. The TM is an emulator that simplifies the original model M by using an approximated and averaged forcing \widetilde{f} in Eq. (27) and a linear approximation of the spatial discretisation, compared to nonlinear advection schemes typically used in ocean models. For the case of a spin-up, as mentioned above, a reduction of accuracy can be achieved by introducing a different criterion that specifies when a tolerable steady periodic solution as been approached.

When using dynamic emulators, it is often insufficient to take the output of the faster but less accurate coarse model during optimisation, because the accuracy of the coarse model \widetilde{M} might be too low to effectively support parameter search process. It can be worthwhile or even necessary to gradually enhance (or update) the emulator’s accuracy during the optimisation procedure by introducing special alignment operators. To explain their definition, let us assume we have computed state vectors of the original and of the coarse model with a current set of values for the parameter vector Θ_ℓ in the ℓ -th step of the optimisation run, i.e.

$$\begin{aligned} \mathbf{x}_{i+1} &= M[\mathbf{x}_i, \Theta_\ell, \mathbf{f}_i], \\ \widetilde{\mathbf{x}}_{i+1} &= \widetilde{M}[\widetilde{\mathbf{x}}_i, \Theta_\ell, \widetilde{\mathbf{f}}_i], \quad i = 0, \dots, N_t - 1. \end{aligned}$$

We recall that the model state vector \mathbf{x}_i consists of the values of the N_x state variables. Thus, in a spatially distributed model, \mathbf{x}_i is a vector where every element represents the values at a certain spatial grid point. We here assume that the same numbering is used for the coarse model state $\widetilde{\mathbf{x}}_i$.

The alignment operator in optimisation step ℓ is then defined element-wise for \mathbf{x}_i and point-wise in time by

$$\mathbf{A}_{\ell i} \widetilde{M}[\widetilde{\mathbf{x}}_i, \Theta_\ell, \widetilde{\mathbf{f}}_i] = M[\mathbf{x}_i, \Theta_\ell, \mathbf{f}_i]. \quad (28)$$

Thus, every $\mathbf{A}_{\ell i}$ is a diagonal matrix. At the current iterate Θ_ℓ , the emulator equals the original model, and the idea of this *response correction method* is that the deviation between both models remains uncritically similar in a vicinity of Θ_ℓ . The



emulator is thus not just the coarse model \widetilde{M} , but an *aligned* one, $A_{\ell_i}\widetilde{M}$, that is now locally optimised. When this inner optimisation gives some new parameter vector $\Theta_{\ell+1}$, the original model is evaluated once again, and the procedure in Eq. (28) is repeated, defining the new emulator for the $(\ell + 1)$ -th outer optimisation step. In the inner optimisation loop no runs of the original model are needed, and the total number of outer iterations is expected to be lower than in an classical direct optimisation using M . This type of optimisation procedure fits in the framework of trust region methods, a class of state-of-the-art algorithms for which a mathematical convergence analysis is shown in Conn et al. (2000).

The method was successfully applied for parameter identification of a transient 1D configuration with a NPZD ecosystem model and for periodic states with climatological forcing in a three-dimensional setting in a N-based model with dissolved organic phosphorus (DOP) (Prieß et al., 2013a, b). Therein, a coarser time-stepping and a less accurate computation of the fixed-point (i.e. a shorter spin-up), respectively, was used to construct the simple model \widetilde{M} . For this computationally very costly 3D model, it turns out that the most efficient way is to start the optimisation using the emulator- or surrogate-based optimisation procedure (with a very coarse model), and then increase its accuracy during the outer optimisation (Slawig et al., 2014).

8.2 Statistical Emulators

In contrast to a dynamical emulator, statistical emulators relate the input parameters statistically to the model output and thus to $H(\mathbf{x})$ regardless of the dynamical model structure. Generally, statistical emulators interpolate the results of a numerical model from a set of training runs with differing parameters. The aim is to approximate the unknown model output for other input parameters, not included in the training parameter set. Common approaches are based on a polynomial fit (of varying degree). Typically, such interpolations are extended by Bayesian techniques to also obtain uncertainty estimates. For this purpose it is commonly assumed that the model outcome can be represented by a Gaussian process and also that the model output changes smoothly as parameter values are varied. Prior assumptions about reliable parameter ranges and their distribution are required. Another necessary a priori choice is to determine the respective model output of interest, e.g. results needed for $H(\mathbf{x})$ to determine $p(\Theta | \mathbf{y})$ or $L(\mathbf{y} | \Theta)$, Sect. (2.2). Although there are methods available to reduce the dimensionality for multi-dimensional model output (e.g. Higdon et al., 2008; Leeds et al., 2014), it remains practically infeasible to capture the complete output of a 3D-coupled ocean ecosystem model.

While the theory for statistical emulation is relatively well described (e.g., Kennedy and O’Hagan, 2000; O’Hagan, 2006; Liu and West, 2009; Conti and O’Hagan, 2010), statistical emulators are so far rarely applied in biogeochemical ocean modelling. Here we provide an example in an idealised 0D setup (Fig. 6). All simulations are based on a NPZD model, assuming a system that is homogenous in space, both in horizontal and in vertical direction, as described in Löptien and Dietze (2015). Daily means of photosynthetically available radiation (PAR) averaged over the surface mixed layer are prescribed. Respective PAR values range from 2.5 W m^{-2} in winter to 50 W m^{-2} in summer. These PAR-conditions are representative for mixed layer conditions typically observed in the Baltic Sea (Leppäranta and Myrberg, 2009). We define, a priori, our own “synthetic observations” by integrating the model with an arbitrary but representative set of parameter values: $\text{HI}=15 \text{ W m}^{-2}$; $\text{m}=0.06$



d^{-1} ; $\mu_{max}=0.51 d^{-1}$; $Hn=0.8 \text{ mmol N m}^{-3}$; $m_{PD}=0.1 d^{-1}$; $m_{DN}=0.1 d^{-1}$; $H_Z=0.9 \text{ mmol N m}^{-6}$; $m_{ZN}=0.01 d^{-1}$; $m_{ZD}=0.01 d^{-1}$; $g_{max}=0.21 d^{-1}$.

The respective model simulation is perturbed by reddish noise with a standard deviation of $0.09 \text{ mmol N m}^{-3}$. The goal of this twin experiment is to retrieve the original parameter values used to generate the unperturbed model solution. Generally, such a simple setup would not require emulation (since it is cheap to run), but it allows for the evaluation of many model simulations and is thus well suited for testing an emulator.

Figure (6) depicts simulated and emulated RMS (root mean square) error with respect to all prognostic variables and nitrate only, depending on the maximum growth rate of phytoplankton and the maximum grazing rate. All other model parameters are chosen to match the values underlying the synthetic observations. The emulation is based on a second order polynomial, following the approach of Kennedy and O'Hagan (2000). The training runs comprise 25 model simulations in a Latin hypercube design according to (Urban and Fricker, 2010).

In our example, we obtained similar optimisation results with the emulator and with the full model. For both cases, the underlying truth (i.e. the original parameter values) could be identified well, in spite of the noise added to the original model solution. The agreement between emulated and simulated model-data misfit is satisfactory and might be enhanced further by considering higher order polynomials and/or more trainings data sets. Thus, for this testcase, the parameter retrieval can be successful if based on the emulator instead of the real model. Note that the complexity of the problem increases strongly with the number of free parameters. Particularly, the numerous parameter collinearities in biogeochemical models (e.g. Matear, 1995; Kreuz and Schartau, 2015; Löptien and Dietze, 2015) can complicate emulation. Increasing dimensions brings in additional difficulties. One suggestion on how to treat this problem is given by Hooten et al. (2011). The authors decomposed modelled surface Chl a concentrations for 50 training runs of a coupled ocean-ecosystem model by singular vectors and predicted these in dependence of a suite of biological and physical model parameters. During the subsequent parameter optimisation with respect to satellite chlorophyll, the zooplankton grazing rate and the light response of phytoplankton were identified as the most influential parameters. In contrast to most other approaches, where variances are estimated based on Bayesian techniques, Hooten et al. (2011) used a Bayesian approach to estimate the mean values. The study of Leeds et al. (2014) applied a similar technique for DA.

Another example for statistical emulation in biogeochemical modelling is presented by Mattern et al. (2012). Their emulator approach was based on polynomial chaos expansion (e.g. Askey and Wilson, 1985; Wan and Karniadakis, 2006). Mattern et al. (2012) emulated simulation results of Chl a concentrations as a function of "maximum zooplankton grazing rate" and the Chl a :C-ratio in the Middle Atlantic Bight in year 2006. The authors used an emulator instead of the model to minimise the model-data misfit with respect to daily Chl a concentrations observed from remote sensing. They optimised time-constant as well as time-varying parameter estimates. Both approaches improved the overall model performance with respect to Chl a . While the original time-varying estimates disregard the actual state of the system, the use of the polynomial chaos method formed the basis of an updated, more reliable method in the study of Mattern et al. (2014) previously discussed in Sect. (7).

Another study of Mattern et al. (2013b) analysed the uncertainty of modelled hypoxia for the Texas-Louisiana shelf based on statistical emulators. The authors investigated the uncertainty due to initial and boundary conditions of biological variables



as well as river nutrient loads and phytoplankton growth rate. Additionally, physical factors like river runoff, wind forcing and ocean mixing coefficients were taken into account. The authors revealed considerable uncertainties as their estimates for the hypoxic area varied by more than 40%, when considering reasonable uncertainties in freshwater runoff. Such an extensive analysis would not have been possible without taking advantage of emulators. Furthermore, the use of emulators opens up the possibility of new approaches to exploring the parameter space. One emulator-based technique referred to as “history matching” (Craig et al., 1996), now well-established in other fields and recently applied to the constraint of coupled ocean-atmosphere model parameters (Williamson et al., 2013), seems a particularly promising approach for parameter identification in marine ecosystem modelling. This relatively simple method uses Bayesian inference to rule out areas of parameter space as implausible, given some set of observations. Estimated uncertainties in both the observations (with respect to the truth) and the emulator (with respect to the model) can be taken into account. The method can be applied iteratively with different observation sets to reduce the size of the plausible region at each stage, either as a precursor to more formal model calibration or as a parameter identification method in its own right.

8.3 Combining dynamical and statistical approaches

The principal advantage of statistical emulators is speed. Dynamical emulators, on the other hand, have the advantage of being inherently related to the models they are emulating. This makes them much less reliant on model output than statistical emulators that rely totally on that output to provide their training data. Suitable training data sets are easy to generate for 3D models with limited domains or fairly coarse resolution. However, the increased integration times required for high resolution 3D simulations or for long spin-up periods inevitably reduce the size of ensemble simulations that can be used for generating training data. Otherwise the need to explore large high-dimensional parameter spaces for comprehensive model analyses demands relatively large ensemble integrations to produce adequate training sets. This problem motivates the combination of dynamical and statistical emulators, exploiting the advantages of both.

A two stage emulation process is suggested by Hemmings et al. (2015). Their idea is to use a set of 1D models as a dynamical emulator that describes the evolution of the 3D model at representative sites. This Stage 1 emulator allows large ensemble simulations to be run, providing output that could be used as training data for construction of a statistical emulator (Stage 2). The dynamical emulator of Hemmings et al. (2015) is not used in an inner optimisation loop but is used instead to predict 3D model output for arbitrary parameter vectors. It is thus used more like a statistical emulator. In fact, a major innovation in their study was to quantify uncertainty in the emulator outputs for inference purposes. Another innovation was the inclusion of biogeochemical perturbations associated with lateral advection that are typically ignored in 1D calibration studies. These were derived by averaging 3D model diagnostics over a 10-member ensemble simulation. To account for the lateral flux information was helpful contributed strongly to the emulator accuracy. The emulator with uncertainty estimates gave robust results for the surface Chl a concentration of an ecosystem model of intermediate complexity, considering variation in 8 parameters.



9 Parameter estimation of large-scale biogeochemical ocean circulation models

Global biogeochemical ocean models are commonly used to investigate the mutual interactions between ocean biota and climate change, a famous example being coupled earth system models applied in the IPCC assessments and evaluated as part of the Coupled Model Intercomparison Project (CMIP5; Taylor et al., 2012). Besides separate evaluation of the biogeochemical ocean model components (e.g., Ilyina et al., 2013; Tjiputra et al., 2013), the models are analysed with respect to their representation and projection of the carbon cycle (e.g., Schwinger et al., 2016), or oxygen minimum zones (Cocco et al., 2013; Cabre et al., 2015). Assessment of model skill is usually done with respect to climatological data sets, e.g. of nutrients and oxygen, components of the carbonate system, and/or diagnostics derived from remotely sensed data such as primary production or chlorophyll (e.g., Watanabe et al., 2011; Tjiputra et al., 2013; Nevison et al., 2015). Considering the often high level of structural complexity of these models, which include many components and feedbacks among these, at first sight it seems astonishing that there are only few model assessments against more elaborate data such as organism groups or fluxes of organic matter. Examples for this type of model assessment can be found in Gehlen et al. (2006), who compared simulated and observed particle fluxes, or Aumont et al. (2015), who compared simulated and observed dissolved iron concentrations and nitrogen fixation rates.

9.1 Data availability and computational time

One reason for the usual fallback to rather basic data types such as nutrients for global model evaluation is the sparsity of observations for more “sophisticated” data, which sometimes also suffer from methodological problems and uncertainties (e.g. particle fluxes measured by sediment traps, or observations of nitrogen fixation). In addition, some data sets have a strong bias towards certain areas (e.g. towards the coastal areas, summer season in the high latitudes, and the northern hemisphere, Kriest et al., 2010; Kriest and Oschlies, 2013). Therefore, comparison against observations of dissolved inorganic tracers, for which large, easily accessible and quasi-synoptic data sets exist, appear to be a relatively straightforward way for global biogeochemical model evaluation. Biogeochemical tracer distributions are also close to the heart of working group I of the IPCC where carbon-cycle climate feedbacks are more in the focus than ecological patterns or changes.

A complication arises from the fact that dissolved inorganic tracers (as available from global climatologies) often do not show a normal distribution, as illustrated in Fig. (7). Both phosphate and nitrate rather show a bimodal distribution, where the first peak of very low concentrations can probably be related to biogeochemical processes at the sea surface (in particular: nutrient uptake by phytoplankton), and the second peak (around ≈ 2.2 and $33 \mu M$ for phosphate and nitrate, respectively) may be associated with combined effects of circulation and deep remineralisation. This non-gaussian data distribution may question the suitability of tools for model skill assessment that rely on Gaussian distributions, as commonly employed in 3D model evaluation (e.g. Taylor plots that display simulated and observed standard deviation). Figure (7) also shows the difference in data distribution between spatially interpolated and “raw” data sets, where only grid boxes containing at least one observation are considered. For reasons mentioned above, the raw data show a bias towards low nutrient concentrations, and lower data frequency for higher concentrations, most likely caused by the sampling bias towards shallower waters and / or



summer seasons. It depends on the research question posed at the model, whether one opts for one or the other data set, and remains to be investigated, whether this causes a large difference in global parameter estimation. However, we argue a more balanced distribution, as available from interpolated data sets, should not be rejected per se.

A further difficulty for model calibration on a global scale arises from the fact that global models require many millennia until the simulated tracer distributions are in equilibrium with the given circulation field and biogeochemical processes (Wunsch and Heimbach, 2008). Tracer equilibrium should be aimed for before evaluating simulated against observed tracer distributions. It is usually achieved by integrating tracer fields for several thousand years in a so-called model spin-up with some seasonally cycling climatological circulation fields. For current biogeochemical models it has been found that after several thousand years of simulation time, the seasonally cycling steady state reached is independent of the initial conditions except for the global ocean inventory of phosphorus (Kriest and Oeschler, 2015). Oxygen and nitrogen (and carbon) adjust via biogeochemical feedbacks in the models, in conjunction with physical forcing and surface boundary conditions, such as air-sea gas exchange. That is, in this steady state simulated tracer fields are the sole product of the combined, physico-chemical framework, independent of poorly known initial conditions. It is important to note that the convergence of the model fields towards steady state is not necessarily a monotonous function of time, but may exhibit inflection points, which mirror the interaction of different processes with different time scales (Kriest and Oeschler, 2015). Convergence to steady state conditions also strongly depends on the region, tracer type, and form of boundary condition (Wunsch and Heimbach, 2008; Primeau and Deleersnijder, 2009; Siberlin and Wunsch, 2011). Unfortunately, simulation times of several thousand years can be computationally very expensive for global biogeochemical circulation models. Until very recently, this has made dense scans of the models' parameter space for spun-up states essentially impossible.

Considering the ocean's key role in the global carbon cycle and hence climate system, three types of data are considered essential for model assessment and calibration: 1) distributions of dissolved inorganic tracers, such as nutrients, oxygen, alkalinity and dissolved inorganic carbon, 2) plankton primary production, which turns inorganic dissolved carbon into organic particulate form, and 3) gravitational flux of organic particles to the ocean interior, which moves carbon through the water (and not - in contrast to the flotation of plankton or dissolved constituents - with it). Different data sets exist with respect to the latter two types of observations: primary production simulated by global models can be compared to data sets derived from remotely sensed ocean colour spectra (e.g., Carr et al., 2006). It should be noted, that these are not direct measurements of primary production, but are based on algorithms to derive production rates from ocean colour and additional parameters, including assumptions required for vertical extrapolation and seasonal interpolation that might introduce artifacts (e.g. Karl et al., 1998). Ship-based direct observations of production are usually sparse in space and time (for logistic reasons); in addition, also here the methodology has to be assessed carefully for artefacts. Observations of oceanic particle flux by sediment traps or optical methods are also subject to large uncertainties (e.g., Gardner, 2000; Buesseler, 1991). They are sparse in space and time, therefore providing a rather patchy impression about the particle flux in the world ocean. In addition, particles produced at the surface are subject to horizontal transport by advection, hampering the establishment of correlations between surface and deep fluxes, particularly for slowly sinking particles (e.g. a meter per day) in energetic current fields (e.g. a meter per second, i.e. close to 100 km per day) (e.g., Siegel et al., 2008; Frigstad et al., 2015).



It is possibly for these reasons, that attempts to calibrate global models against individual observations of particle flux have not yet revealed any unique “best” model (Gehlen et al., 2006; Kriest and Oschlies, 2013), although they provide some insight into the general ability of models to reproduce the observed magnitude of the deep particle flux (Kriest and Oschlies, 2013). Calibration against primary production also may not provide much insight into the long-term behaviour of global models, as this diagnostic is biased towards quite short time scales. A side effect of this is that simulated primary production can be tuned to (almost) any desired value, by increasing that carbon (nutrient) turnover in shallow waters, without changing the long-term model behaviour, ocean interior tracer concentrations, and the flux of organic matter into the ocean interior (Oschlies, 2001). In addition, simulated global primary production does not seem to be related to any other diagnostic, and thus is not indicative of the overall, long-term biogeochemical model fit to dissolved tracers, that can be measured with rather high accuracy. In contrast, global particle export at 2000m or below shows a clear relationship to the model fit to dissolved nutrients or oxygen (Kriest et al., 2012), indicating the relevance of the model fit to these tracers for its prognostic skill of particle flux and carbon storage in the ocean.

9.2 Parameters that connect surface production with deep particle flux and long-term storage of carbon

It is attractive to use nutrients and / or oxygen data in order to inversely determine the otherwise weakly constrained model parameters for particle flux and remineralisation. The joint effect of particle flux and remineralisation is often described by one or two parameters in global models. Early models referred to an exponential function of remineralisation with depth (Bacastow and Maier-Reimer, 1991), which - in equilibrium - would correspond to constant particle sinking rate and remineralisation. Another, very popular approach to describing particle flux (and hence subsequent remineralisation) in ocean models is a power law of depth: $F(z) z^{-b}$, where b is usually set to $b = 0.858$, representing the open-ocean composite value derived by Martin et al. (1987) from sediment traps (e.g., Maier-Reimer, 1993). Empirical observations suggest that b may vary between 0.3-1.4 (Martin et al., 1987; Berelson, 2001; Van Mooy et al., 2002; Buesseler et al., 2007). This range of variation has been tested in global biogeochemical models e.g. for its effect on dissolved tracer concentrations (Kwon and Primeau, 2006, 2008; Kriest et al., 2010, 2012). Kwon et al. (2009) coupled a simple global biogeochemical model with a 1-box atmosphere, and found a large effect of this parameter on atmospheric $p\text{CO}_2$. Considering the continuing popularity of this parameterisation (e.g., Kwon and Primeau, 2006, 2008; Najjar et al., 2007; Parekh et al., 2005) it seems worthwhile to have a closer look at its implicit assumptions and at potential ways to constrain its parameters.

As shown by Kriest and Oschlies (2008), under steady state conditions b can be regarded as equivalent to the rate of vertical increase in particle sinking speed a over constant remineralisation rate r : $b = r/a$. Potential mechanisms that may lead to a vertical increase in sinking speed include selective export of large and fast particles to deeper layers, or repackaging of small particles into larger ones by zooplankton egestion. Alternatively, one may consider sinking speed to be constant with depth, and remineralisation rate to decrease with depth, e.g., by particles becoming more refractory and less susceptible to bacterial degradation, or because of a temperature-dependent decline in bacterial activity. However, other parameterisations of particle flux profiles have been applied in global models, e.g., constant sinking and remineralisation (leading to an exponential flux curve; e.g., Bacastow and Maier-Reimer, 1991), or models that explicitly simulate different groups of particles with different



size and properties (e.g., Gehlen et al., 2006; Schwinger et al., 2016). Cabre et al. (2015) provide an excellent overview about different parameterisations for models applied in CMIP5.

Even though there exists a variety of such structurally simple parameterisations of particle export and remineralisation, so far few attempts have been made to calibrate these in global models in a systematic manner, most likely because of the computational and observational constraints mentioned above. Kwon and Primeau (2006) used a simple biogeochemical model coupled to global circulation to optimise b against observations of annual mean phosphate, and found an optimal and well constrained b of ≈ 1 . This is in some contrast to recent attempts by Wilson et al. (2015), who could not diagnose flux profiles from phosphate changes derived from simulated circulation divergence (within a model time step). They attributed this to the errors in circulation-driven transport of phosphate dominating over the small remineralisation rates, together with errors in observations. Given the successful calibration by Kwon and Primeau (2006), it remains to be investigated whether these different results are associated with the different time scales considered in both approaches. Recent optimisations of a more complex biogeochemical model against similar data sets (and using the same circulation fields as used by Wilson et al., 2015) could successfully recover b (Kriest et al., in preparation), resulting in optimal values of ≈ 1.3 , i.e. slightly larger than the optimal b recovered by Kwon and Primeau (2006). We note that all of these studies are likely very dependent on the applied circulation fields, which are also uncertain. Studies comparing the effects of different circulation fields on parameter estimates are so far lacking, due to the high computational demands. One exception is the study by Kriest and Oschlies (2013), who found the same sensitivity of model fit to observed dissolved tracers for a coupled global model forced by two different circulation fields.

It should be kept in mind that parameters associated with processes acting in the sunlit surface layers of the ocean and those responsible for deep sedimentation and long term-storage of carbon act on very different spatial and temporal scales, posing a challenge for simultaneous estimation on a global scale. Kriest et al. (in preparation) carried out a set of optimisations of six biogeochemical parameters against climatologies of annual mean oxygen, nitrate and phosphate, within a global, offline circulation model. Two parameters were associated with phytoplankton growth, and two with zooplankton grazing and mortality, i.e. processes confined to the surface layer. Two additional parameters were associated with deep processes, interacting more closely on long (circulation) timescales, namely the stoichiometric ratio of oxygen to phosphate, $R_{-O_2:P}$, and particle sinking profile, expressed as b (see Kriest and Oschlies, 2015, for more information on the biogeochemical model and its coupling to the circulation fields). The optimisation used an “Estimation of Distribution Algorithm” with a population size of 10 individuals (model runs) per generation, and finished after 182 generations, resulting in a total of 1820 model simulations.

Kriest et al. (in preparation) found that particularly zooplankton mortality (but also other parameters related to phytoplankton and zooplankton turnover) were more weakly constrained by the data than the “deep” parameters $R_{-O_2:P}$ and b , which can be explained by the choice of the misfit function (annual mean dissolved tracers on a global scale). The sensitivity of two contrasting parameters to this function is illustrated in Fig. (8), showing the parameter-cost function manifold projected onto values quadratic zooplankton mortality κ_{zoo} (left panels) and rate of vertical increase of particle sinking speed, a , expressed as quotient $b = r/a$ (r is particle remineralisation rate; right panels). To examine the parameter hyperspace, in analogy to Eq. (13), we defined two criteria for individuals sufficiently close to the optimum, via $\Delta_J = J(\Theta)/J(\hat{\Theta}) - 1$, namely $\Delta_J = 0.01$ and



$\Delta_J = 0.001$. All individuals that satisfied one of these criteria were selected from the entire population trajectory, and grouped into 50 classes distributed evenly over the predefined parameter range. As can be seen from the plots in Fig. (8), b (or particle sinking speed) has a very well defined minimum, resulting in a unimodal distribution for this parameter, regardless of the Δ_J criterion. It is different for the zooplankton mortality that exhibits a bimodal distribution for solutions where $\Delta_J = 0.01$.

5 Obviously, annual mean climatologies of dissolved inorganic tracers provide little information on the - dynamic - behaviour of zooplankton in the upper layers, while particle sinking and decay, which integrates over large spatial and temporal scales, is well defined by the large-scale distribution of dissolved inorganic tracers. We note that the half-saturation constant for phosphate uptake by phytoplankton shows a pattern similar to zooplankton mortality, which indicates a collinearity with both parameters being mutually dependent. Thus, in the presence of very diverse time and space scales, as typical for global biogeochemical

10 ocean models, the choice of the data set and misfit strongly affects the detectability of parameters.

9.3 Impact of parameter uncertainties on climate model projections into the future

A typical large-scale application of marine biogeochemical models is their use in Earth system models from which projections of future climate change can be derived for different emission and land-use scenarios. Output of such models helps to inform scientists, but also society and policymakers about possible consequences of human action on the climate system. A key

15 example is the most recent assessment report of the Intergovernmental Panel on Climate Change (IPCC) that featured Earth system models with fully interactive carbon cycle. An appropriate treatment of the uncertainties contained in the applied scenarios and employed models is crucial for correctly interpreting model projections, informing the societal debate about climate policies and thus strengthening the base for developing relevant measures.

A comprehensive attempt to account for uncertainties in the models when determining likelihoods of reaching certain climate

20 goals like the politically widely accepted 2°C warming goal, was presented by Steinacher et al. (2013) and Steinacher and Joos (2016). Employing a somewhat simplified Earth system model of intermediate complexity, they ran perturbed parameter ensembles with some ad hoc assumptions about prior probability distributions of the model parameters. The skill of individual ensemble members was then measured by comparison of model hindcasts with available observations of the current state of the Earth system. A single, pragmatic skill score was used in the assessment and led to an improved posterior estimate of parameter

25 probability distributions. The model dynamics then mapped the parametric uncertainty onto the model projections. From the large ensemble of model solutions that were, in hindcast mode, not inconsistent with the observational constraints, the authors could then successfully derive likelihoods of reaching various climate goals.

Note that reproducing the current climate state is merely a necessary condition for model skill, but may not constrain the model's ability to correctly simulate the sensitivity to natural or anthropogenic environmental change. Observational informa-

30 tion on past climate change, such as glacial-interglacial changes may help to better constrain the models' sensitivity to changing environmental conditions, even though no historical analog to the current anthropogenic perturbation is known in terms of the rapid rate of change. Still, any information about model sensitivities to applied perturbations is extremely valuable, be it derived from lab or mesocosm experiments or from historical information. DA is a promising tool to combine such information



on very different space and time scales and to develop an improved understanding of how the earth system works and may respond to ongoing environmental change.

10 Summary and perspectives

The survey done by Arhonditsis and Brett (2004) revealed only a small fraction of all aquatic biogeochemical modelling studies
5 a) considered parameter optimisation (8.5%), b) provided values of data-model misfit (30 %), or c) performed quantitative
parameter sensitivity analyses (28%). Since then there has been a vast increase in the number of those studies where the
assimilation of biological and chemical data into planktonic ecosystem models are described. Likewise, we now find a wide
field of different studies that address problems of parameter identification. Although positive, this development has also brought
up diverse approaches whose contexts and connections are sometimes difficult to understand. Furthermore, we face a variety
10 in terminology and notation, which makes it even more arduous to distinguish between negligible and important findings. With
this review we aim to provide support to readers.

The theoretical backbone for studies of parameter estimation and uncertainty builds first of all on how model errors and
observational errors are treated. Specifying the error model is an essential first step in the workflow of parameter identification,
enabling the subsequent derivation of conditional probabilities and cost functions. Our review shows that there is no ultimate
15 standard error model or procedure but a meaningful practice is to become explicit about these errors and to reconsider the
underlying assumptions for discussions of parameter estimates and model results. Whether the DA approach conserves mass
and/or energy is relevant in this respect.

As in many other fields of science, the basic estimation methods considered in plankton ecosystem DA studies are Bayesian
estimation and Maximum Likelihood. Their major difference is how prior information enters the DA approach and how the
20 posterior is evaluated. The consideration of prior parameter values from preceding studies is meaningful and likely alleviates
parameter identification problems. A drawback then is that asymptotic (point-wise) approximations of posterior uncertainty
covariance matrices, as described herein, may not apply. But when the model parameters in question have been estimated
before in a number of comparable settings, it may seem a tragic waste of effort and information to pursue a ML approach
without prior information. A similar issue arises in specifying an “ignorance” prior and the choice of using BEs when no prior
25 information is available can also be questioned.

We included a section on typical basic parameterisations of plankton models, mainly to stress that the treatment of light- and
nutrient limitation may differ between modelling studies. Furthermore, we touched on the problem of resolving phytoplankton
losses specified by e.g. grazing and aggregation parameters. Latest plankton growth models account for physiological accli-
30 mation effects, responsible for variations between carbon fixation, cellular allocation of nitrogen and phosphorus, and Chl*a*
synthesis. Those variations are relevant for DA, in particular if flux estimates of carbon (e.g. CO₂ utilisation and respiration)
are of primary concern. It is thus worthwhile to discuss some of the underlying dynamics that can be resolved with the plankton
ecosystem model rather than treating it as a “black box” for simulating Chl*a* concentrations as in some DA approaches.



Many acclimation or optimality-based models have been qualitatively calibrated with data from laboratory experiments. DA approaches for parameter estimation were only done in a few of these studies. Going from laboratory data to the assimilation of data from mesocosm experiments can be a useful intermediate step for testing e.g. acclimation or adaptive models and for assessing uncertainty ranges of parameter values. In this respect, parameter estimates of one experiment can be used for cross-validation with data of another independent mesocosm experiment. On the one hand, a main advantage is that simulations of the physical environment of mesocosms are easier to implement, compared e.g. to setting up a 1D-model for an ocean site. On the other hand, a drawback is that parameter estimates obtained from the assimilation of mesocosm data might not be representative for ocean simulations. Although more difficult, model cross-validations between different ocean sites or regions provide valuable insight, eventually specifying a model's predictive skill under oceanic conditions.

Some studies have shown that an increase in model complexity may not automatically improve predictive skill. This can partially be attributed to over-fitting, which can yield parameter estimates that improve model-data misfits at one site but induce unreasonable model results at other ocean sites. Such results illustrate the vital role played by well-designed cross-validation experiments. A critical element of cross-validation is whether the assimilated data are truly independent from the data used for testing model skill. This is, for instance, not really the case if observations from different years but of the same characteristic region are used. Regional differences between parameter estimates are informative and they rigorously disclose a model's merits and limitations.

Parameter identification becomes more difficult as we go from local and regional scale to large-scale and global model simulations. Algorithms for parameter optimisation require multiple model evaluations, which can be computationally expensive for global biogeochemical models. The procedure for optimising parameter values can be accelerated with the application of an emulator. We discussed the usage of dynamical and statistical emulators. Both emulator approaches have been shown to efficiently support the search for optimal parameter values. The development and usage of emulators of biogeochemical models will likely gain in importance along with improved computer performance. A promising approach is to use models with coarser resolution or a series of 1D-models (distributed over ocean regions) as dynamical emulators for 3D-global biogeochemical model simulations. Studies have shown that sufficient accuracy of the emulator can be achieved with repeated intermediate alignments of the dynamical emulator. Alternatively, differences between 1D- and 3D results can be statistically evaluated as emulator error during the parameter search process, which is then used to update the "emulator" based cost function.

Parameter identification in global marine biogeochemical circulation models is still in its infancy, due to the high computational requirements, the huge range of spatial and temporal scales to be covered, and the comparatively sparse spatial-temporal distribution of data in the ocean. In contrast to local optimisations, the consideration of all relevant spatial and temporal scales has one major advantage in that it provides the opportunity to rigorously test and benchmark biogeochemical models. In addition to tasks and complications mentioned in our review, care must be taken in the selection of appropriate data sets, assuring their relevancy (or potential) for answering the questions posed. Moreover a critical evaluation of the respective roles of physics, biogeochemistry, exchanges across the model's boundaries and, possibly, ecology is an as yet unresolved task.



10.1 Grasping complexity of a plankton ecosystem but keeping number of free parameters low

A desirable state for modelling plankton dynamics and biogeochemical cycles is to require some minimum number of parameters while capturing most of the complexity involved in the transfer of energy and mass in the ocean (e.g., Denman, 2003). To accomplish this we may not only think of new model approaches, but also of collecting respective data that can help to constrain solutions of these models. Analyses of plankton size measurements and the derivation of plankton size density spectra is one good example in this respect. A commonality of new model formulations is to focus on principles, e.g. adaptation of traits towards optimal trade-offs (e.g., Wirtz and Pahlow, 2010; Dutkiewicz et al., 2009; Smith et al., 2015), allometric relationships in growth and plankton interaction (e.g., Banas, 2011; Ward et al., 2012; Acevedo-Trejos et al., 2015). Perhaps one of the most remarkable developments is the revival of thermodynamically inspired ecosystem theories for modelling biogeochemical cycling in the oceans (e.g., Vallino, 2011). In the review of Vallino and Algar (2016) the concept and potential of the maximum entropy production principle is addressed. In this modelling approach life in the ocean is perceived as units of e.g. covalent bonded chains of carbon atoms that create disequilibria of energy and mass between organisms. These disequilibria lead to different functional pathways in biogeochemical cycling, accompanied by a flexible evolution of structural dependencies between nutrient or substrate availability, plankton and other organisms. Such novel (or revised) approaches are expedient and help create new ideas in terms of what to measure and what kind of corresponding model would be needed, thereby reducing problems of parameter identification.

10.2 Harmonising research foci in marine ecosystem modelling and data assimilation

The application of DA methods has become standard for calibrating marine ecosystem- and biogeochemical models. But scientific insight can differ between DA studies considerably. In the literature we find a growing disproportion between level of sophistication of the ecosystem model used and DA method employed, for example when obsolete parameterisations of plankton growth are combined with an up-to-date, sophisticated DA approach, or vice versa. This dissonance is likely owed to the fact that marine ecosystem-/biogeochemical modelling studies integrate knowledge from different scientific fields, of which each has its own foci, objectives, and expertise i.e. plankton ecology, physical oceanography, marine geochemistry, and mathematics and statistics. It is difficult to track major advancements in marine ecosystem modelling when considering the different views from each of these research fields. Furthermore, the design of experimental studies and the collection of field data are often achieved without harmonising the needs of biologists with the modelers' exigencies (Flynn, 2010).

Facets of parameter identification in biological modelling disclose major commonalities and disparities between the objectives expressed in these different research fields. Discussions on parameter identification are therefore helpful to achieve a common understanding and to promote communication between observers, modelers, and statisticians.

Author contributions. Individual sections of our review were written by one or more lead author(s), with contributions from the other authors (Phil Wallhead, PW; John Hemmings, JH; Ben Ward, BW; Ulrike Loeptin, UL; Thomas Slawig, TS; Iris Kriest, IK; Andreas Oschlies, OA, and Markus Schartau, MS). All authors were involved in mutual revisions of the individual sections. The sections' lead authors are:



1. Introduction (MS), 2. Theoretical background (PW, MS, and JH), 3. Error models (PW), 4. Parameter uncertainties (MS), 5. Typical parameterisations of plankton models (MS), 6. Cross-validation and model complexity (BW), 7. Space-time variations in model parameters (JH), 8. Emulator approaches (UL and TS), 9. Parameter estimation of large-scale biogeochemical ocean circulation models (IK and AO), 10. Summary and perspectives (MS), Appendix A (PW), Appendix B (MS), and Appendix C (MS and TS). Shubham Krishna performed parameter optimisations, MCMC computations of the mesocosm modelling example, as well as calculations of the 2D parameter arrays.

Acknowledgements. We gratefully acknowledge the support from the International Space Science Institute (ISSI). This publication is an outcome of the ISSI's Working Group on "Carbon Cycle Data Assimilation: How to consistently assimilate multiple data streams". Examples of mesocosm data assimilation are based on the mesocosm modelling environment designed for the large integrated projects Surface Ocean Processes in the Anthropocene (SOPRAN, 03F0662A) and BIOACID (03F0728A), both funded by the German Federal Ministry of Education and Research (BMBF). Contributions from Iris Kriest, Ulrike Löptin, and Thomas Slawig were supported by the BMBF funded PalMod - Paleo Modelling: A national paleo climate modelling initiative.

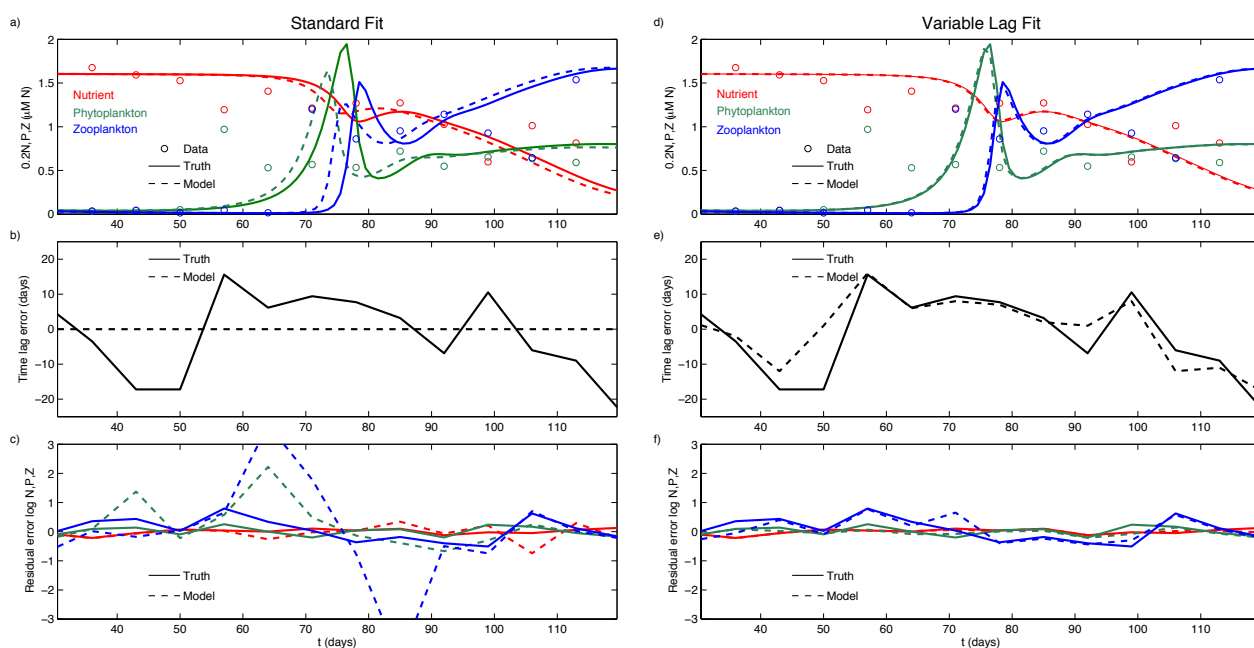


Figure 1. Demonstration of the Variable Lag Fit (VLF) applied to a simulated data set. a) shows the system trajectory with the true parameter values (solid lines), the data (dots) simulated assuming normal and independent time lag errors ($\sigma_\tau = 10$ days) and residual errors ($\sigma_{\log N,P,Z} = 0.1, 0.2, 0.3$, see Table A), and the system trajectory with the VLF parameter estimates (dashed lines, overlapping with solid). b) compares the true time lags (solid) with those estimated from the VLF (dashed). c) compares the true residual errors with those estimated by the VLF (dashed, same colour code as in a)). Three years of data were assimilated but only the initial and post-bloom period of the first year is shown for clarity.

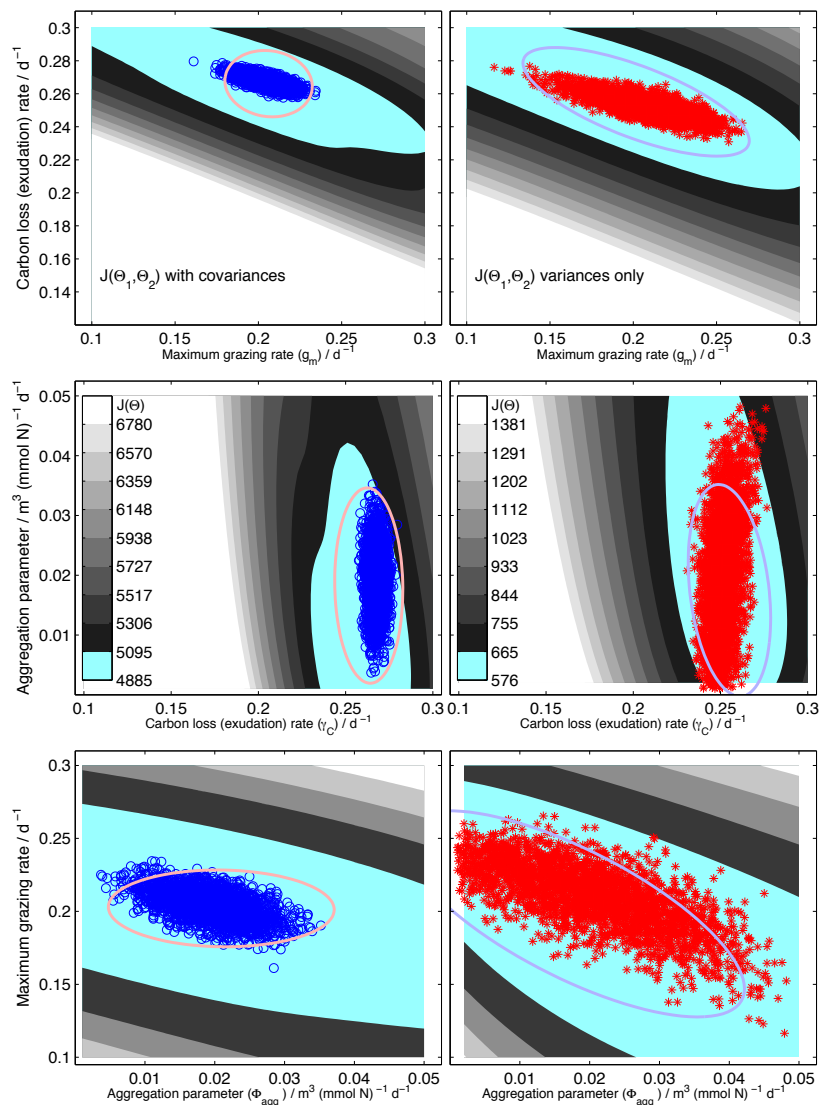


Figure 2. Cost function contours when varying values of a combination of two parameters $J(\hat{\Theta}_m \pm \Delta_m, \hat{\Theta}_n \pm \Delta_n)$ around the optimum estimate at $(\hat{\Theta}_m, \hat{\Theta}_n, \min(J))$, while values of all other parameters remain fixed. Each plot resolves a pairwise combination out of three parameters that all specify phytoplankton biomass losses: 1) carbon exudation rate ($\Theta_1 = \gamma_C$), 2) maximum grazing rate ($\Theta_2 = g_m$), and 3) aggregation parameter ($\Theta_3 = \Phi_{\text{agg}}$). Markers show credible regions of parameter estimates obtained with Markov Chain Monte-Carlo (MCMC) method (dots for J with covariances, asterisks for J with variances only). Error ellipses (lines) depict point-wise 95% confidence regions derived from an approximated and inverted Hessian matrix, according Eq. (19). The cyan colored region embeds all cost function values that are lower than an upper threshold $\Delta J^*(\alpha = 0.05)$, derived from a distribution of $J(\hat{\Theta}) - J^*(\hat{\Theta})$, where $J^*(\hat{\Theta})$ are cost function values at $\hat{\Theta}$ using resampled data (Fig. B in Appendix).

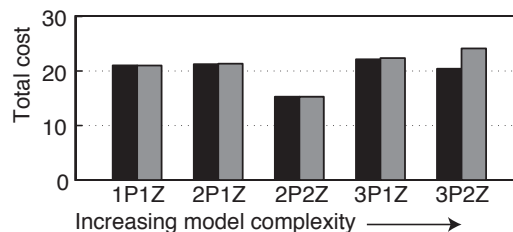


Figure 3. Predictive skill for five ecosystem models of different complexity, after assimilation of satellite data (black) and after assimilation of satellite data with 20% added noise (grey) (Xiao and Friedrichs, 2014a). The most complex model appear to be the most sensitive to errors in the data, in terms of its cross-validated predictive skill.

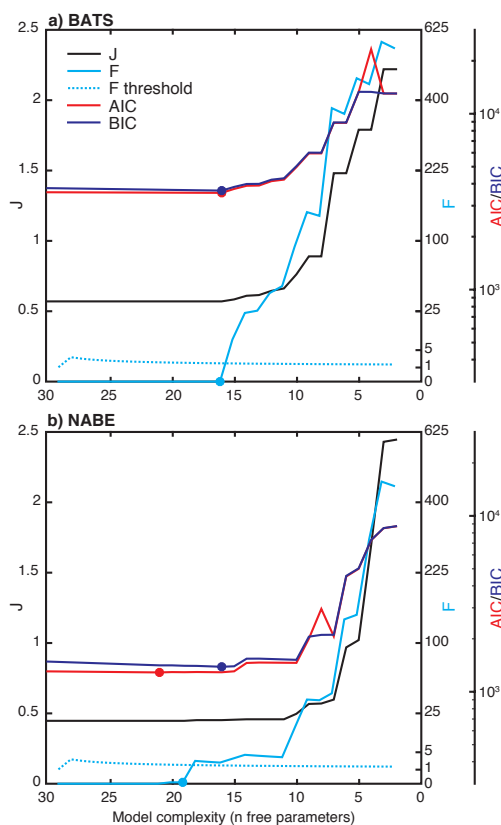


Figure 4. Model selection metrics at the Bermuda Atlantic Time-series Study (BATS) and the North Atlantic Bloom Experiment (NABE), as a function of complexity across a suite of nested ocean biogeochemical models (Ward et al., 2013). The least-squares misfit, J (left-hand axis), increases monotonically with decreasing complexity, as it does not penalise model complexity. The likelihood ratio test, F (first right-hand axis), compares each reduced model to the full model, and selects the simplest that is not significantly worse than the full model ($F < F$ threshold). The AIC and BIC (second right-hand axis) both contain terms that account for model data misfit and complexity, and the optimal model is the one with the lowest score. In each case, the optimal model is indicated by a dot.

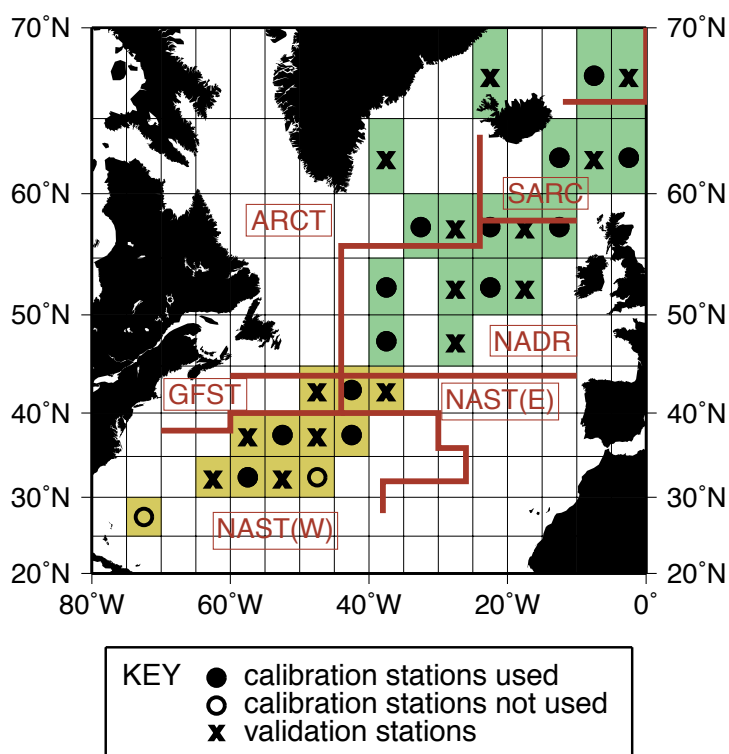


Figure 5. Geographic extent of the two sub-domains giving the optimal calibration in the split- domain calibration study of Hemmings et al. (2004). Biogeochemical provinces defined by Longhurst (1998) are shown for reference. ARCT: Atlantic Arctic Province; SARC: Atlantic Subarctic Province; NADR: North Atlantic Drift Province; GFST: Gulf Stream Province; NAST: North Atlantic Subtropical Gyral Province.

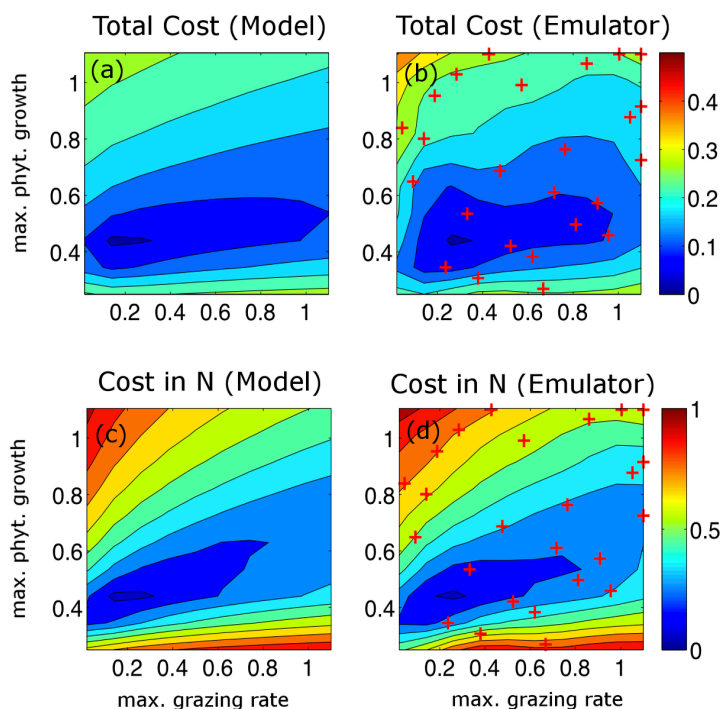


Figure 6. Simulated (a,c) and emulated (b,d) RMS (root mean square) error depending on the "maximum growth rate of phytoplankton" and the "maximum grazing rate". Sub panels (a,b) are based on all prognostic variables, while the RMS error in (c,d) is based on nitrate (NO_3^-) only (c,d). Red crosses mark the training data.

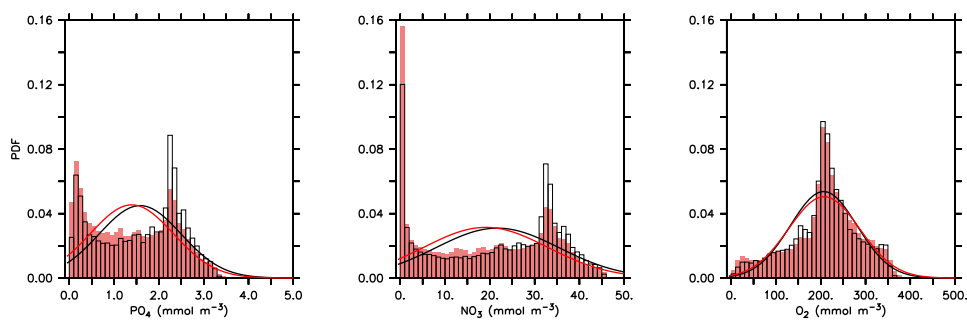


Figure 7. Probability densities (PDFs) of climatological data: observed annual mean phosphate (PO_4 , left), nitrate (NO_3 , middle), and oxygen (O_2 , right), derived from Garcia et al. (2006a, b). Observations were gridded onto ECCO model grid (Stammer et al., 2004); $1^\circ \times 1^\circ$ horizontal resolution, 23 vertical levels), then grouped into 50 bins between 0-5 (phosphate), 0-50 (nitrate) and 0-500 (oxygen) mmol m^{-3} . Light red bars denote frequency densities of non-interpolated values, open bars interpolated (analysed) values. Lines illustrate normal distribution calculated from mean and variance of the unbinned data sets, scaled to the match the y-axis of the discrete PDF (red: non-interpolated; black: interpolated).

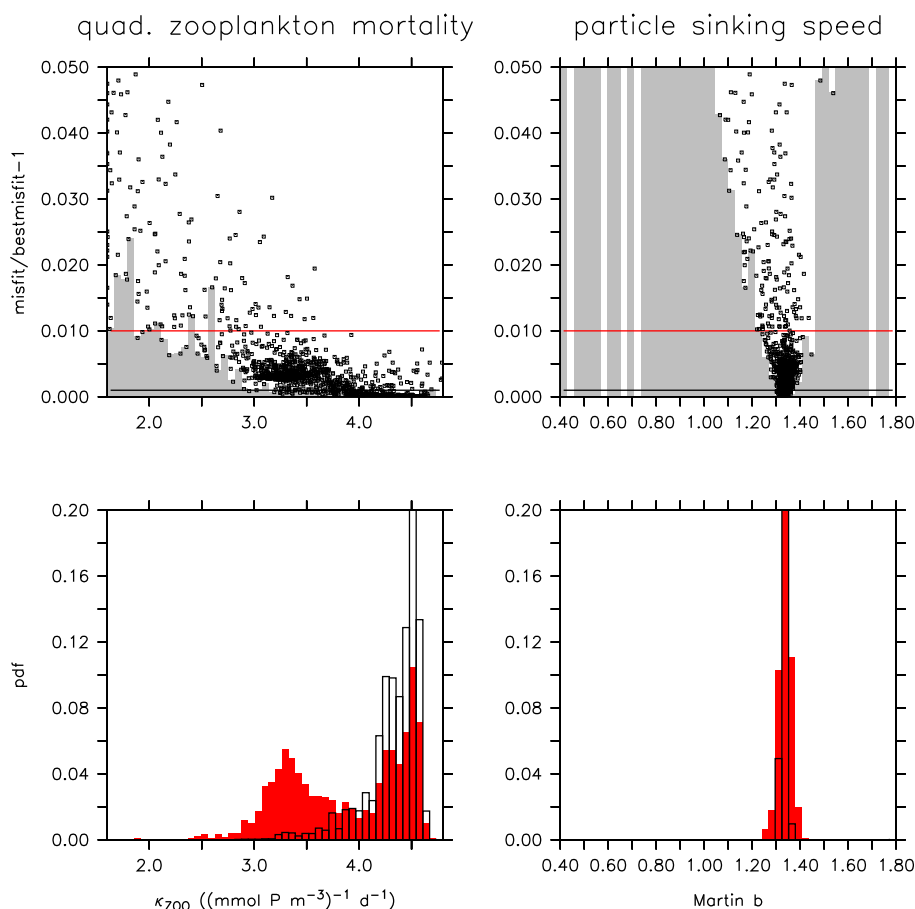


Figure 8. Projections from parameter-cost function manifold $(\hat{\Theta}_I, J(\Theta))$ as obtained during the optimisation of six biogeochemical parameters. Parameters shown are quadratic zooplankton mortality κ_{zoo} (left panels) and rate of vertical increase of particle sinking speed, a , expressed as quotient $b = r/a$, where r is particle remineralization rate (right panels). Upper panels: cost function (volume-weighted root-mean square error, divided by global mean concentration of each tracer) expressed as its deviation from the minimum. Parameters of all model simulations in the optimisation trajectory were grouped into 50 classes. Grey bars show minimum cost within each class. Red and black horizontal lines indicate deviation from minimum cost of 1% and 0.1%, respectively. Squares show the cost of each individual. Note that the y-axis only extends to 5% above minimum cost at $(\hat{\Theta}, J(\hat{\Theta}))$. Lower panels: parameter distribution (PDF) of all model simulations, whose cost do not exceed a threshold limit of $\Delta_J = 1.01 \cdot J(\hat{\Theta})$ (1%, red bars) or $\Delta_J = 1.001 \cdot J(\hat{\Theta})$ (0.1%, open bars) of the minimum cost, see Eq. (13 and text).



Appendix A: The Variable Lag Fit with unknown error variances (Sect. 3.4)

In a Variable Lag Fit (VLF), we assume that the truth at time t_i is related to the model output by a kinematic model error (ζ) in phase or time lag τ_i . Equation (2) becomes:

$$\mathbf{x}^t(t_i) = \mathbf{x}(t_i + \tau_i) \quad (\text{A1})$$

- 5 A notable feature of this model error representation is that it introduces unknowns τ that can be conditionally optimised by searching forwards and backwards in time within saved model output, i.e. *without rerunning the dynamical model*. For the demonstration in Fig. (1) we assumed that the time lag errors are normal and independent: $\tau_i \sim N(0, \sigma_\tau^2)$. This independence assumption may seem restrictive; for example, a misplaced eddy might be expected to impose some correlation between the τ_i for a set of cruise data. Nevertheless, we find that the method is somewhat robust to neglected lag correlation. Moreover, this formal neglect enables a large computational simplification since the lags can
 10 then be optimised one by one, see Wallhead et al. (2006).

For the observational error in Fig. (1) we assumed lognormal errors with no interpolation or conversion factors, and that all measured variables were sampled simultaneously. Equation (3) becomes:

$$y_{ij} = x_{ij}^t \cdot \exp\left(\epsilon_{ij} - \frac{\sigma_j^2}{2}\right) \quad (\text{A2})$$

- at each measurement time t_i and for each measured variable j (Nutrient, Phytoplankton and Zooplankton). For simplicity we further
 15 assumed that the observational errors were independent between measurements and data types, hence $\epsilon_{ij} \sim N(0, \sigma_j^2)$. Note that the ϵ may be considered to include a component of kinematic model error (ζ) without affecting the parameter estimation, hence we refer to them as *residual* errors below. Assuming that the ecosystem parameters θ_e , time lags τ , time lag variance σ_τ and observational error variances σ are all unknown, a joint posterior mode estimate of $\Theta = (\theta_e, \tau, \sigma_\tau, \sigma)$ is obtained by maximising the posterior density $p(\Theta | \mathbf{y})$, equivalent to minimising the following cost function:

$$20 \quad J(\Theta) = n \log \sigma_\tau^2 + \sum_i \frac{\tau_i^2}{\sigma_\tau^2} + n \sum_j \log \sigma_j^2 + \sum_{ij} \frac{(\log y_{ij} - \log x_j(t_i + \tau_i) + 0.5\sigma_j^2)^2}{\sigma_j^2} \quad (\text{A3})$$

- To test this cost function, we simulated data from the NPZD model of Oschlies and Garçon (1999) in a 0D setting using the parameters values and sine-squared forcing function from Wallhead et al. (2013). Three years of simultaneous weekly samples of N , P , and Z were simulated assuming independent normal time lag errors with standard deviation $\sigma_\tau = 10$ days and independent normal residual errors $\sigma_{\log N} = 0.1$,
 25 $\sigma_{\log P} = 0.2$, $\sigma_{\log Z} = 0.3$. The data were assimilated into the same NPZD model by one of two methods. In the ‘standard fit’, no time lag error was assumed and search parameters $\Theta = \{\theta_e, \sigma_{\log N}, \sigma_{\log P}, \sigma_{\log Z}\}$ were estimated by minimising only the final two terms in A3 with $\tau_i = 0$ for all i . In the VLF, $\Theta = \{\theta_e, \tau, \sigma_\tau, \sigma_{\log N}, \sigma_{\log P}, \sigma_{\log Z}\}$ was estimated by minimising Eq. (A3). In both cases, we assume uncertainty in only two of the 15 biological parameters, namely the phytoplankton maximum uptake rate V_m and the zooplankton maximum grazing rate g (hence $\theta_e = (V_m, g)$). For all search parameters, allowed ranges were $\pm 50\%$ about the true values, equivalent to unbiased uniform priors
 30 with 29% prior uncertainty. Initial values of the search parameters were chosen at random from this prior, and optimisations were repeated over 10 random restarts to avoid local minima. The experiment was repeated over 20 simulated data sets to obtain the statistics in Table (A).

Caution must be exercised here regarding the estimation of σ_τ . If the prior for σ_τ permits very low or zero values then the MAP estimation will push the estimate of σ_τ towards zero irrespective of its true value. This is because, unlike the fourth term in Eq. (A3), the second term



can be made exactly zero with $\tau = 0$ as long as $\sigma_\tau^2 > 0$, in which case the negative contribution of $n \log \sigma_\tau^2$ may produce a spurious, deeper minimum of J near to $\sigma_\tau = 0$. We have found that this spurious minimum need not influence estimation as long as the sample size and the lower limit of the allowed range or rectangular prior for σ_τ are sufficiently large, Fig. (A). An alternative solution may be to assume a prior that drops smoothly to zero as $\sigma_\tau^2 \rightarrow 0$, such as an inverse gamma distribution (cf., Kavetski et al., 2006a).

- 5 To investigate estimation of the time lag variance parameter σ_τ we obtained cost function profiles by fitting the same data set using a range of fixed values of σ_τ , Fig. (A). We see that with three years of weekly NPZ sampling the cost function function has a strong minimum close to the true value of 10 days, and this minimum should be approached even if the allowed range (prior uncertainty) for σ_τ reaches as low as 1 day. However, if we decrease the number of sampled years, or especially the number of sampled variables, the minimum becomes weaker and a spurious minimum close to $\sigma_\tau = 0$ starts to encroach on the profile. A sufficiently low minimum allowed value $\sigma_\tau^{(\min)}$ may then lead
- 10 to estimates converging to this spurious minimum.

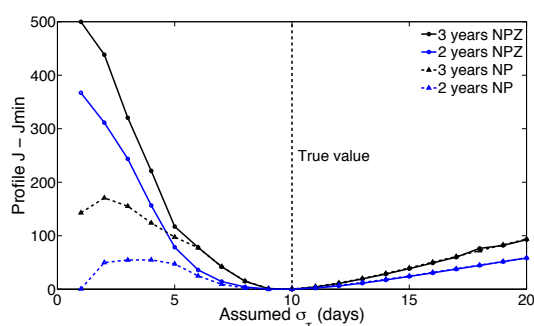


Figure A. Profiles of the Variable Lag Fit cost function ($-2 \times$ posterior density) relative to the minimum value for a range of assumed values of the time lag error standard deviation σ_τ . For each σ_τ , Eq. (A3) was minimised over $(\theta, \tau, \sigma_{\log N, P, Z})$ for the same data set. Different curves correspond to different scenarios for the number of sampled years (at weekly sampling frequency) and number of simultaneously sampled variables (black = 3 years, blue = 2 years, solid lines with circles = Nutrient-Phytoplankton-Zooplankton sampling, dashed lines with triangles = Nutrient-Phytoplankton sampling). The extent to which each curve has a deep minimum close to the true value $\sigma_\tau(\text{true}) = 10$ days indicates the feasibility of estimating σ_τ for the corresponding sampling plan.



Table A. True parameter values and means ± 1 SD of estimates over 20 simulated data sets, using a standard fit method and a variable lag fit method (see Eq. A3). Three years of weekly NPZ data were simulated using the true values (first row) for the maximum nutrient uptake rate V_m , zooplankton grazing rate g , residual standard deviations $\sigma_{\log N, P, Z}$, and time lag standard deviation σ_τ (for experiments with lags imposed). With no time lags, the standard fit accurately recovers the true parameter values (third row), but with time lags (fourth row) the standard grazing rate estimates are biased and imprecise, while the residual variances have strong positive bias as they are forced to account for the time lag errors. The variable lag fit avoids these biases and accurately partitions the variance between residual error and time lag error (fifth row).

	Lags?	V_m (day ⁻¹)	g (day ⁻¹)	$\sigma_{\log N}$	$\sigma_{\log P}$	$\sigma_{\log Z}$	σ_τ (days)
True values	—	0.66	2.00	0.10	0.20	0.30	10.0
First guesses	—	0.66 \pm 0.19	2.00 \pm 0.58	0.10 \pm 0.03	0.20 \pm 0.06	0.30 \pm 0.09	10.0 \pm 2.9
Standard fit	No	0.66 \pm 0.00	2.03 \pm 0.07	0.10 \pm 0.01	0.20 \pm 0.01	0.31 \pm 0.01	—
Standard fit	Yes	0.68 \pm 0.03	2.61 \pm 0.44	0.27 \pm 0.02	0.46 \pm 0.07	0.75 \pm 0.14	—
Variable Lag Fit	Yes	0.67 \pm 0.01	2.03 \pm 0.19	0.07 \pm 0.01	0.18 \pm 0.02	0.29 \pm 0.02	9.2 \pm 0.7

Appendix B: Mesocosm example (Sect. 5.3.3)

For our example we account for six types of measurements from mesocosms of the Pelagic Ecosystem CO₂ Enrichment Study (PeECE I, Engel et al., 2005; Delille et al., 2005): 1) dissolved inorganic carbon (DIC, mmol m⁻³), 2) nitrate (NO₃⁻, mmol m⁻³), 3) nitrite (NO₂⁻, mmol m⁻³), 4) Chl_a (mg m⁻³), 5) PON (mmol m⁻³), 6) POC (mmol m⁻³). Concentrations of NO₃⁻ and NO₂⁻ are not explicitly resolved by the model and therefore these measurements are combined. We refer to their sum as dissolved inorganic nitrogen (DIN). Thus, the number of components of the observation vector is \mathbf{y} is $N_y = 5$. Observations are available on a daily basis over a period of 23 days ($N_t = 23$). The vector includes daily means of nine mesocosms at t_i , $i = 1, \dots, N_t$:

$$\mathbf{y}_i = \begin{pmatrix} \text{DIC}_i \\ (\text{NO}_3^- + \text{NO}_2^-)_i \\ \text{Chl}_{a_i} \\ \text{PON}_i \\ \text{POC}_i \end{pmatrix} \quad (\text{B1})$$

The dynamical model equations determine twelve state variables ($N_x = 12$). The corresponding vector of model counterparts to observations (also daily means of nine mesocosm simulations):

$$H_i(\mathbf{x}) = \begin{pmatrix} \text{DIC}_i \\ \text{DIN}_i \\ \theta_i^{\text{chl:C}} \cdot \text{PhyC}_i \\ (\text{PhyN} + \text{ZooN} + \text{DetN})_i \\ (\text{PhyC} + \text{ZooC} + \text{DetC} + \text{GelC})_i \end{pmatrix} \quad (\text{B2})$$

with carbon and nitrogen biomass concentrations of phytoplankton (PhyN & PhyC), of zooplankton (ZooN & ZooC), of detritus (DetN & DetC), and carbon concentration of (particulate) macrogels (GelC). Standard errors (σ_i) can be written in matrix notation with off-diagonal



elements being zero:

$$\mathbf{S}_i = \begin{pmatrix} \sigma_i^{(\text{DIC})} & 0 & \dots & 0 \\ 0 & \sigma_i^{(\text{DIN})} & \dots & \vdots \\ \vdots & \vdots & \ddots & 0 \\ 0 & \dots & 0 & \sigma_i^{(\text{POC})} \end{pmatrix} \quad (\text{B3})$$

Correlations during exponential growth (t_i ; $i = 1, \dots, 13$):

$$\mathbf{C}_{(y)} = \begin{pmatrix} & \text{DIC} & \text{DIN} & \text{Chla} & \text{PON} & \text{POC} \\ \text{DIC} & 1 & 0.96 & -0.95 & -0.97 & -0.97 \\ \text{DIN} & . & 1 & -0.96 & -0.95 & -0.95 \\ \text{Chla} & . & . & 1 & 0.96 & 0.92 \\ \text{PON} & . & . & . & 1 & 0.94 \\ \text{POC} & . & . & . & . & 1 \end{pmatrix} \quad (\text{B4})$$

5 Correlations of post-bloom period (t_i ; $i = 14, \dots, 22$) are:

$$\mathbf{C}_{(y)} = \begin{pmatrix} 1 & 0.2 & -0.22 & \mathbf{0.20} & -0.64 \\ . & 1 & -0.37 & -0.26 & \mathbf{0.16} \\ . & . & 1 & 0.63 & \mathbf{-0.26} \\ . & . & . & 1 & \mathbf{-0.55} \\ . & . & . & . & 1 \end{pmatrix} \quad (\text{B5})$$

For days with some missing observations (e.g. no PON measurements), the dimension of the vectors $H_i(\mathbf{x})$ and \mathbf{y}_i and matrices $\mathbf{S}_{(y_i)}$ and $\mathbf{C}_{(y)}$ have to be adjusted for that date accordingly.

10 The mesocosm model environment was coded in FORTRAN and compiled as shared library so that we could use R as free software environment for statistical computations. For parameter optimisation and for the analysis of the posterior (Markov chain Monte Carlo method) we applied the R package FME of Soetaert and Petzoldt (2010).

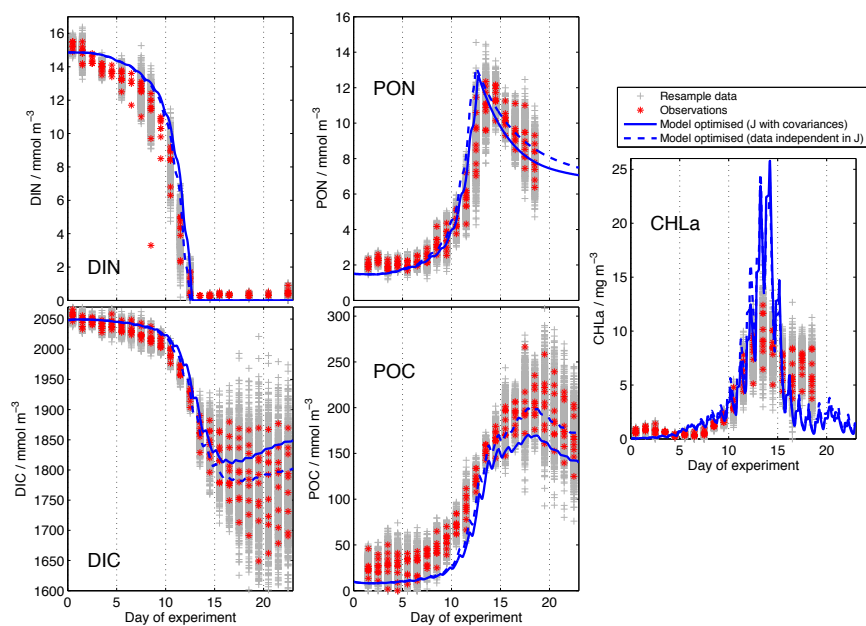


Figure B. Observations of nine mesocosms (red asterisks), resampled data (gray markers) and optimised simulation results (blue lines): Dissolved inorganic nitrogen and carbon (DIN and DIC), particulate nitrogen and carbon (PON and POC), and chlorophyll *a* concentration (CHLa).



Appendix C: Development of an adjoint model (Sect. 4.2.3)

Adjoint models can be used to efficiently compute the derivative (or gradient) of the cost function J . In a parameter identification problem, J depends on Θ both indirectly via the state variable \mathbf{x} and also directly if prior information is incorporated. The optimisation problem can thus be written as

$$5 \quad \min_{\Theta} J(\mathbf{x}(\Theta), \Theta), \quad (C1)$$

where $\mathbf{x} = (\mathbf{x}_i)_{i=0}^{N_t}$ summarize all time instances of the model variables. To evaluate the derivative of the cost w.r.t. the parameters Θ , we may apply the chain rule and obtain

$$\frac{dJ}{d\Theta} = \sum_{i=0}^{N_t} \frac{\partial J}{\partial \mathbf{x}_i} \frac{d\mathbf{x}_i}{d\Theta} + \frac{\partial J}{\partial \Theta}, \quad (C2)$$

where we omitted the arguments $\mathbf{x}(\Theta)$ and Θ for brevity.

- 10 The needed derivatives of the model variables \mathbf{x}_i w.r.t. the parameters Θ can be obtained by taking the total derivative w.r.t. Θ of the equations of the dynamical model, Eq. (1):

$$\frac{d\mathbf{x}_{i+1}}{d\Theta} = \frac{\partial M}{\partial \mathbf{x}_i} \frac{d\mathbf{x}_i}{d\Theta} + \frac{\partial M}{\partial \Theta}, \quad i = 0, \dots, N_t - 1. \quad (C3)$$

This time propagation scheme for the derivatives is often called the tangent linear model.

- 15 The idea behind adjoint models is to avoid this direct computation, whose effort grows linear with the number of parameters Θ . For this purpose, we re-formulate Eq. (C1), treat both arguments of J independently and use the model equation as a constraint in the optimisation process. This can be expressed as

$$\min_{(\mathbf{x}, \Theta)} J(\mathbf{x}, \Theta) \text{ s. t. } \mathbf{x}_{i+1} = M[\mathbf{x}_i, \theta_e, \mathbf{f}], i = 0, \dots, N_t - 1. \quad (C4)$$

- 20 A useful overview of adjoint model construction and applications is given in Kasibhatla (2000). An established approach to construct an adjoint model is to generate adjoint code directly from the numerical code of a model, based on algorithms that implement the chain rule for automatic differentiation (Griewank, 1989, 2003). According to the description of Giering and Kaminski (1998), a numerical model can be treated as a composition of differentiable functions, where each function represents a statement in the numerical code. The differentiation of such composition can be automated by highly sophisticated tools that yield tangent linear and adjoint FORTRAN code (e.g., Faure and Papegay, 1997; Giering and Kaminski, 1998). The application of adjoint construction tools (e.g., Tangent linear and Adjoint Model compiler, TAMC, of Giering and Kaminski, 1998) have been shown to perform well for studies with large-scale ocean general circulation models that include even complicated boundary conditions (e.g., Stammer et al., 1997; Marotzke et al., 1999; Wunsch and Heimbach, 2007; Heimbach et al., 2011).

Another approach is based on a discretised extended Lagrange equation. Under certain mathematical assumptions, a solution of Eq. (C4) corresponds to a saddle-point $(\mathbf{x}, \Theta, \boldsymbol{\lambda})$ of the Lagrangian

$$\mathcal{L}(\mathbf{x}, \Theta, \boldsymbol{\lambda}) = J(\mathbf{x}, \Theta) + \sum_{i=0}^{N_t-1} \boldsymbol{\lambda}_i^\top (M[\mathbf{x}_i, \theta_e, \mathbf{f}] - \mathbf{x}_{i+1}). \quad (C5)$$



The vector $\boldsymbol{\lambda} = (\lambda_i)_{i=0}^{N_t-1}$ contains the Lagrange multipliers λ_i , each of which corresponds to one time step in the model. A saddle-point of \mathcal{L} satisfies the conditions

$$0 = \frac{\partial \mathcal{L}}{\partial \mathbf{x}_i} = \frac{\partial J}{\partial \mathbf{x}_i} + \boldsymbol{\lambda}_i^\top \frac{\partial M}{\partial \mathbf{x}_i} - \boldsymbol{\lambda}_{i-1}^\top, \quad i = 1, \dots, N_t \quad (\text{C6})$$

$$0 = \frac{\partial \mathcal{L}}{\partial \Theta} = \frac{\partial J}{\partial \Theta} + \sum_{i=0}^{N_t-1} \boldsymbol{\lambda}_i^\top \frac{\partial M}{\partial \Theta} \quad (\text{C7})$$

$$5 \quad 0 = \frac{\partial \mathcal{L}}{\partial \boldsymbol{\lambda}} \quad (\text{C8})$$

Here, we again omitted the arguments, and set $\lambda_{N_t} = 0$ in the first equation to keep the compact notation. Note that all derivatives are partial ones since the idea is to decouple \mathbf{x} and Θ and realize their dependency by implying the constraint in Eq. (C4). For simplicity we neglect additional parameter bounds which otherwise would affect Eq. (C7). Taking the derivative in Eq. (C8) for each λ_i separately results in the model equations (Eq. 1) again. From (C6) we deduce

$$10 \quad \frac{\partial J}{\partial \mathbf{x}_i} \frac{d\mathbf{x}_i}{d\Theta} = \boldsymbol{\lambda}_{i-1}^\top \frac{d\mathbf{x}_i}{d\Theta} - \boldsymbol{\lambda}_i^\top \frac{\partial M}{\partial \mathbf{x}_i} \frac{d\mathbf{x}_i}{d\Theta}, \quad i = 1, \dots, N_t$$

and apply Eq. (C3) to obtain

$$\frac{\partial J}{\partial \mathbf{x}_i} \frac{d\mathbf{x}_i}{d\Theta} = \boldsymbol{\lambda}_{i-1}^\top \frac{d\mathbf{x}_i}{d\Theta} - \boldsymbol{\lambda}_i^\top \left(\frac{d\mathbf{x}_{i+1}}{d\Theta} - \frac{\partial M}{\partial \Theta} \right), \quad i = 1, \dots, N_t$$

where $\lambda_{N_t} = 0$ as above. Summing up gives

$$15 \quad \begin{aligned} \sum_{i=1}^{N_t} \frac{\partial J}{\partial \mathbf{x}_i} \frac{d\mathbf{x}_i}{d\Theta} &= \boldsymbol{\lambda}_0^\top \frac{d\mathbf{x}_1}{d\Theta} + \sum_{i=1}^{N_t} \boldsymbol{\lambda}_i^\top \frac{\partial M}{\partial \Theta} \\ &= \boldsymbol{\lambda}_0^\top \frac{\partial M}{\partial \mathbf{x}_0} \frac{d\mathbf{x}_0}{d\Theta} + \sum_{i=0}^{N_t} \boldsymbol{\lambda}_i^\top \frac{\partial M}{\partial \Theta} \end{aligned}$$

where we used again Eq. (C3) for $i = 1$. The first term includes the derivative of the initial values \mathbf{x}_0 w.r.t. the parameters and in many cases will be zero. As result, the derivative of the cost can be computed from Eq. (C2) using the multiplier vector $\boldsymbol{\lambda}$, but without the tangent linear model. Note that the derivative of the model w.r.t. Θ in the sum is a *partial* derivative only, thus it does not include the derivative of the model variables, but only those of the model equations w.r.t. Θ .

20 The multipliers λ_i satisfy a time-stepping scheme themselves, but in reverse direction. Using the transposed form of (C6), we obtain

$$\boldsymbol{\lambda}_{i-1} = \left(\frac{\partial M}{\partial \mathbf{x}_i} \right)^\top \boldsymbol{\lambda}_i + \left(\frac{\partial J}{\partial \mathbf{x}_i} \right)^\top, \quad i = N_t, \dots, 1, \quad (\text{C9})$$

with $\lambda_{N_t} = 0$ (see above) as starting point of the computation. Since here the transposed (or adjoint) of the linearisation of the model operator M occurs, these equations are referred to as the adjoint equations or the adjoint model. Accordingly, the multipliers $\boldsymbol{\lambda}$ are also referred to as adjoint variables or adjoints. Given a model trajectory \mathbf{x} and using Eq. (C9), the trajectory of the adjoints $\boldsymbol{\lambda}$ can be computed. It is crucial to
 25 note that both time-stepping schemes, for the variables \mathbf{x} and the adjoints $\boldsymbol{\lambda}$, have opposite directions. This requires – except for the case of a linear model M – the complete model trajectory to be stored or recomputed in order to compute $\boldsymbol{\lambda}$.

The adjoint model construction starting from a discretised extended Lagrange equation, Eq. (C5) can easily become extensive, in particular when discretisations of advection and mixing are included in the model dynamics. Furthermore, even small changes in the equations can entail considerable additional efforts in updating the adjoint model equations. The application of automatic differentiation tools may therefore
 30 be better suited for cases where the ecosystem dynamical model is subject to regular modifications.



References

- Acevedo-Trejos, E., Brandt, G., Bruggeman, J., and Merico, A.: Mechanisms shaping size structure and functional diversity of phytoplankton communities in the ocean, *Scientific Reports*, 5, 2015.
- Aksnes, D. L. and Egge, J. K.: A theoretical model for nutrient uptake in phytoplankton., *Marine Ecology Progress Series*, 70, 65–72, 1991.
- 5 Anderson, T. R.: Plankton functional type modelling: running before we can walk?, *Journal of Plankton Research*, 27, doi:10.1093/plankt/fbi076, 2005.
- Anning, T., MacIntyre, H. L., Pratt, S. M., Sammes, P. J., Gibb, S., and Geider, R. J.: Photoacclimation in the marine diatom *Skeletonema costatum*, *Limnology and Oceanography*, 45, 1807–1817, 2000.
- Arhonditsis, G. and Brett, M.: Evaluation of the current state of mechanistic aquatic biogeochemical modeling, *Marine Ecology Progress Series*, 271, 13–26, doi:10.3354/meps271013, 2004.
- 10 Arhonditsis, G. B., Papantou, D., Zhang, W., Perhar, G., Massos, E., and Shi, M.: Bayesian calibration of mechanistic aquatic biogeochemical models and benefits for environmental management, *Journal of Marine Systems*, 73, 8–30, 2008.
- Armi, L. and Flament, P.: Cautionary remarks on the spectral interpretation of turbulent flows, *Journal of Geophysical Research: Oceans* (1978–2012), 90, 11 779–11 782, 1985.
- 15 Armstrong, R. A.: Optimality-based modeling of nitrogen allocation and photoacclimation in photosynthesis, *Deep Sea Research Part II: Topical Studies in Oceanography*, 53, 513–531, 2006.
- Armstrong, R. A.: Nutrient uptake rate as a function of cell size and surface transporter density: A Michaelis-like approximation to the model of Pasciak and Gavis, *Deep Sea Research Part I: Oceanographic Research Papers*, 55, 1311–1317, 2008.
- Arrhenius, S.: Über die Dissociationswärme und den Einfluss der Temperatur auf den Dissociationsgrad der Elektrolyte, *Wilhelm Engelmann*, 20 1889.
- Askey, R. and Wilson, J. A.: Some basic hypergeometric orthogonal polynomials that generalize Jacobi polynomials, vol. 319, *American Mathematical Society*, 1985.
- Aumont, O., Ethe, C., Tagliabue, A., Bopp, L., and Gehlen, M.: PISCES-v2: an ocean biogeochemical model for carbon and ecosystem studies, *Geoscientific Model Development*, 8, 2465–2513, doi:10.5194/gmd-8-2465-2015, www.geosci-model-dev.net/8/2465/2015/, 25 2015.
- Bacastow, R. and Maier-Reimer, E.: Dissolved organic carbon in modeling oceanic new production, *Global Biogeochemical Cycles*, 5, 71–85, 1991.
- Banas, N. S.: Adding complex trophic interactions to a size-spectral plankton model: Emergent diversity patterns and limits on predictability, *Ecological Modelling*, 222, 2663–2675, 2011.
- 30 Baretta-Bekker, J. G., Riemann, B., Baretta, J. W., and Rasmussen, E. K.: Testing the microbial loop concept by comparing mesocosm data with results from a dynamical simulation-model, *Marine Ecology Progress Series*, 106, 187–198, 1994.
- Baretta-Bekker, J. G., Baretta, J. W., Hansen, A. S., and Riemann, B.: An improved model of carbon and nutrient dynamics in the microbial food web in marine enclosures, *Aquatic Microbial Ecology*, 1998.
- Baumert, H.: On the theory of photosynthesis and growth in phytoplankton. Part I: Light limitation and constant temperature, *Internationale Revue der gesamten Hydrobiologie und Hydrographie*, 81, 109–139, 1996.
- 35 Bayes, T.: A letter from the late Reverend Mr. Thomas Bayes, F. R. S. to John Canton, A.M.F.R.S., *Philosophical Transactions* (1683-1775), pp. 269–271, 1763.



- Béal, D., Brasseur, P., Brankart, J.-M., Ourmieres, Y., and Verron, J.: Characterization of mixing errors in a coupled physical biogeochemical model of the North Atlantic: implications for nonlinear estimation using Gaussian anamorphosis, *Ocean Science*, 6, 247–262, 2010.
- Bennett, A. F.: *Inverse modeling of the ocean and atmosphere*, Cambridge University Press, 2002.
- Berelson, W.: The flux of particulate organic carbon into the ocean interior: A comparison of four US JGOFS regional studies, *Oceanography*, 5 14, 59–67, 2001.
- Bertino, L., Evensen, G., and Wackernagel, H.: Sequential data assimilation techniques in oceanography, *International Statistical Review*, 71, 223–241, 2003.
- Blackman, F. F.: Optima and limiting factors, *Annals of Botany*, 19, 281–295, 1905.
- Bliznyuk, N., Ruppert, D., Shoemaker, C., Regis, R., Wild, S., and Mugunthan, P.: Bayesian calibration and uncertainty analysis for computationally expensive models using optimization and radial basis function approximation, *Journal of Computational and Graphical Statistics*, 10 17, 2008.
- Bocquet, M.: An introduction to inverse modelling and parameter estimation for atmosphere and ocean sciences, in: *International Summer School - Advanced Data Assimilation for Geosciences*, edited by Blayo, E., Bocquet, M., Cosme, E., and Cugliandolo, L. F., p. 608, Oxford University Press, 2014.
- 15 Box, G. E. and Cox, D. R.: An analysis of transformations, *Journal of the Royal Statistical Society. Series B (Methodological)*, pp. 211–252, 1964.
- Brasseur, P., Baharel, P., Bertino, L., Birol, F., Brankart, J.-M., Ferry, N., Losa, S., Rémy, E., Schröter, J., Skachko, S., et al.: Data assimilation for marine monitoring and prediction: the MERCATOR operational assimilation systems and the MERSEA developments, *Quarterly Journal of the Royal Meteorological Society*, 131, 3561–3582, 2005.
- 20 Brown, J. H., Gillooly, J. F., Allen, A. P., Savage, V. M., and West, G. B.: Toward a metabolic theory of ecology, *Ecology*, 85, 1771–1789, 2004.
- Bruggeman, J.: A phylogenetic approach to the estimation of phytoplankton traits, *Journal of Phycology*, 47, 52–65, 2011.
- Bruggeman, J., Heringa, J., and Brandt, B. W.: PhyloPars: estimation of missing parameter values using phylogeny, *Nucleic Acids Research*, 37, W179–W184, 2009.
- 25 Brun, R., Reichert, P., and Künsch, H. R.: Practical identifiability analysis of large environmental simulation models, *Water Resources Research*, 37, 1015–1030, 2001.
- Brun, R., Kühni, M., Siegrist, H., Gujer, W., and Reichert, P.: Practical identifiability of ASM2d parameters – systematic selection and tuning of parameter subsets, *Water Research*, 36, 4113–4127, 2002.
- Buesseler, K.: Do upper-ocean sediment traps provide an accurate record of particle flux?, *Nature*, 353, 420–423, 1991.
- 30 Buesseler, K., Lamborg, C., Boyd, P., Lam, P., Trull, T., Bidigare, R., Bishop, J., Casciotti, K., Dehairs, F., Elskens, M., Honda, M., Karl, D., Siegel, D., Silver, M., Steinberg, D., Valdes, J., Mooy, B. V., and Wilson, S.: Revisiting carbon flux through the ocean’s twilight zone, *Science*, 316, 567–570, doi:10.1126/science.1137959, 2007.
- Buitenhuis, E., Le Quéré, C., Aumont, O., Beaugrand, G., Bunker, A., Hirst, A., Ikeda, T., O’Brien, T., Piontkovski, S., and Straile, D.: Biogeochemical fluxes through mesozooplankton, *Global Biogeochemical Cycles*, 20, 2006.
- 35 Buitenhuis, E. T., Rivkin, R. B., Salliey, S., and Le Quéré, C.: Biogeochemical fluxes through microzooplankton, *Global Biogeochemical Cycles*, 24, 2010.
- Burd, A. B. and Jackson, G. A.: Particle aggregation, *Annual Review of Marine Science*, 1, 65–90, 2009.



- Burnham, K. P. and Anderson, D. R.: Model selection and multimodel inference: a practical information-theoretic approach, Springer Science & Business Media, 2002.
- Cabre, A., Marinov, I., Bernadello, R., and Bianchi, D.: Oxygen minimum zones in the tropical Pacific across CMIP5 models: mean state differences and climate change trends, *Biogeosciences*, 12, 5429–5454, doi:10.5194/bg-12-5429-2015, www.biogeosciences.net/12/5429/2015/, 2015.
- 5 Cao, X. and Spall, J.: Comparison of Expected and Observed Fisher Information in Variance Calculations for Parameter Estimates, Johns Hopkins APL technical digest, 28, 294, 2010.
- Carr, M.-E., Friedrichs, M. A. M., Schmeltz, M., Aitac, M. N., Antoine, D., Arrigo, K. R., Asanuma, I., Aumont, O., Barber, R., Behrenfeld, M., Bidigare, R., Buitenhuis, E. T., Campbell, J., Ciotti, A., Dierssen, H., Dowell, M., Dunne, J., Esaias, W., Gentili, B., Gregg, W., Groom, S., Hoepffner, N., Ishizaka, J., Kameda, T., Quéré, C. L., Lohrenz, S., Marra, J., Mélin, F., Moore, K., Morel, A., Reddy, T., Ryan, J., Scardi, M., Smyth, T., Turpie, K., Tilstone, G., Waters, K., and Yamanaka, Y.: A comparison of global estimates of marine primary production from ocean color, *Deep Sea Research Part II: Topical Studies in Oceanography*, 53, 741–770, doi:10.1016/j.dsr2.2006.01.028, 2006.
- Castelletti, A., Galelli, S., Ratto, M., Soncini-Sessa, R., and Young, P.: A general framework for dynamic emulation modelling in environmental problems, *Environmental Modelling & Software*, 34, 5–18, 2012.
- 15 Cocco, V., Joos, F., Steinacher, M., Frölicher, T., Bopp, L., Dunne, J., Gehlen, M., Heinze, C., Orr, J., Oschlies, A., Schneider, B., Segsneider, J., and Tjiputra, J.: Oxygen and indicators of stress for marine life in multi-model global warming projections, *Biogeosciences*, 10, 1849–1868, doi:10.5194/bg-10-1849-2013, 2013.
- Conn, A. R., Gould, N. I. M., and Toint, P. L.: Trust-region methods, MPS-SIAM Series on Optimization, Society for Industrial and Applied Mathematics, Philadelphia, 2000.
- 20 Conti, S. and O’Hagan, A.: Bayesian emulation of complex multi-output and dynamic computer models, *Journal of Statistical Planning and Inference*, 140, 640–651, 2010.
- Conti, S., Gosling, J. P., Oakley, J. E., and O’Hagan, A.: Gaussian process emulation of dynamic computer codes, *Biometrika*, p. asp028, 2009.
- 25 Côté, B. and Platt, T.: Day-to-day variations in the spring-summer photosynthetic parameters of coastal marine phytoplankton, *Limnology and Oceanography*, 28, 320–344, 1983.
- Cox, D.: Frequentist and Bayesian statistics: a critique, *Proceedings of the Statistical Problems in Particle Physics, Astrophysics and Cosmology*, 2005.
- Cox, D. R. and Hinkley, D. V.: *Theoretical Statistics*, CRC Press, 1974.
- 30 Craig, P., Goldstein, M., Seheult, A., and Smith, J.: Bayes linear strategies for matching hydrocarbon reservoir history, in: *Bayesian statistics 5: Proceedings of the Fifth Valencia International Meeting, June 5-9, 1994*, edited by Bernardo, J., Berger, J., Dawid, A., and Smith, A., pp. 69–95, Oxford University Press, 1996.
- Crout, N. M., Tarsitano, D., and Wood, A. T.: Is my model too complex? Evaluating model formulation using model reduction, *Environmental Modelling & Software*, 24, 1–7, 2009.
- 35 Cullen, J. J., Yang, X., and MacIntyre, H. L.: Nutrient limitation of marine photosynthesis, in: *Primary Productivity and Biogeochemical Cycles in the Sea*, edited by Falkowski, P., Woodhead, A., and Vivirito, K., vol. 43 of *Environmental Science Research*, pp. 69–88, Springer, 1992.



- Delille, B., Harlay, J., Zondervan, I., Jacquet, S., Chou, L., Wollast, R., Bellerby, R. G., Frankignoulle, M., Borges, A. V., Riebesell, U., and Gattuso, J.-P.: Response of primary production and calcification to changes of pCO₂ during experimental blooms of the coccolithophorid *Emiliania huxleyi*, *Global Biogeochemical Cycles*, 19, 2005.
- Denman, K.: Modelling planktonic ecosystems: parameterizing complexity, *Progress in Oceanography*, 57, 429–452, doi:10.1016/S0079-6611(03)00109-5, 2003.
- 5 Doney, S. C., Glover, D. M., and Najjar, R. G.: A new coupled, one-dimensional biological-physical model for the upper ocean: Applications to the JGOFS Bermuda Atlantic Time-series Study (BATS) site, *Deep Sea Research Part II: Topical Studies in Oceanography*, 43, 591–624, 1996.
- Doron, M., Brasseur, P., Brankart, J.-M., Losa, S. N., and Melet, A.: Stochastic estimation of biogeochemical parameters from Globcolour ocean colour satellite data in a North Atlantic 3D ocean coupled physical–biogeochemical model, *Journal of Marine Systems*, 117, 81–95, 2013.
- 10 Doucet, A. and Robert, C. P.: Introduction to Special Issue on Monte Carlo Methods in Statistics, *ACM Transactions on Modeling and Computer Simulation (TOMACS)*, 23, 1, 2013.
- Dowd, M.: A sequential Monte Carlo approach for marine ecological prediction, *Environmetrics*, 17, 435–455, 2006.
- 15 Dowd, M.: Bayesian statistical data assimilation for ecosystem models using Markov Chain Monte Carlo, *Journal of Marine Systems*, 68, 439–456, 2007.
- Dowd, M.: Estimating parameters for a stochastic dynamic marine ecological system, *Environmetrics*, 22, 501–515, 2011.
- Dowd, M. and Meyer, R.: A Bayesian approach to the ecosystem inverse problem, *Ecological Modelling*, 168, 39–55, doi:10.1016/S0304-3800(03)00186-8, 2003.
- 20 Dowd, M., Jones, E., and Parslow, J.: A statistical overview and perspectives on data assimilation for marine biogeochemical models, *Environmetrics*, 25, 203–213, 2014.
- Droop, M.: 25 Years of Algal Growth Kinetics A Personal View, *Botanica Marina*, 26, 99–112, 1983.
- Dutkiewicz, S., Follows, M. J., and Bragg, J. G.: Modeling the coupling of ocean ecology and biogeochemistry, *Global Biogeochemical Cycles*, 23, 2009.
- 25 Edwards, K. F., Thomas, M. K., Klausmeier, C. A., and Litchman, E.: Allometric scaling and taxonomic variation in nutrient utilization traits and maximum growth rate of phytoplankton, *Limnology and Oceanography*, 57, 554–566, 2012.
- Efron, B.: Bootstrap confidence intervals for a class of parametric problems, *Biometrika*, 72, 45–58, 1985.
- Efron, B.: Why isn't everyone a Bayesian?, *The American Statistician*, 40, 1–5, 1986.
- Efron, B. and Hinkley, D. V.: Assessing the accuracy of the maximum likelihood estimator: Observed versus expected Fisher information, *Biometrika*, 65, 457–483, 1978.
- 30 Efron, B. and Tibshirani, R.: Bootstrap methods for standard errors, confidence intervals, and other measures of statistical accuracy, *Statistical science*, pp. 54–75, 1986.
- El Jarbi, M., Rückelt, J., Slawig, T., and Oschlies, A.: Reducing the model-data misfit in a marine ecosystem model using periodic parameters and linear quadratic optimal control, *Biogeosciences*, 10, 1169–1182, 2013.
- 35 Engel, A., Zondervan, I., Aerts, K., Beaufort, L., Benthien, A., Chou, L., Delille, B., Gattuso, J.-P., Harlay, J., Heemann, C., Hoffmann, L., Jacquet, S., Nejstgaard, J., Pizay, M.-D., Rochelle-Newall, E., Schneider, U., Terbrueggen, A., and Riebesell, U.: Testing the direct effect of CO₂ concentration on a bloom of the coccolithophorid *Emiliania huxleyi* in mesocosm experiments, *Limnology and Oceanography*, 50, 493–507, 2005.



- Eppley, R. W.: Temperature and phytoplankton growth in the sea, *Fishery Bulletin*, 70, 1063–1085, 1972.
- Eppley, R. W., Rogers, J. N., and McCarthy, J. J.: Half-saturation constants for uptake of nitrate and ammonium by marine phytoplankton, *Limnology and Oceanography*, 14, 912–920, 1969.
- Evans, G. T.: A framework for discussing seasonal succession and coexistence of phytoplankton species, *Limnology and Oceanography*, 33, 5 1988.
- Evans, G. T.: Defining misfit between biogeochemical models and data sets, *Journal of Marine Systems*, 40, 49–54, 2003.
- Evans, G. T. and Parslow, J. S.: A model of annual plankton cycles, *Biological Oceanography*, 3, 327–347, 1985.
- Falkowski, P. G.: Nitrate uptake in marine phytoplankton: Comparison of half-saturation constants from seven species¹, *Limnology and Oceanography*, 20, 412–417, 1975.
- 10 Fan, W. and Lv, X.: Data assimilation in a simple marine ecosystem model based on spatial biological parameterizations, *Ecological Modelling*, 220, 1997–2008, 2009.
- Fasham, M., Ducklow, H., and McKelvie, S.: A nitrogen-based model of plankton dynamics in the oceanic mixed layer, *Journal of Marine Research*, 48, 591–639, 1990.
- Fasham, M. J. R. and Evans, G. T.: The use of optimization techniques to model marine ecosystem dynamics at the JGOFS station 47 Deg N 15 20 Deg W, *Philosophical Transactions of The Royal Society: Biological Sciences*, 348, 203–209, 1995.
- Faugeras, B., Lévy, M., Mémery, L., Verron, J., Blum, J., and Charpentier, I.: Can biogeochemical fluxes be recovered from nitrate and chlorophyll data? A case study assimilating data in the Northwestern Mediterranean Sea at the JGOFS-DYFAMED station, *Journal of Marine Systems*, 40-41, 99–125, doi:10.1016/S0924-7963(03)00015-0, 2003.
- Faure, C. and Papegay, Y.: *Odyssée Version 1.6, the language reference manual*, *Rapport Technique*, 211, 1997.
- 20 Fennel, K., Losch, M., Schroter, J., and Wenzel, M.: Testing a marine ecosystem model : sensitivity analysis and parameter optimization, *Journal of Marine Systems*, 28, 45–63, 2001.
- Fiechter, J., Herbei, R., Leeds, W., Brown, J., Milliff, R., Wikle, C., Moore, A., and Powell, T.: A Bayesian parameter estimation method applied to a marine ecosystem model for the coastal Gulf of Alaska, *Ecological Modelling*, 258, 122–133, 2013.
- Fiksen, Ø., Follows, M. J., and Aksnes, D. L.: Trait-based models of nutrient uptake in microbes extend the Michaelis-Menten framework, 25 *Limnology and Oceanography*, 58, 193–202, 2013.
- Fisher, R. A.: On the mathematical foundations of theoretical statistics, *Philosophical Transactions of the Royal Society of London. Series A, Containing Papers of a Mathematical or Physical Character*, pp. 309–368, 1922.
- Fisher, R. A.: Two new properties of mathematical likelihood, *Proceedings of the Royal Society of London. Series A, Containing Papers of a Mathematical and Physical Character*, 144, 285–307, 1934.
- 30 Fletcher, S.: Mixed Gaussian-lognormal four-dimensional data assimilation, *Tellus A*, 62, 266–287, 2010.
- Flynn, K., Davidson, K., and Leftley, J.: Carbon-nitrogen relations at whole-cell and free-amino-acid levels during batch growth of *Isochrysis galbana* (Prymnesiophyceae) under conditions of alternating light and dark, *Marine Biology*, 118, 229–237, 1994.
- Flynn, K. J.: Modelling multi-nutrient interactions in phytoplankton; balancing simplicity and realism, *Progress in Oceanography*, 56, 249–279, 2003.
- 35 Flynn, K. J.: Ecological modelling in a sea of variable stoichiometry: dysfunctionality and the legacy of Redfield and Monod, *Progress in Oceanography*, 84, 52–65, 2010.
- Flynn, K. J., Marshall, H., and Geider, R. J.: A comparison of two N-irradiance interaction models of phytoplankton growth, *Limnology and Oceanography*, 46, 1794–1802, 2001.



- Franks, P. J.: NPZ models of plankton dynamics: their construction, coupling to physics, and application, *Journal of Oceanography*, 58, 379–387, 2002.
- Franks, P. J.: Plankton patchiness, turbulent transport and spatial spectra, *Marine Ecology Progress Series*, 294, 295–309, 2005.
- Franks, P. J. S.: Planktonic ecosystem models: perplexing parameterizations and a failure to fail, *Journal of Plankton Research*, 31, 1299–1306, doi:10.1093/plankt/fbp069, 2009.
- Freeman, J. and Modarres, R.: Inverse Box–Cox: the power-normal distribution, *Statistics & Probability Letters*, 76, 764–772, 2006.
- Friedrichs, M. A. M.: A data assimilative marine ecosystem model of the central Equatorial Pacific: Numerical twin experiments, *Journal of Marine Research*, 59, 859–894, 2001.
- Friedrichs, M. A. M.: Assimilation of JGOFS EqPac and SeaWiFS data into a marine ecosystem model of the central equatorial Pacific Ocean, *Deep Sea Research Part II: Topical Studies in Oceanography*, 49, 289–319, 2002.
- Friedrichs, M. A. M., Hood, R. R., and Wiggert, J. D.: Ecosystem model complexity versus physical forcing: Quantification of their relative impact with assimilated Arabian Sea data, *Deep Sea Research Part II: Topical Studies in Oceanography*, 53, 576–600, doi:10.1016/j.dsr2.2006.01.026, 2006.
- Friedrichs, M. A. M., Dusenberry, J. A., Anderson, L. A., Armstrong, R. A., Chai, F., Christian, J. R., Doney, S. C., Dunne, J., Fujii, M., Hood, R., McGillicuddy, D. J., Moore, J. K., Schertau, M., Spitz, Y. H., and Wiggert, J. D.: Assessment of skill and portability in regional marine biogeochemical models: Role of multiple planktonic groups, *Journal of Geophysical Research*, 112, C08 001, doi:10.1029/2006JC003852, 2007.
- Frigstad, H., Henson, S., Hartman, S., Omar, A., Jeansson, E., Cole, H., Pebody, C., and Lampitt, R.: Links between surface productivity and deep ocean particle flux at the Porcupine Abyssal Plain sustained observatory, *Biogeosciences*, 12, 5885–5897, 2015.
- Fulton, E. A., Smith, A. D. M., and Johnson, C. R.: Effect of complexity on marine ecosystem models, *Marine Ecology Progress Series*, 253, 1–16, doi:10.3354/meps253001, 2003.
- Garcia, H. E., Locarnini, R. A., Boyer, T. P., and Antonov, J. I.: World Ocean Atlas 2005, Vol. 4: Nutrients (phosphate, nitrate, silicate), in: NOAA Atlas NESDIS 64, edited by Levitus, S., U.S. Government Printing Office, Wash.,D.C., 2006a.
- Garcia, H. E., Locarnini, R. A., Boyer, T. P., and Antonov, J. I.: World Ocean Atlas 2005, Vol. 3: Dissolved Oxygen, Apparent Oxygen Utilization, and Oxygen Saturation, in: NOAA Atlas NESDIS 63, edited by Levitus, S., U.S. Government Printing Office, Wash.,D.C., 2006b.
- Garcia-Gorriz, E., Hoepffner, N., and Ouberdous, M.: Assimilation of SeaWiFS data in a coupled physical–biological model of the Adriatic Sea, *Journal of Marine Systems*, 40, 233–252, 2003.
- Gardner, W.: Sediment trap sampling in surface waters: issues and recommendations, in: *The Changing Ocean Carbon Cycle*, edited by *et al.*, R. H., pp. 240–284, Cambridge University Press, 2000.
- Gehlen, M., Bopp, L., Emprin, N., Aumont, O., Heinze, C., and Ragueneau, O.: Reconciling surface ocean productivity, export fluxes and sediment composition in a global biogeochemical ocean model, *Biogeosciences*, 3, 521–537, 2006.
- Geider, R. J., MacIntyre, H. L., and Kana, T. M.: A dynamic regulatory model of phytoplankton acclimation to light, nutrients, and temperature, *Limnology and Oceanography*, 43, 679–694, 1998.
- Gentleman, W., Leising, A., Frost, B., Strom, S., and Murray, J.: Functional responses for zooplankton feeding on multiple resources: a review of assumptions and biological dynamics, *Deep Sea Research Part II: Topical Studies in Oceanography*, 50, 2847–2875, doi:10.1016/j.dsr2.2003.07.001, 2003.



- Giering, R. and Kaminski, T.: Recipes for adjoint code construction, *ACM Transactions on Mathematical Software (TOMS)*, 24, 437–474, 1998.
- Gill, J. and King, G.: Numerical Issues Involved in Inverting Hessian Matrices, in: *Numerical Issues in Statistical Computing for the Social Scientist*, edited by Altman, M., Gill, J., and McDonald, M. P., chap. 6, pp. 143–176, John Wiley and Sons, Inc., Hoboken, NJ, 2003.
- 5 Gordon, N., Salmond, D., and Smith, A.: Novel approach to nonlinear/non-Gaussian Bayesian state estimation, *IEE Proceedings F (Radar and Signal Processing)*, 140, 107–113, doi:10.1049/ip-f-2.1993.0015, 1993.
- Gregg, W. W., Friedrichs, M., Robinson, A. R., Rose, K. a., Schlitzer, R., Thompson, K. R., and Doney, S. C.: Skill assessment in ocean biological data assimilation, *Journal of Marine Systems*, 76, 16–33, doi:10.1016/j.jmarsys.2008.05.006, 2009.
- Griewank, A.: On automatic differentiation, *Mathematical Programming: recent developments and applications*, 6, 83–107, 1989.
- 10 Griewank, A.: A mathematical view of automatic differentiation, *Acta Numerica*, 12, 321–398, 2003.
- Gunson, J., Oschlies, A., and Garçon, V.: Sensitivity of ecosystem parameters to simulated satellite ocean color data using a coupled physical-biological model of the North Atlantic, *Journal of Marine Research*, 57, 613–639, doi:10.1357/002224099321549611, 1999.
- Hald, A.: On the history of maximum likelihood in relation to inverse probability and least squares, *Statistical Science*, pp. 214–222, 1999.
- Harmon, R. and Challenor, P.: A Markov chain Monte Carlo method for estimation and assimilation into models, *Ecological Modelling*, 101, 15 41–59, 1997.
- Hastings, W. K.: Monte Carlo sampling methods using Markov chains and their applications, *Biometrika*, 57, 97–109, 1970.
- Healey, F. P.: Interacting effects of light and nutrient limitation on the growth rate of *Synechococcus linearis* (cyanophyceae) 1, *Journal of Phycology*, 21, 134–146, 1985.
- Heath, M. R.: Ecosystem limits to food web fluxes and fisheries yields in the North Sea simulated with an end-to-end food web model, 20 *Progress in Oceanography*, 102, 42–66, 2012.
- Heimbach, P., Wunsch, C., Ponte, R. M., Forget, G., Hill, C., and Utke, J.: Timescales and regions of the sensitivity of Atlantic meridional volume and heat transport: Toward observing system design, *Deep Sea Research Part II: Topical Studies in Oceanography*, 58, 1858–1879, 2011.
- Hemmings, J. C. and Challenor, P. G.: Addressing the impact of environmental uncertainty in plankton model calibration with a dedicated software system: the Marine Model Optimization Testbed (MarMOT 1.1 alpha), *Geoscientific Model Development*, 5, 471–498, doi:10.5194/gmd-5-471-2012, 2012.
- 25 Hemmings, J. C., Srokosz, M. A., Challenor, P., and Fasham, M. J.: Assimilating satellite ocean-colour observations into oceanic ecosystem models, *Philosophical Transactions of the Royal Society of London A: Mathematical, Physical and Engineering Sciences*, 361, 33–39, 2003.
- 30 Hemmings, J. C., Srokosz, M. A., Challenor, P., and Fasham, M. J.: Split-domain calibration of an ecosystem model using satellite ocean colour data, *Journal of Marine Systems*, 50, 141–179, 2004.
- Hemmings, J. C., Challenor, P. G., and Yool, A.: Mechanistic site-based emulation of a global ocean biogeochemical model (MEDUSA 1.0) for parametric analysis and calibration: an application of the Marine Model Optimization Testbed (MarMOT 1.1), *Geoscientific Model Development*, 8, 697–731, doi:10.5194/gmd-8-697-2015, 2015.
- 35 Higdon, D., Gattiker, J., Williams, B., and Rightley, M.: Computer model calibration using high-dimensional output, *Journal of the American Statistical Association*, 103, 2008.
- Hoffman, R. N., Liu, Z., Louis, J.-F., and Grassoti, C.: Distortion representation of forecast errors, *Monthly Weather Review*, 123, 2758–2770, 1995.



- Hooten, M. B., Leeds, W. B., Fiechter, J., and Wikle, C. K.: Assessing first-order emulator inference for physical parameters in nonlinear mechanistic models, *Journal of Agricultural, Biological, and Environmental Statistics*, 16, 475–494, 2011.
- Huisman, J. and Weissing, F. J.: Biodiversity of plankton by species oscillations and chaos, *Nature*, 402, 407–410, 1999.
- Huret, M., Gohin, F., Delmas, D., Lunven, M., and Garçon, V.: Use of SeaWiFS data for light availability and parameter estimation of a phytoplankton production model of the Bay of Biscay, *Journal of Marine Systems*, 65, 509–531, 2007.
- Hurt, G. C. and Armstrong, R. A.: A pelagic ecosystem model calibrated with BATS data, *Deep Sea Research Part II: Topical Studies in Oceanography*, 43, 653–683, 1996.
- Hurt, G. C. and Armstrong, R. A.: A pelagic ecosystem model calibrated with BATS and OWSI data, *Deep Sea Research Part I: Oceanographic Research Papers*, 46, 27–61, 1999.
- Ilyina, T., Six, K. D., Segschneider, J., Maier-Reimer, E., Li, H., and Núñez-Riboni, I.: Global ocean biogeochemistry model HAMOCC: Model architecture and performance as component of the MPI-Earth System Model in different CMIP5 experimental realizations, *Journal of Advances in Modeling Earth Systems*, 5, 287–315, 2013.
- Jassby, A. D. and Platt, T.: Mathematical formulation of the relationship between photosynthesis and light for phytoplankton, *Limnology and Oceanography*, 21, 540–547, 1976.
- Jazwinski, A. H.: *Stochastic processes and filtering theory*, Courier Corporation, 2007.
- Ji, R., Davis, C. S., Chen, C., Townsend, D. W., Mountain, D. G., and Beardsley, R. C.: Modeling the influence of low-salinity water inflow on winter-spring phytoplankton dynamics in the Nova Scotian Shelf–Gulf of Maine region, *Journal of Plankton Research*, 30, 1399–1416, 2008.
- Joassin, P., Delille, B., Soetaert, K., Harlay, J., Borges, A. V., Chou, L., Riebesell, U., Suykens, K., and Grégoire, M.: Carbon and nitrogen flows during a bloom of the coccolithophore *Emiliania huxleyi*: Modelling a mesocosm experiment, *Journal of Marine Systems*, 85, 71–85, 2011.
- Johnson, J. B. and Omland, K. S.: Model selection in ecology and evolution, *Trends in ecology & evolution*, 19, 101–108, 2004.
- Jones, E., Parslow, J., and Murray, L.: A Bayesian approach to state and parameter estimation in a Phytoplankton-Zooplankton model, *Australian Meteorological and Oceanographic Journal*, 59, 7–16, 2010.
- Kane, A., Moulin, C., Thiria, S., Bopp, L., Berrada, M., Tagliabue, A., Crépon, M., Aumont, O., and Badran, F.: Improving the parameters of a global ocean biogeochemical model via variational assimilation of in situ data at five time series stations, *Journal of Geophysical Research: Oceans*, 116, 2011.
- Karl, D., Hebel, D., Björkmann, K., and Letelier, R.: The role of dissolved organic matter release in the productivity of the oligotrophic North Pacific Ocean, *Limnology and Oceanography*, 43, 1270–1286, 1998.
- Kasibhatla, P.: Inverse methods in global biogeochemical cycles, 114, American Geophysical Union, 2000.
- Kavetski, D., Kuczera, G., and Franks, S. W.: Bayesian analysis of input uncertainty in hydrological modeling: 1. Theory, *Water Resources Research*, 42, 2006a.
- Kavetski, D., Kuczera, G., and Franks, S. W.: Bayesian analysis of input uncertainty in hydrological modeling: 2. Application, *Water Resources Research*, 42, 2006b.
- Kennedy, M. C. and O’Hagan, A.: Predicting the output from a complex computer code when fast approximations are available, *Biometrika*, 87, 1–13, 2000.
- Kennedy, M. C. and O’Hagan, A.: Bayesian calibration of computer models, *Journal of the Royal Statistical Society. Series B, Statistical Methodology*, pp. 425–464, 2001.



- Khatiwala, S.: A computational framework for simulation of biogeochemical tracers in the ocean, *Global Biogeochemical Cycles*, 21, 2007.
- Kidston, M., Matear, R., and Baird, M. E.: Parameter optimisation of a marine ecosystem model at two contrasting stations in the Sub-Antarctic Zone, *Deep Sea Research Part II: Topical Studies in Oceanography*, 58, 2301–2315, 2011.
- Klausmeier, C. A. and Litchman, E.: Algal games: The vertical distribution of phytoplankton in poorly mixed water columns, *Limnology and Oceanography*, 46, 1998–2007, 2001.
- 5 Kooijman, S.: Population dynamics on basis of budgets, in: *The dynamics of physiologically structured populations*, vol. 68, pp. 266–297, Springer Berlin, 1986.
- Kreus, M. and Schartau, M.: Variations in the elemental ratio of organic matter in the central Baltic Sea: Part II–Sensitivities of annual mass flux estimates to model parameter variations, *Continental Shelf Research*, 100, 46–63, 2015.
- 10 Kriest, I. and Oschlies, A.: On the treatment of particulate organic matter sinking in large-scale models of marine biogeochemical cycles, *Biogeosciences*, 5, 55–72, 2008.
- Kriest, I. and Oschlies, A.: Swept under the carpet: organic matter burial decreases global ocean biogeochemical model sensitivity to remineralization length scale, *Biogeosciences*, 10, 8401–8422, 2013.
- Kriest, I. and Oschlies, A.: MOPS-1.0: towards a model for the regulation of the global oceanic nitrogen budget by marine biogeochemical processes, *Geoscientific Model Development*, 8, 2929–2957, 2015.
- 15 Kriest, I., Khatiwala, S., and Oschlies, A.: Towards an assessment of simple global marine biogeochemical models of different complexity, *Progress in Oceanography*, 86, 337–360, doi:10.1016/j.pocean.2010.05.002, 2010.
- Kriest, I., Oschlies, A., and Khatiwala, S.: Sensitivity analysis of simple global marine biogeochemical models, *Global Biogeochemical Cycles*, 26, 2012.
- 20 Kriest, I., Sauerland, V., Khatiwala, S., Srivastav, A., and Oschlies, A.: Calibrating a global three-dimensional biogeochemical ocean model, *Geoscientific Model Development Discussions*, in preparation.
- Kuczera, G.: Assessing hydrologic model nonlinearity using response surface plots, *Journal of Hydrology*, 118, 143–161, 1990.
- Kwon, E. Y. and Primeau, F.: Optimization and sensitivity study of a biogeochemistry ocean model using an implicit solver and in situ phosphate data, *Global Biogeochemical Cycles*, 20, 2006.
- 25 Kwon, E. Y. and Primeau, F.: Optimization and sensitivity of a global biogeochemistry ocean model using combined in situ DIC, alkalinity, and phosphate data, *Journal of Geophysical Research: Oceans*, 113, 2008.
- Kwon, E. Y., Primeau, F., and Sarmiento, J. L.: The impact of remineralization depth on the air–sea carbon balance, *Nature Geoscience*, 2, 630–635, 2009.
- Laws, E. A. and Bannister, T.: Nutrient-and light-limited growth of *Thalassiosira fluviatilis* in continuous culture, with implications for phytoplankton growth in the ocean, *Limnology and Oceanography*, 25, 457–473, 1980.
- 30 Laws, E. A., Redalje, D. G., Karl, D. M., and Chalup, M. S.: A theoretical and experimental examination of the predictions of two recent models of phytoplankton growth, *Journal of theoretical biology*, 105, 469–491, 1983.
- Lawson, L. M., Hofmann, E. E., and Spitz, Y. H.: Time series sampling and data assimilation in a simple marine ecosystem model, *Deep Sea Research Part II: Topical Studies in Oceanography*, 43, 625–651, doi:10.1016/0967-0645(95)00096-8, 1996.
- 35 Lawson, W. G. and Hansen, J. A.: Alignment error models and ensemble-based data assimilation, *Monthly Weather Review*, 133, 1687–1709, 2005.
- Le Dimet, F.-X. and Talagrand, O.: Variational algorithms for analysis and assimilation of meteorological observations: theoretical aspects, *Tellus A*, 38, 97–110, 1986.



- Le Queré, C.: Reply to Horizons Article ‘Plankton functional type modelling: running before we can walk’ Anderson (2005): I. Abrupt changes in marine ecosystems?, *Journal of Plankton Research*, 28, 871–872, 2006.
- Leeds, W., Wikle, C., and Fiechter, J.: Emulator-assisted reduced-rank ecological data assimilation for nonlinear multivariate dynamical spatio-temporal processes, *Statistical Methodology*, 17, 126–138, 2014.
- 5 Leeds, W. B., Wikle, C. K., Fiechter, J., Brown, J., and Milliff, R. F.: Modeling 3-D spatio-temporal biogeochemical processes with a forest of 1-D statistical emulators, *Environmetrics*, 24, 1–12, 2013.
- Lele, S. R. and Dennis, B.: Bayesian methods for hierarchical models: are ecologists making a Faustian bargain, *Ecological Applications*, 19, 581–584, 2009.
- Leppäranta, M. and Myrberg, K.: *Physical oceanography of the Baltic Sea*, Springer Science & Business Media, 2009.
- 10 Lewis, F., Butler, A., and Gilbert, L.: A unified approach to model selection using the likelihood ratio test, *Methods in Ecology and Evolution*, 2, 155–162, doi:10.1111/j.2041-210X.2010.00063.x, 2011.
- Li, X., McGillicuddy, D. J., Durbin, E. G., and Wiebe, P. H.: Biological control of the vernal population increase of *Calanus finmarchicus* on Georges Bank, *Deep Sea Research Part II: Topical Studies in Oceanography*, 53, 2632–2655, 2006.
- Li, X., Wang, C., Fan, W., and Lv, X.: Optimization of the Spatiotemporal Parameters in a Dynamical Marine Ecosystem Model Based on the Adjoint Assimilation, *Mathematical Problems in Engineering*, 2013, 2013.
- 15 Lignell, R., Haario, H., Laine, M., and Thingstad, T. F.: Getting the “right” parameter values for models of the pelagic microbial food web, *Limnology and Oceanography*, 58, 301–313, 2013.
- Link, W. A. and Barker, R. J.: Model weights and the foundations of multimodel inference, *Ecology*, 87, 2626–2635, 2006.
- Liu, F. and West, M.: A dynamic modelling strategy for Bayesian computer model emulation, *Bayesian Analysis*, 4, 393–411, 2009.
- 20 Longhurst, A.: Seasonal cycles of pelagic production and consumption, *Progress in Oceanography*, 36, 77–167, 1995.
- Longhurst, A. R.: *Ecological Geography of the Sea*, San Diego, Academic Press, 1998.
- Löptien, U. and Dietze, H.: Constraining parameters in state-of-the-art marine pelagic ecosystem models—is it actually feasible with typical observations of standing stocks?, *Ocean Science Discussions*, 12, 227–274, 2015.
- Löptien, U. and Meier, H. M.: The influence of increasing water turbidity on the sea surface temperature in the Baltic Sea: A model sensitivity study, *Journal of Marine Systems*, 88, 323–331, 2011.
- 25 Löptien, U., Eden, C., Timmermann, A., and Dietze, H.: Effects of biologically induced differential heating in an eddy-permitting coupled ocean-ecosystem model, *Journal of Geophysical Research: Oceans (1978–2012)*, 114, 2009.
- Losa, S. N., Kivman, G. A., Schröter, J., and Wenzel, M.: Sequential weak constraint parameter estimation in an ecosystem model, *Journal of Marine Systems*, 43, 31–49, 2003.
- 30 Losa, S. N., Kivman, G. A., and Ryabchenko, V. A.: Weak constraint parameter estimation for a simple ocean ecosystem model: what can we learn about the model and data?, *Journal of Marine Systems*, 45, 1–20, 2004.
- Losa, S. N., Vézina, A., Wright, D., Lu, Y., Thompson, K., and Dowd, M.: 3D ecosystem modelling in the North Atlantic: Relative impacts of physical and biological parameterizations, *Journal of marine systems*, 61, 230–245, 2006.
- Lucia, D. J., Beran, P. S., and Silva, W. A.: Reduced-order modeling: new approaches for computational physics, *Progress in Aerospace Sciences*, 40, 51–117, 2004.
- 35 Maier-Reimer, E.: Geochemical cycles in an ocean general circulation model. Preindustrial tracer distributions, *Global Biogeochemical Cycles*, 7, 645–677, 1993.



- Malve, O., Laine, M., Haario, H., Kirkkala, T., and Sarvala, J.: Bayesian modelling of algal mass occurrences—using adaptive MCMC methods with a lake water quality model, *Environmental Modelling & Software*, 22, 966–977, 2007.
- Marotzke, J., Giering, R., Zhang, K. Q., Stammer, D., Hill, C., and Lee, T.: Construction of the adjoint MIT ocean general circulation model and application to Atlantic heat transport sensitivity, *Journal of Geophysical Research*, 104, 529–548, 1999.
- 5 Marsili-Libelli, S., Guerrizio, S., and Checchi, N.: Confidence regions of estimated parameters for ecological systems, *Ecological Modelling*, 165, 127–146, 2003.
- Martin, A.: Phytoplankton patchiness: the role of lateral stirring and mixing, *Progress in Oceanography*, 57, 125–174, 2003.
- Martin, J. H., Knauer, G. A., Karl, D. M., and Broenkow, W. W.: VERTEX: carbon cycling in the northeast Pacific, *Deep Sea Research Part A. Oceanographic Research Papers*, 34, 267–285, 1987.
- 10 Matear, R. J.: Parameter optimization and analysis of ecosystem models using simulated annealing: A case study at Station P, *Journal of Marine Research*, 53, 571–607, doi:10.1357/0022240953213098, 1995.
- Mattern, J. P., Fennel, K., and Dowd, M.: Estimating time-dependent parameters for a biological ocean model using an emulator approach, *Journal of Marine Systems*, 96, 32–47, 2012.
- Mattern, J. P., Dowd, M., and Fennel, K.: Particle filter-based data assimilation for a three-dimensional biological ocean model and satellite
15 observations, *Journal of Geophysical Research: Oceans*, 118, 2746–2760, 2013a.
- Mattern, J. P., Fennel, K., and Dowd, M.: Sensitivity and uncertainty analysis of model hypoxia estimates for the Texas-Louisiana shelf, *Journal of Geophysical Research: Oceans*, 118, 1316–1332, 2013b.
- Mattern, J. P., Fennel, K., and Dowd, M.: Periodic time-dependent parameters improving forecasting abilities of biological ocean models, *Geophysical Research Letters*, 41, 6848–6854, 2014.
- 20 McDonald, C. P. and Urban, N. R.: Using a model selection criterion to identify appropriate complexity in aquatic biogeochemical models, *Ecological Modelling*, 221, 428–432, 2010.
- Meeker, W. Q. and Escobar, L. A.: Teaching about approximate confidence regions based on maximum likelihood estimation, *The American Statistician*, 49, 48–53, 1995.
- Melbourne-Thomas, J., Wotherspoon, S., Corney, S., Molina-Balari, E., Marini, O., and Constable, A.: Optimal control and system limitation
25 in a Southern Ocean ecosystem model, *Deep Sea Research Part II: Topical Studies in Oceanography*, 2013.
- Merico, A., Bruggeman, J., and Wirtz, K.: A trait-based approach for downscaling complexity in plankton ecosystem models, *Ecological Modelling*, 220, 3001–3010, 2009.
- Metropolis, N., Rosenbluth, A. W., Rosenbluth, M. N., Teller, A. H., and Teller, E.: Equation of state calculations by fast computing machines, *The Journal of Chemical Physics*, 21, 1087–1092, 1953.
- 30 Mittermaier, M. P.: Improving short-range high-resolution model precipitation forecast skill using time-lagged ensembles, *Quarterly Journal of the Royal Meteorological Society*, 133, 1487–1500, 2007.
- Monod, J.: Recherches sur la croissance des cultures bacteriennes, Ph. D Thesis, 1942.
- Monod, J.: The growth of bacterial cultures, *Selected Papers in Molecular Biology by Jacques Monod*, p. 139, 2012.
- Murtugudde, R., Beauchamp, J., McClain, C. R., Lewis, M., and Busalacchi, A. J.: Effects of penetrative radiation on the upper tropical
35 ocean circulation, *Journal of Climate*, 15, 470–486, 2002.
- Najjar, R. G., Jin, X., Louanchi, F., Aumont, O., Caldeira, K., Doney, S. C., Dutay, J.-C., Follows, M., Gruber, N., Joos, F., Lindsay, K., Maier-Reimer, E., Matear, R., Matsumoto, K., Monfray, P., Mouchet, A., Orr, J. C., Plattner, G.-K., Sarmiento, J. L., Schlitzer, R., Slater, R. D., Weirig, M.-F., Yamanaka, Y., and Yool, A.: Impact of circulation on export production, dissolved organic matter and dissolved oxygen in



- the ocean: Results from Phase II of the Ocean Carbon-cycle Model Intercomparison Project (OCMIP-2), *Global Biogeochemical Cycles*, 21, doi:10.1029/2006GB002857, 2007.
- Natvik, L.-J. and Evensen, G.: Assimilation of ocean colour data into a biochemical model of the North Atlantic: Part I. Data assimilation experiments, *Journal of Marine Systems*, 40, 127–153, 2003.
- 5 Nerger, L. and Gregg, W. W.: Improving assimilation of SeaWiFS data by the application of bias correction with a local SEIK filter, *Journal of marine systems*, 73, 87–102, 2008.
- Nevison, C., Manizza, M., Keeling, R., Kahru, M., Bopp, L., Dunne, J., Tiputra, J., Ilyina, T., and Mitchell, B.: Evaluating the ocean biogeochemical components of Earth system models using atmospheric potential oxygen and ocean color data, *Biogeosciences*, 12, 193–208, doi:10.5194/bg-12-193-2015, 2015.
- 10 Omlin, M. and Reichert, P.: A comparison of techniques for the estimation of model prediction uncertainty, *Ecological Modelling*, 115, 45–59, 1999.
- Omlin, M., Reichert, P., and Forster, R.: Biogeochemical model of Lake Zürich: model equations and results, *Ecological Modelling*, 141, 77–103, 2001.
- Oschlies, A.: Model-derived estimates of new production: New results point towards lower values, *Deep Sea Research Part II: Topical Studies in Oceanography*, 48, 2173–2197, 2001.
- 15 Oschlies, A.: Feedbacks of biotically induced radiative heating on upper-ocean heat budget, circulation, and biological production in a coupled ecosystem-circulation model, *Journal of Geophysical Research: Oceans*, 109, 2004.
- Oschlies, A. and Garçon, V.: An eddy-permitting coupled physical-biological model of the North Atlantic: 1. Sensitivity to advection numerics and mixed layer physics, *Global Biogeochemical Cycles*, 13, 135–160, 1999.
- 20 Oschlies, A. and Schartau, M.: Basin-scale performance of a locally optimized marine ecosystem model, *Journal of Marine Research*, 63, 335–358, 2005.
- O’Hagan, A.: Bayesian analysis of computer code outputs: a tutorial, *Reliability Engineering & System Safety*, 91, 1290–1300, 2006.
- Pahlow, M.: Linking chlorophyll-nutrient dynamics to the Redfield N:C ratio with a model of optimal phytoplankton growth, *Marine Ecology Progress Series*, 287, 33–43, 2005.
- 25 Pahlow, M. and Oschlies, A.: Chain model of phytoplankton P, N and light colimitation, *Marine Ecology Progress Series*, 376, 2009.
- Pahlow, M. and Oschlies, A.: Optimal allocation backs Droop’s cell-quota model, *Marine Ecology Progress Series*, 473, 1–5, 2013.
- Pahlow, M., Vézina, A. F., Casault, B., Maass, H., Malloch, L., Wright, D. G., and Lu, Y.: Adaptive model of plankton dynamics for the North Atlantic, *Progress in Oceanography*, 76, 151–191, 2008.
- Parekh, P., Follows, M. J., and Boyle, E. A.: Decoupling of iron and phosphate in the global ocean, *Global Biogeochemical Cycles*, 19, 2005.
- 30 Parslow, J., Cressie, N., Campbell, E. P., Jones, E., and Murray, L.: Bayesian learning and predictability in a stochastic nonlinear dynamical model, *Ecological Applications*, 23, 679–698, 2013.
- Pelc, J. S., Simon, E., Bertino, L., El Serafy, G., and Heemink, A. W.: Application of model reduced 4D-Var to a 1D ecosystem model, *Ocean Modelling*, 57, 43–58, 2012.
- Peterson, D., Perry, M., Bencala, K., and Talbot, M.: Phytoplankton productivity in relation to light intensity: a simple equation, *Estuarine, Coastal and Shelf Science*, 24, 813–832, 1987.
- Phillips, J. R.: Projection-based approaches for model reduction of weakly nonlinear, time-varying systems, *Computer-Aided Design of Integrated Circuits and Systems*, *IEEE Transactions on*, 22, 171–187, 2003.



- Platt, T. and Jassby, A. D.: The relationship between photosynthesis and light for natural assemblages of coastal marine phytoplankton, *Journal of Phycology*, 12, 421–430, 1976.
- Platt, T., Caverhill, C., and Sathyendranath, S.: Basin-scale estimates of oceanic primary production by remote sensing: The North Atlantic, *Journal of Geophysical Research: Oceans*, 96, 15 147–15 159, 1991.
- 5 Platt, T., Sathyendranath, S., Ulloa, O., and Harrison, W.: Nutrient control of phytoplankton photosynthesis in the Western North Atlantic, *Nature*, 356, 229–231, 1992.
- Powell, T. M., Lewis, C. V., Curchitser, E. N., Haidvogel, D. B., Hermann, A. J., and Dobbins, E. L.: Results from a three-dimensional, nested biological-physical model of the California Current System and comparisons with statistics from satellite imagery, *Journal of Geophysical Research: Oceans*, 111, 356–362, doi:10.1029/2004JC002506, 2006.
- 10 Prieß, M., Koziel, S., and Slawig, T.: Marine ecosystem model calibration with real data using enhanced surrogate-based optimization, *Journal of Computational Science*, 4, 423–437, 2013a.
- Prieß, M., Piwonski, J., Koziel, S., Oschlies, A., and Slawig, T.: Accelerated parameter identification in a 3D marine biogeochemical model using surrogate-based optimization, *Ocean Modelling*, 68, 22–36, 2013b.
- Primeau, F. and Deleersnijder, E.: On the time to tracer equilibrium in the global ocean, *Ocean Science*, 5, 13–28, 2009.
- 15 Prunet, P., Minster, J.-F., Echevin, V., and Dadou, I.: Assimilation of surface data in a one-dimensional physical-biogeochemical model of the surface ocean: 2. Adjusting a simple trophic model to chlorophyll, temperature, nitrate, and pCO₂ data, *Global Biogeochemical Cycles*, 10, 139–158, 1996.
- Raue, A., Kreutz, C., Maiwald, T., Bachmann, J., Schilling, M., Klingmüller, U., and Timmer, J.: Structural and practical identifiability analysis of partially observed dynamical models by exploiting the profile likelihood, *Bioinformatics*, 25, 1923–1929, 2009.
- 20 Raue, A., Kreutz, C., Maiwald, T., Klingmüller, U., and Timmer, J.: Addressing parameter identifiability by model-based experimentation, *Systems Biology, IET*, 5, 120–130, 2011.
- Ravela, S., Emanuel, K., and McLaughlin, D.: Data assimilation by field alignment, *Physica D: Nonlinear Phenomena*, 230, 127–145, 2007.
- Rayner, P., Michalak, A. M., and Chevallier, F.: Fundamentals of Data Assimilation, *Biogeosciences Discussions*, submitted.
- Rückelt, J., Sauerland, V., Slawig, T., Srivastav, A., Ward, B., and Patvardhan, C.: Parameter optimization and uncertainty analysis in a
- 25 model of oceanic CO₂ uptake using a hybrid algorithm and algorithmic differentiation, *Nonlinear Analysis: Real World Applications*, 11, 3993–4009, 2010.
- S., B. F. R. and Price: An Essay towards solving a Problem in the Doctrine of Chances. By the late Rev. Mr. Bayes, F. R. S. communicated by Mr. Price, in a letter to John Canton, A. M. F. R. S., *Philosophical Transactions (1683-1775)*, pp. 370–418, 1763.
- Sarmiento, J. L., Slater, R. D., Fasham, M. J. R., Ducklow, H. W., Toggweiler, J. R., and Evans, G. T.: A seasonal three-dimensional ecosystem
- 30 model of nitrogen cycling in the North Atlantic Euphotic Zone, *Global Biogeochemical Cycles*, 7, 417–450, 1993.
- Sasaki, Y.: Some basic formalisms in numerical variational analysis, *Monthly Weather Review*, 98, 875–883, 1970.
- Schartau, M. and Oschlies, A.: Simultaneous data-based optimization of a 1D-ecosystem model at three locations in the North Atlantic: Part I – Method and parameter estimates, *Journal of Marine Research*, 61, 765–793, 2003.
- Schartau, M., Oschlies, A., and Willebrand, J.: Parameter estimates of a zero-dimensional ecosystem model applying the adjoint method,
- 35 Deep Sea Research Part II: Topical Studies in Oceanography, 48, 1769–1800, doi:10.1016/S0967-0645(00)00161-2, 2001.
- Schartau, M., Engel, A., Schröter, J., Thoms, S., Völker, C., and Wolf-Gladrow, D.: Modelling carbon overconsumption and the formation of extracellular particulate organic carbon, *Biogeosciences*, 4, 433–454, 2007.



- Schwinger, J., Goris, N., Tjiputra, J., Kriest, I., Bentsen, M., Bethke, I., Ilicak, M., Assmann, K., and Heinze, C.: Evaluation of NorESM-OC (versions 1 and 1.2), the ocean carbon-cycle stand-alone configuration of the Norwegian Earth System Model (NorESM1), *Geoscientific Model Development Discussions*, pp. 1–73, 2016.
- Shuter, B.: A model of physiological adaptation in unicellular algae, *Journal of Theoretical Biology*, 78, 519–552, 1979.
- 5 Siberlin, C. and Wunsch, C.: Oceanic tracer and proxy time scales revisited, *Climate of the Past*, 7, 27–39, 2011.
- Siegel, D. A., Fields, E., and Buesseler, K. O.: A bottom-up view of the biological pump: Modeling source funnels above ocean sediment traps, *Deep Sea Research Part I: Oceanographic Research Papers*, 55, 108–127, 2008.
- Simon, E. and Bertino, L.: Gaussian anamorphosis extension of the DEnKF for combined state parameter estimation: application to a 1D ocean ecosystem model, *Journal of Marine Systems*, 89, 1–18, 2012.
- 10 Sinha, B., Buitenhuis, E. T., Le Quéré, C., and Anderson, T. R.: Comparison of the emergent behavior of a complex ecosystem model in two ocean general circulation models, *Progress in Oceanography*, 84, 204–224, 2010.
- Slawig, T., Prieß, M., and Kratzenstein, C.: Surrogate-Based and One-Shot Optimization Methods for PDE-Constrained Problems with an Application in Climate Models, in: *Solving Computationally Expensive Engineering Problems*, edited by Koziel, S., Leifsson, L., and Yang, X.-S., vol. 97 of *Springer Proceedings in Mathematics & Statistics*, pp. 1–24, Springer International Publishing, 2014.
- 15 Smith, E. L.: Photosynthesis in relation to light and carbon dioxide, *Proceedings of the National Academy of Sciences of the United States of America*, 22, 504, 1936.
- Smith, R. A.: The theoretical basis for estimating phytoplankton production and specific growth rate from chlorophyll, light and temperature data, *Ecological Modelling*, 10, 243–264, 1980.
- Smith, S. L. and Yamanaka, Y.: Quantitative comparison of photoacclimation models for marine phytoplankton, *Ecological Modelling*, 201, 20 547–552, 2007a.
- Smith, S. L., Yamanaka, Y., Pahlow, M., and Oschlies, A.: Optimal uptake kinetics: physiological acclimation explains the pattern of nitrate uptake by phytoplankton in the ocean, *Marine Ecology Progress Series*, 384, 1–12, 2009.
- Smith, S. L., Merico, A., Wirtz, K. W., and Pahlow, M.: Leaving misleading legacies behind in plankton ecosystem modelling, *Journal of Plankton Research*, 36, 613–620, 2014.
- 25 Smith, S. L., Pahlow, M., Merico, A., Acevedo-Trejos, E., Sasai, Y., Yoshikawa, C., Sasaoka, K., Fujiki, T., Matsumoto, K., and Honda, M. C.: Flexible phytoplankton functional type (FlexPFT) model: size-scaling of traits and optimal growth, *Journal of Plankton Research*, p. fbv038, 2015.
- Soetaert, K. and Petzoldt, T.: Inverse Modelling, Sensitivity and Monte Carlo Analysis in R Using Package FME, *Journal of Statistical Software*, 33, 2010.
- 30 Spitz, Y. H., Moisan, J. R., Abbott, M. R., and Richman, J. G.: Data assimilation and a pelagic ecosystem model: parameterization using time series observations, *Journal of Marine Systems*, 16, 51–68, doi:10.1016/S0924-7963(97)00099-7, 1998.
- Spitz, Y. H., Moisan, J. R., and Abbott, M. R.: Configuring an ecosystem model using data from the Bermuda Atlantic Time Series (BATS), *Deep Sea Research Part II: Topical Studies in Oceanography*, 48, 1733–1768, 2001.
- Stammer, D., Wunsch, C., Giering, R., Zhang, Q., Marotzke, J., Marshall, J., and Hill, C.: The global ocean circulation estimated from TOPEX/POSEIDON altimetry and the MIT general circulation model, *MIT Center for Global Change Science Report*, No. 49, 1997.
- 35 Stammer, D., Ueyoshi, K., Köhl, A., Large, W. G., Josey, S. A., and Wunsch, C.: Estimating air-sea fluxes of heat, freshwater, and momentum through global ocean data assimilation, *Journal of Geophysical Research: Oceans*, 109, 2004.



- Steinacher, M. and Joos, F.: Transient Earth system responses to cumulative carbon dioxide emissions: linearities, uncertainties, and probabilities in an observation-constrained model ensemble, *Biogeosciences*, 13, 1071–1103, 2016.
- Steinacher, M., Joos, F., and Stocker, T. F.: Allowable carbon emissions lowered by multiple climate targets, *Nature*, 499, 197–201, 2013.
- Stock, C. A., McGillicuddy, D. J., Solow, A. R., and Anderson, D. M.: Evaluating hypotheses for the initiation and development of *Alexandrium fundyense* blooms in the western Gulf of Maine using a coupled physical–biological model, *Deep Sea Research Part II: Topical Studies in Oceanography*, 52, 2715–2744, 2005.
- Tarantola, A.: *Inverse problems theory, Methods for Data Fitting and Model Parameter Estimation*. Elsevier, Southampton, 1987.
- Tarantola, A.: *Inverse problem theory and methods for model parameter estimation*, siam, 2005.
- Taylor, K. E., Stouffer, R. J., and Meehl, G. A.: An overview of CMIP5 and the experiment design, *Bulletin of the American Meteorological Society*, 93, 485–498, 2012.
- Terry, K. L., Hirata, J., and Laws, E. A.: Light-limited growth of two strains of the marine diatom *Phaeodactylum tricornutum* Bohlin: chemical composition, carbon partitioning and the diel periodicity of physiological processes, *Journal of Experimental Marine Biology and Ecology*, 68, 209–227, 1983.
- Terry, K. L., Hirata, J., and Laws, E. A.: Light-, nitrogen-, and phosphorus-limited growth of *Phaeodactylum tricornutum* Bohlin strain TFX-1: Chemical composition, carbon partitioning, and the diel periodicity of physiological processes, *Journal of Experimental Marine Biology and Ecology*, 86, 85–100, 1985.
- Thacker, W. C.: The role of the Hessian matrix in fitting models to measurements, *Journal of Geophysical Research: Oceans*, 94, 6177–6196, 1989.
- Tjiputra, J., Roelandt, C., Bentsen, M., Lawrence, D., Lorentzen, T., Schwinger, J., Seland, Ø., and Heinze, C.: Evaluation of the carbon cycle components in the Norwegian Earth System Model (NorESM), *Geoscientific Model Development*, 6, 301–325, 2013.
- Tjiputra, J. F., Polzin, D., and Winguth, A. M.: Assimilation of seasonal chlorophyll and nutrient data into an adjoint three-dimensional ocean carbon cycle model: Sensitivity analysis and ecosystem parameter optimization, *Global Biogeochemical Cycles*, 21, 2007.
- Urban, N. M. and Fricker, T. E.: A comparison of Latin hypercube and grid ensemble designs for the multivariate emulation of an Earth System Model, *Computers & Geosciences*, 36, 746–755, 2010.
- Vallino, J.: Differences and implications in biogeochemistry from maximizing entropy production locally versus globally, *Earth System Dynamics*, 2, 69–85, 2011.
- Vallino, J. J.: Improving marine ecosystem models: Use of data assimilation and mesocosm experiments, *Journal of Marine Research*, 58, 117–164, doi:10.1357/002224000321511223, 2000.
- Vallino, J. J. and Algar, C. K.: The Thermodynamics of Marine Biogeochemical Cycles: Lotka Revisited, *Annual Review of Marine Science*, 8, 333–356, 2016.
- Van den Meersche, K., Middelburg, J. J., Soetaert, K., Van Rijswijk, P., Boschker, H. T., and Heip, C. H.: Carbon-nitrogen coupling and algal-bacterial interactions during an experimental bloom: Modeling a ¹³C tracer experiment, *Limnology and Oceanography*, 49, 862–878, 2004.
- van der Meer, J.: Metabolic theories in ecology, *Trends in Ecology & Evolution*, 21, 136–140, 2006.
- van der Merwe, R., Leen, T. K., Lu, Z., Frolov, S., and Baptista, A. M.: Fast neural network surrogates for very high dimensional physics-based models in computational oceanography, *Neural Networks*, 20, 462–478, 2007.
- van Leeuwen, P. J.: Particle Filtering in Geophysical Systems, *Monthly Weather Review*, 137, 4089–4114, 2009.



- van Leeuwen, P. J.: Nonlinear data assimilation in geosciences: an extremely efficient particle filter, *Quarterly Journal of the Royal Meteorological Society*, 136, 1991–1999, 2010.
- Van Mooy, B. A., Keil, R. G., and Devol, A. H.: Impact of suboxia on sinking particulate organic carbon: Enhanced carbon flux and preferential degradation of amino acids via denitrification, *Geochimica et Cosmochimica Acta*, 66, 457–465, 2002.
- 5 Venzon, D. and Moolgavkar, S.: A method for computing profile-likelihood-based confidence intervals, *Applied Statistics*, pp. 87–94, 1988.
- Wallhead, P. J., Martin, A. P., Srokosz, M. a., and Fasham, M. J. R.: Accounting for unresolved spatial variability in marine ecosystems using time lags, *Journal of Marine Research*, 64, 881–914, doi:10.1357/002224006779698387, 2006.
- Wallhead, P. J., Garçon, V. C., and Martin, A. P.: Efficient upscaling of ocean biogeochemistry, *Ocean Modelling*, doi:10.1016/j.ocemod.2012.12.002, 2013.
- 10 Wallhead, P. J., Garçon, V. C., Casey, J. R., and Lomas, M. W.: Long-term variability of phytoplankton carbon biomass in the Sargasso Sea, *Global Biogeochemical Cycles*, 28, 825–841, 2014.
- Wan, X. and Karniadakis, G. E.: Beyond Wiener–Askey expansions: handling arbitrary pdfs, *Journal of Scientific Computing*, 27, 455–464, 2006.
- Ward, B. A., Friedrichs, M. A., Anderson, T. R., and Oschlies, A.: Parameter optimisation techniques and the problem of underdetermination
15 in marine biogeochemical models, *Journal of Marine Systems*, 81, 34–43, 2010.
- Ward, B. A., Dutkiewicz, S., Jahn, O., and Follows, M.: A size-structured food-web model for the global ocean, *Limnology and Oceanography*, 57, 1877–1891, 2012.
- Ward, B. A., Schartau, M., Oschlies, A., Martin, A. P., Follows, M. J., and Anderson, T. R.: When is a biogeochemical model too complex? Objective model reduction and selection for North Atlantic time-series sites, *Progress in Oceanography*, 116, 49–65,
20 doi:10.1016/j.pocean.2013.06.002, 2013.
- Watanabe, S., Hajima, T., Sudo, K., Nagashima, T., Takemura, T., Okajima, H., Nozawa, T., Kawase, H., Abe, M., Yokohata, T., Ise, T., Sato, H., Kato, E., Takata, K., Emori, S., and Kawamiya, M.: MIROC-ESM 2010: model description and basic results of CMIP5-20c3m experiments, *Geoscientific Model Development*, 4, 845–872, doi:10.5194/gmd-4-845-2011, <http://www.geosci-model-dev.net/4/845/2011/>, 2011.
- 25 Watts, M. C. and Bigg, G. R.: Modelling and the monitoring of mesocosm experiments: two case studies, *Journal of Plankton Research*, 23, 1081–1093, 2001.
- Weir, B., Miller, R. N., and Spitz, Y. H.: Implicit estimation of ecological model parameters, *Bulletin of mathematical biology*, 75, 223–257, 2013.
- Wikle, C. K., Milliff, R. F., Herbei, R., Leeds, W. B., et al.: Modern statistical methods in oceanography: A hierarchical perspective, *Statistical
30 Science*, 28, 466–486, 2013.
- Williamson, D., Goldstein, M., Allison, L., Blaker, A., Challenor, P., Jackson, L., and Yamazaki, K.: History matching for exploring and reducing climate model parameter space using observations and a large perturbed physics ensemble, *Climate Dynamics*, 41, 1703–1729, doi:10.1007/s00382-013-1896-4, 2013.
- Wilson, J., Ridgwell, A., and Barker, S.: Can organic matter flux profiles be diagnosed using remineralisation rates derived from observed tracers and modelled ocean transport rates?, *Biogeosciences*, 12, 5547–5562, doi:10.5194/bg-12-5547-2015, 2015.
- Wirtz, K.-W. and Eckhardt, B.: Effective variables in ecosystem models with an application to phytoplankton succession, *Ecological Modelling*, 92, 33–53, 1996.



- Wirtz, K. W. and Pahlow, M.: Dynamic chlorophyll and nitrogen: carbon regulation in algae optimizes instantaneous growth rate, *Marine Ecology Progress Series*, 402, 81–96, 2010.
- Wood, S. N.: Statistical inference for noisy nonlinear ecological dynamic systems, *Nature*, 466, 1102–1104, 2010.
- Wunsch, C. and Heimbach, P.: Practical global oceanic state estimation, *Physica D: Nonlinear Phenomena*, 230, 197–208, 2007.
- 5 Wunsch, C. and Heimbach, P.: How long to oceanic tracer and proxy equilibrium?, *Quaternary Science Reviews*, 27, 637–651, doi:10.1016/j.quascirev.2008.01.006, 2008.
- Wunsch, C., Heimbach, P., and Ponte, R. M.: The Global General Circulation of the Ocean estimated by the ECCO-consortium, *Oceanography*, 22, 88, 2009.
- Xiao, Y. and Friedrichs, M. A. M.: Using biogeochemical data assimilation to assess the relative skill of multiple ecosystem models in the
10 Mid-Atlantic Bight: effects of increasing the complexity of the planktonic food web, *Biogeosciences*, 11, 3015–3030, doi:10.5194/bg-11-3015-2014, 2014a.
- Xiao, Y. and Friedrichs, M. A. M.: The assimilation of satellite-derived data into a one-dimensional lower trophic level marine ecosystem model, *Journal of Geophysical Research: Oceans*, 119, 2691–2712, 2014b.
- Young, G. A. and Smith, R. L.: *Essentials of statistical inference*, vol. 16, Cambridge University Press, 2005.
- 15 Zhang, W. and Arhonditsis, G. B.: A Bayesian hierarchical framework for calibrating aquatic biogeochemical models, *Ecological Modelling*, 220, 2142–2161, 2009.
- Zhao, L., Wei, H., Xu, Y., and Feng, S.: An adjoint data assimilation approach for estimating parameters in a three-dimensional ecosystem model, *Ecological Modelling*, 186, 235–250, 2005.
- Ziegeler, S. B., Dykes, J. D., and Shriver, J. F.: Spatial error metrics for oceanographic model verification, *Journal of Atmospheric and
20 Oceanic Technology*, 29, 260–266, 2012.